2010

Fabrication of Receptor-Modified Microfluidic Surfaces for Applications in Glycoprotein Screening

Jennifer Macalindong De Guzman
Louisiana State University and Agricultural and Mechanical College

FABRICATION OF RECEPTOR–MODIFIED MICROFLUIDIC SURFACES FOR APPLICATIONS IN GLYCOPROTEIN SCREENING

A Dissertation

Submitted to the Graduate Faculty of the
Louisiana State University and
Agricultural and Mechanical College
in partial fulfillment of the
requirements for the degree of
Doctor of Philosophy

in

the Department of Chemistry

By
Jennifer Macalindong De Guzman
B.S., University of the Philippines at Los Baños, 2000
December 2010

DEDICATION

This dissertation is dedicated to my family:

My Mom, Daisy S. Macalindong

My Dad, Noli M. Macalindong

My Sister, Dr. Shiela S. Macalindong

And to

My dear husband, Christian T. De Guzman

ACKNOWLEDGMENTS

First of all, I would like to thank God and the Lord Jesus Christ for the bountiful blessings that They shower upon me everyday.

I would like to thank Dr. Robin L. McCarley, for providing me with the opportunity to work under his supervision and guidance. I feel fortunate that I got to work in your research group. Words can't express how truly grateful I am.

To my committee members, Dr. Steve A. Soper, Dr. David Spivak, and Dr. Jayne C. Garno, thank you for taking the time to help me with my dissertation. To my Dean's representative, Dr. Lucina E. Lampila, thank you for agreeing to be a part of my dissertation in such short notice.

To the McCarley research group, I will treasure your friendship forever. You have made working in the laboratory enjoyable despite the challenges that we faced. I am glad that I came to meet people who are so good in many ways.

I would also like to extend my gratitude to those who unselfishly helped me in the conduct of my research. Thank you most especially to Dr. Sreelatha Balamurugan, Dr. Subramanian Balamurugan, Dr. Rafael Cueto, and Dr. Dongmei Cao.

To my sister, your passion, hard work and determination are constant inspiration. How you handle the challenges that you face everyday reminds me that there is no problem that cannot be solved if you are willing.

To my mom and dad, I offer you this dissertation. You have made it possible for me to be where I am at now because of your guidance and support, and most especially your sacrifices. For all this, I thank you.

To my dear husband, Stan, thank you for being so supportive and understanding in my decision to pursue graduate studies here in the U.S, and realize this dream, despite of us being away from each other. You are the source of my strength everyday. I would not have accomplished what I have today if not for your love, patience, and kindness.

And last but certainly not the least, I thank the Department of Chemistry and LSU for providing an excellent graduate study environment.

TABLE OF CONTENTS

LIST OF TABLES

LIST OF FIGURES

LIST OF SCHEMES

LIST OF ABBREVIATIONS

μTAS	Micrototal analysis systems
AECPBA	4-[(2-aminoethyl)carbamoyl]phenylboronic acid
CM5	Carboxymethyl dextran
SPR	Surface plasmon resonance
PMMA	Poly(methyl methacrylate)
S–LAC	Serial lectin affinity chromatography
M–LAC	Multi-lectin affinity chromatography
ZIC–HILIC	Zwitterionic hydrophilic interaction liquid chromatography
HC	Hydrazide chemistry
HA	Hydrophilic affinity liquid chromatography (other term for HILIC)
XPS	X-ray photoelectron spectroscopy
ATRP	Atom transfer radical polymerization
SI–ATRP	Surface-initiated atom transfer radical polymerization
RU	Resonance units
p*I*	Isoelectric point
CT–PMMA	Carboxylic acid-terminated poly(methyl methacrylate)
AECPBA–PMMA	4-[(2-aminoethyl)carbamoyl]phenylboronic acid-modified poly(methyl methacrylate)
EDC	1-ethyl-3-[3-dimethylaminopropyl]carbodiimide
NHS	*N*-hydroxysuccinimide
Tris	Tris(hydroxymethyl)aminomethane
BSA	Bovine serum albumin

NIPAAM	*N*-isopropylacrylamide
NAS	*N*-acryloxysuccinimide
tBA	*Tert*-butyl acrylate
GMA	Glycidyl methacrylate
LCST	Lower critical solution temperature
CP	Cloud point
RCA_{120}	*Ricinus communis* agglutinin
TFA	Trifluoroacetic acid
Poly(NIPAAM–NAS–tBA)	Terpolymer consisting of *N*-isopropylacrylamide, *N*-acryloxysuccinimide, and *tert*-butyl acrylate
Poly(NIPAAM–GMA–tBA)	Terpolymer consisting of *N*-isopropylacrylamide, glycidyl methacrylate, and *tert*-butyl acrylate
Poly(NIPAAM–ppg–tBA)	Terpolymer consisting of *N*-isopropylacrylamide, propargyl and *tert*-butyl acrylate
Poly(NIPAAM–lac–tBA)	Terpolymer consisting of *N*-isopropylacrylamide, lactose, and *tert*-butyl acrylate
Poly(NIPAAM–lac–Aac)	Terpolymer consisting of *N*-isopropylacrylamide, lactose, and acrylic acid
Poly(NIPAAM–lac–RCA_{120})	Terpolymer consisting of *N*-isopropylacrylamide, lactose, and *Ricinus communis* agglutinin

ABSTRACT

Glycoproteins have long been identified to have a profound association with human pathological processes, and they are much sought after as potential biomarkers to aid in the early diagnosis and clinical prognosis of cancers and diseases. There is currently high demand for high-throughput and low–limit–of–detection techniques that can afford profiling of the glycoproteome. Micro-total analysis systems (μTAS) based on microfluidics have the potential to fulfill these requirements, but in order to reduce the complexity of the protein pool, the μTAS devices must contain a pre-isolation and enrichment component.

The research project undertaken here involved derivatization of microfluidic surfaces with ligands to allow for capture and isolation of glycoproteins in solution. It is envisioned that a microfluidic device operating in a serial affinity mode can be fabricated whereby a large set of glycoproteins are captured by a global capture element, followed by further fractionation of the previously captured glycoprotein pool into unique glycoproteins by capture elements specific to each unique protein. To that end, the research here involved (1) modification of poly(methyl methacrylate) surfaces with a boronic acid derivative as the global glycoprotein receptor and (2) investigation of a surface-amenable synthetic route for the creation of a thermoresponsive scaffold with immobilized lectin, as the specific glycoprotein receptor, and its complementary eluting sugar. Creation of these surfaces is the first step toward realizing a μTAS for glycoprotein analysis.

The novel boronic acid derivative 4-[(2-aminoethyl)carbamoyl]phenylboronic acid was immobilized on carboxymethyl dextran surfaces, and its protein interaction analysis was investigated by surface plasmon resonance spectroscopy. Poly(methyl methacrylate) microfluidic surfaces were then functionalized with the novel boronic acid derivative to yield a

first-generation global capture modality. Glycoprotein binding to and elution from the global capture surface was afforded using glycine- and Tris-binding buffer systems and borate-eluting buffer systems, respectively, with the aid of Tween 20. A thermoresponsive terpolymer poly(*N*-isopropylacrylamide–lactose–RCA_{120}), with the lectin *Ricinus communis* agglutinin (RCA_{120}) as the specific capture element, was successfully prepared by surface-amenable synthetic protocols. The synthetic strategy proposed in this work can be easily adapted in the creation of microfluidic devices that can afford the capture of specific glycoproteins.

CHAPTER 1

INTRODUCTION

1.1 Research Goals and Aims

The goal of this research is the creation of microfluidic surfaces that possess glycoprotein receptors for applications in glycoproteome profiling and screening. In particular, receptor-modified surfaces capable of isolating a large set of glycoproteins and another surface that allows for the fractionation of the previously captured set of glycoproteins into a specific glycoprotein component are to be prepared to realize an affinity system that can operate in a serial fashion (i.e. general isolation to specific isolation).

The association of glycoproteins with human physiological and pathological processes has generated a lot of interest and has been the subject of much research on structure-function relationships. In fact, a number of current clinically-important biomarkers are glycoproteins,[1-5] and there is reason to believe that more glycoproteins have yet to be identified as biomarkers, but that will require the aid of developing technologies. Profiling of the whole glycoproteome remains a challenge because of the inherent microheterogeneity of glycoproteins and their existence in minute quantities in biological specimens. When glycoproteins are differentiated in response to diseases or cancer, this not only increases the heterogeneity of the pool but also further decreases the quantity that can be detected. A pre-isolation or enrichment methodology is almost exclusively required in all glycoprotein analysis. Owing to the reasons given above, a high demand is placed on high-throughput systems, especially because identification of a viable biomarker requires profiling of biological specimens from a large population of human subjects in order to improve bias against sample-to-sample variations. The rationale for developing systems that can afford a general to specific glycoprotein affinity, in a serial processing mode, is

two-fold in nature. First, the general to specific modality basically constitutes a fractionation method. Fractionation of glycoproteins/glycopeptides is a necessary step in order to obtain pure glycoproteins/glycopeptides that result from differentiation in response to pathological processes. This rationale stems from the fact that the glycoprotein pool is very heterogeneous. This serial processing approach is not uncommon in glycoprotein analysis. Cummings and Kornfeld[6] introduced the very first serial affinity approach (as serial lectin affinity chromatography, S–LAC) for glycoprotein fractionation. Since then, a lot of investigators have employed S–LAC to obtain glycoprotein subsets, with each subset containing a glycoprotein with a unique glycan feature.[7-10] Processing by S–LAC normally begins with a lectin that exhibits broad sugar specificity followed by lectins with narrow sugar specificity. However, as Yang and Hancock[11] adequately puts it, even the broadest specificity lectins available do not sufficiently capture all glycoproteins. Hence, they introduced the concept of multi-lectin affinity chromatography (i.e. multiple lectins in one column) in order to increase the range of glycoproteins captured. This is highly desirable because any attempt in glycoprotein analysis that fails to include even a single component glycoprotein is necessarily inadequate. Without an efficient initial global capture methodology, information from other glycoproteins is most likely to be lost in the process of the fractionation. It is therefore desirable to create devices or selection methods that first provide a global capture of all the glycoproteins, followed by a more specific selection method (capture) to isolate a unique glycoprotein. In this way, a global capture would initially give a good representation of the glycoproteome. Although M–LAC proved to be successful in capturing a wider range of glycoproteins, it requires several lectins combined to effect the desired capability. This is not attractive in the standpoint of cost effectivity. Therefore, another global capture element should be sought; boronic acids are good candidates for this.

A viable argument is why not simply use a narrow specificity lectin since the thrust in isolation methodologies is to single out a particular disease- or cancer-related glycoprotein from a heterogeneous protein pool. This brings about the second rationale in employing a general to specific glycoprotein affinity approach. The approach envisioned herein actually attempts, not only to include all glycoproteins from a protein pool before fractionation, but to reduce the complexity of the protein pool using the general capture methodology. Glycoproteins make up within 10% of the protein pool[11] and the quantity of cancer- and disease-differentiated glycoproteins is further reduced to within 1%.[12] If high abundance proteins are not removed, ionization of the low abundance glycoproteins is reduced during mass spectrometric (MS) analysis;[11,13] mass spectrometry is often the method of choice when interrogating glycoproteins because of its structure elucidation capability. The masking of glycoprotein by the high abundance proteins results in the non-identification of low abundance glycoproteins. It is therefore customary to employ broad sugar specificity lectins or protein depletion methods prior to fractionation or MS analysis to reduce the complexity of the protein pool and subsequently allow identification of glycoproteins. Depletion methods in glycoprotein capture function by allowing the high abundance proteins to adsorb on depletion matrices, leaving other proteins, glycoproteins included, unbound.[11,14] However, depletion strategies are not very efficient, as they do not capture all non-glycosylated proteins.

The first aim of this research was to fabricate a boronic acid-derivatized microfluidic surface for applications in the capture, enrichment, and release of large sets of glycoproteins. Boronic acids form heterocyclic diester bonds with 1,2- or 1,3-cis diols[15] that are prominent features in all glycoproteins; use of properly-designed boronic acid capture elements should afford a global analysis of the glycoproteome. Inherent to the aim of the research was the

evaluation of the interactions between glycosylated and non-glycosylated proteins alike with a unique boronicacid-derivatized surface. For this purpose, 4-[(2-aminoethyl)carbamoyl]phenyl-boronic acid, AECPBA, was immobilized on carboxymethyl dextran (CM5) sensor surfaces, thereafter called AECPBA–CM5, and protein interaction studies were carried out using surface plasmon resonance spectroscopy (SPR) to monitor protein-boronic acid interactions. The binding and elution of a model glycosylated protein was examined to determine the appropriate buffer systems that afford adsorption and desorption. Different glycosylated and non-glycosylated proteins were evaluated in order to identify the factors that influence the adsorption of proteins on boronic acids and the underlying substrate. The nature of non-specific adsorption and how to minimize it was also addressed. After the conclusion of that study, poly(methyl methacrylate), a polymeric substrate established for the fabrication of microanalytical devices, was surface-functionalized with the same boronic acid derivative, thereafter called AECPBA–PMMA, with the hope of translating the outcomes obtained from the surface plasmon resonance spectroscopy (SPR) study to a surface that is chemically and structurally different from the CM5 surface. The properties of the AECPBA–PMMA surface were investigated by X-ray photoelectron spectroscopy (XPS), UV-vis absorption spectroscopy, and contact angle goniometry. The ability and selectivity of the AECPBA–PMMA surface to capture glycoproteins and subsequently release them were examined by XPS measurements using model glycosylated and non-glycosylated proteins.

The second aim of this research was to develop a system that would be capable of capturing/releasing specific glycoproteins. In particular, a synthetic strategy was proposed to create a thermoresponsive terpolymer that bears *both* pendant lectin (i.e. ligand or glycoprotein receptor) and its corresponding complementary eluting sugar for applications in the microfluidic-

based capture, enrichment, and elution of more specific glycoproteins (i.e. glycoproteins possessing unique glycan features). Lectins belong to a protein class that contains binding epitopes for specific oligosaccharide moieties. Consequently, elution of bound glycoproteins from a lectin affinity enrichment format is afforded by the same specific sugars. It should be immediately noted that unlike the conventional lectin affinity chromatography wherein the eluting sugar is introduced through the mobile phase, the eluting sugar in the terpolymer format is also immobilized on the same thermoresponsive polymer scaffold along with the lectin. Adsorption and desorption of glycoprotein analytes are envisioned to be facilitated by the expansion and collapse of the terpolymer as a consequence of the coil-to-globule transition of the thermoresponsive polymer support in response to temperature.[16] This is an attractive affinity system because eluates would be free from small interfering eluent molecules, thereby allowing for direct introduction to a mass spectrometer. It is envisioned that a microfluidic surface could be modified with this terpolymer; hence, the synthetic route developed here in solution possesses surface-amenable synthetic protocols. The components of the precursor terpolymer were investigated and atom transfer radical polymerization synthesis was employed. In particular, the combinations *N*-isopropylacrylamide (NIPAAM)–*X*–tert-butyl acrylate (tBA) where *X* is either *N*-acryloxysuccinimide (NAS) or glycidyl methacrylate (GMA) were examined. The subsequent attachment of the lectin *Ricinus communis* agglutinin (RCA_{120}) and its corresponding eluting sugar lactose were performed in a multi-step sequence fashion using biologically-relevant reactions.

Ultimately, fabricated microfluidic surfaces or devices are going to be integrated into a serial fashion such that an affinity system that operates by first non-selectively capturing and enriching a large subset of glycoproteins from a protein pool (boronic acid surface/device) then

followed by the isolation and enrichment of a unique glycoprotein (lectin–NIPAAM–sugar surface/device) is obtained, similar to serial lectin affinity methodologies.

1.2 Glycoproteins and Their Roles in Human Physiology and Pathology

1.2.1 What Are Glycoproteins?

Glycosylation of proteins is a topic that has attracted much attention over the years due to the unique properties that the oligosaccharide chains impart to the overall function of the proteins. In general, proteins are decorated with glycan chains via co- and post-translational modification processes. Glycoproteins are perhaps the most complex biomolecules in existence, because their biosynthetic pathway allows for the creation of structurally-diverse variants of glycoproteins. The glycosylation of the protein is not coded by DNA. Instead, the glycan chains are initiated, elongated, and terminated in the Golgi apparatus (GA) through the sequential action of glycosidases and glycosyltransferases.[17-18] The transfer of the oligosaccharide chain to the protein then occurs *en bloc* and occurs primarily in the rough endoplasmic reticulum (ER).[19] This is the natural biosynthetic pathway for *N*-glycosylated proteins. However, a stepwise addition of monosaccharide units to proteins occurs to yield another broad class of glycoproteins called *O*-glycosylated proteins; this glycosylation process still occurs in the GA and ER.[20] This information, along with the increasing evidence for relationships between aberrant protein glycosylation and diseases, has made glycosyltransferases the targets of carbohydrate-based therapeutics through enzyme inhibition actions.[18]

Glycoproteins make up half of all naturally-occurring proteins known to date.[5,21-22] Based on the increasing number of glycosylated biomarkers discovered each year and the advances in high-throughput systems used to do so, this fraction of the protein population is sure to grow. However, glycoproteins exist in minute quantities in physiological specimens. They

exist within 10% (w/w) of circulating serum proteins,[11] and is further reduced to <1% for glycoproteins that resulted from differentiation with respect to cancers and diseases.[12]

In general, the glycan chains consist of mannose (Man), galactose (Gal), *N*-acetylneuraminic acid (NANA, a.k.a. sialic acid,), fucose (Fuc), and *N*-acetylglucoseamine (GlcNAc) or *N*-acetylgalactoseamine (GalNAc). These monosaccharides are linked together in different: (1) combinations—although a concensus is often found for *N*-linked glycans, *vide supra*; (2) linkages of the glycosidic bonds—typically designated as 1→2 or 1→4 or 1→6; and (3) anomeric configuration of linked monosaccharide units (α or β). They can exist as linear chains or branched chains, with the latter often appearing as bi-, tri-, and tetrantennary structures. There are 2 broad categories of glycosylation that are commonly found in human glycoproteins, namely, *N*-glycosylation and *O*-glycosylation. *N*-glycosylation is well understood and is the subject of much research on glycoproteomics. This is partly because *N*-glycosylation is common in glycoproteins found in serum, the latter being a biological fluid that is easily sampled by non-invasive procedures and one that contains a myriad of information. In addition, the availability of known enzymes (such as PNGase F) that allows cleavage of *N*-glycans from the protein makes the resulting free glycans accessible for identification by chromatography and mass spectrometric techniques.

N-glycosylated proteins have glycans that are linked to the asparagine residue in the protein in the consensus sequence Asn–*Xxx*–Ser/Thr/Cys (where *Xxx* is any amino acid except proline) via the *N*-acetylglucosamine glycan residue. All *N*-glycans share a common conserved chitobiose structure that consists of *N*-GlcNAc and Man residues. Three general types of *N*-glycosylation exist, and the type depends on the nature of the monosaccharide residues that extend from the core—high mannose, complex, or hybrid. With high mannose *N*-glycosylation,

additional mannose residues are present. Hybrid type glycosylation consists of *N*-GlcNAc and galactose extending from the core, while complex types are essentially hybrid types with sialic acid and/or fucose residues included in the structure. A survey of *N*-glycosylated proteins reveals that the glycans are extremely chemically similar in composition; however, the variability in the linkages, the anomeric configuration of linked monosaccharides, the presence/absence of even one residue (especially fucose), and the branching all lead to extreme diversity in glycan structure. In addition, the number of glycosylation sites is variable for every glycoprotein.

Subtle differences in the glycan chains of a particular glycoprotein lead to variants of the glycoprotein (glycoforms) that are functionally different from one another. These are general characteristics that occur even with *O*-glycosylated proteins. Ribonuclease B (RNAse B) is a well-characterized glycoprotein of the high mannose type. Its single glycosylation occurs at Asn 60 and consists of at least nine glycoforms whereby the *N*-glycans are known by NMR and MS studies to be composed of 5, 6, 7, 8, and 9 mannose residues occurring in relative proportions of 57%, 31%, 4%, 7%, and 1%, respectively.[23-24] Human transferrin's two major *N*-glycosylation sites (Asn 432 and Asn 630)[25-26] fall under the complex type[27] and were shown to consist of several glycoforms.[26] Chicken ovalbumin, the very first protein that showed definitive evidence of glycosylation[28] has a single *N*-glycosylation site at Asn 293 that exists with 13 different glycan chains (glycoforms) that are primarily of the high mannose and hybrid types.[29]

O-glycosylation of proteins is less understood, likely owing to the difficulties associated with the identification and isolation of intact glycans that are required for a successful profiling and site mapping. Unlike *N*-glycans that can be cleaved and obtained intact by known *N*-glycosidases, there is no known corresponding glycosidase for cleavage of *O*-linked glycans.

It is rather unfortunate that *O*-glycosylation has received little attention over the years, as proteins modified with *O*-glycans are also candidates for disease[30] and cancer biomarker discovery.[31-32] The most common type of *O*-glycosylation is of the "mucin-type".[20,30,33-34] As the name suggests, these are found in mucus secretions and are considered to be the principal components of mucus. The *O*-glycans comprise ~ 50% of the dry weight of mucins;[20,30] the large carbohydrate component is largely responsible for the gelatinous texture of mucus. Structurally, *O*-glycans are linked through an *N*-acetylgalactosamine residue to serine and threonine in the protein.[33] The glycan is further elaborated in a linear or branched fashion with typical monosaccharides such as Gal, GlcNAc, and NANA. Unlike *N*-glycosylation, there is no common core and consensus sequence to which *O*-glycans are attached. However, mucins are rich in *p*roline, *t*hreonine, and/or *s*erine sequences (*PTS* region) and it is these sites where *O*-glycans are normally localized.[30]

O-glycosylation is also found in extracellular glycoproteins and follows the same linkage and monosaccharide composition as the "mucin-types". They can occur along with *N*-glycosylations in a glycoprotein, underlining the extreme diversity that is often encountered with glycoproteins. Fetuin from bovine fetal serum contains both *N*- and *O*-glycan chains. This glycoprotein has six glycosylation sites divided equally between both glycosylation types. The *N*-glycans are of the triantennary complex type, while the *O*-glycans typically exhibit the glycan sequence Ser/Thr→GalNAc→Gal→NANA, with occasional linkage of NANA to GalNAc.[27,35] *O*-glycosylated proteins also include those that that are linked to the proteins via an *N*-Acetylglucosamine residue. They typically comprise nuclear and cytoplasmic proteins and are generally not elaborated beyond the GlcNAc residue. A recent review detailing the approaches in the study of *O*-GlcNAc is given by Wang and Hart.[36]

1.2.2 Roles and Functions of Glycoproteins

Glycosylation imparts structural, protective, and stabilizing functions in living cells. Glycoproteins are involved in diverse biological mechanisms, such as protein folding, cell-cell recognition, protein-cell interactions, signal transduction, immunity, intra- and intercellular trafficking, and cell adhesion and differentiation.[37] Perhaps the greatest interest in glycoproteins stems from their correlation in human pathological processes. It has long been recognized that glycosylation of cell surface proteins is significantly altered during disease initiation and progression, cancer development, and metastases.[38-40]

Because changes in glycosylation patterns are a reflection of the activity—either upregulated or downregulated—of the corresponding glycosyltransferases, these enzymes are becoming targets for carbohydrate-assisted therapy. Therefore, identification of the changes in the glycosylation profiles of proteins is a necessary step toward identification of the target glycosyltransferases. Several examples of aberrant glycosylation in diseases and cancer are illustrated below; the reader is directed to reviews[18,32,38,41] for more comprehensive information.

Perhaps the most well-known glycosylated tumor marker is the prostate-specific antigen (PSA), which consequently is the marker that is used clinically in the diagnosis of prostate carcinoma (PCa). Increased levels of PSA, a 28.4 kDa glycoprotein that contains a single *N*-glycosylation at Asn 45, is associated with PCa. However, false positives make it difficult to definitively assign high levels of PSA to PCa because other prostatic occurrences such as benign prostate hyperplasia (BPH) can also exhibit high PSA levels. Therefore, investigations of glycosylation patterns are currently of great interest in the hope of providing better specificity to PSA as a tumor marker.[1-2] Comparison of the PSA obtained from human seminal plasma (designated as the normal sample), PCa sera from patients, and LNCaP cell line (human prostate

adenocarcinoma cell line) was performed using lectin detection, immunosorbent assay, and 2-dimensional gel electrophoresis.[1-2] The general observation was that the glycans of the PSA from the seminal plasma and the PCa sera were quite similar to each other compared to the LNCaP cell line. A few differences were observed though between the seminal plasma and the PCa and included decreased fucosylation, as well as α2,3 sialylation and the absence of terminal GalNAc for the latter. However, the opposite was observed for the glycans obtained from the PSA protein isolated from the LNCaP cell line; this conflicting outcome may be attributable to differences in PSA expression from one person to another or masking of PCa-related PSA with normal tissue-shed PSA. In view of this, more effort needs to be put forth in order for glycosylation in PSA to be a clinically-viable marker. However, with the advances in high-throughput systems, this goal should soon be met.

Breast cancer is the most common cancer in women of all races (*http://progressreport.cancer.gov/appendices_incidence-mortality.asp*). Alterations in protein glycosylation patterns are reported, including, but not limited to, increased β1,6-branched *N*-linked oligosaccharides, increased sialylation, and upregulation of the mucin protein MUC1.[3] Pawelek and co-workers[42] demonstrated by immunohistochemical techniques with tissue microarrays using the lectin leukocytic phytohemagglutinin (LPHA) that metastatic tumor tissues of breast cancer patients has greater abundance of β1,6-branched *N*-linked oligosaccharides compared to their primary tumor counterpart, suggesting that the alteration in the glycosylation is a poor prognosis of metastatic potential. However, there is much debate over this glycosylation change as an indicator of metastases because other literature failed to find the same association.[3] Instead, Dwek and co-workers[3] observed that monosialylated oligosaccharides, such as HPAgly-1, were found overexpressed in the MCF7 breast cancer cell line of patients who developed

metastases; an immunohistochemical methodology based on the lectin HPA from the Roman snail *Helix pomatia* and 2-dimensional gel electrophoresis were used to identify the glycoprotein with overexpressed HPAgly-1.[3] Both of these studies demonstrate the utility of lectins as a valuable tool in biomarker discovery.

Serum CA125 is a glycoprotein tumor marker that is routinely used in the clinical diagnosis of ovarian cancer. However, the ability to detect cancer at its later stage using this marker demands that other ovarian tumor markers be sought to facilitate earlier prognosis. It was found in profiling studies of glycans from whole serum that a good indicator of ovarian cancer is the simultaneous doubling of occurrence for sialyl lewis x and core fucosylated agalactosylated biantennary glycans. Studies to identify the glycoproteins containing these glycans led to the discovery of tumor-derived haptoglobulin β-chain, α1-acid glycoprotein, and α1-antichymotrypsin as proteins with altered glycosylation.[4]

In hepatocellular carcinoma that has developed from hepatitis B virus (HBV) and/or hepatitis C virus (HCV) infections, increased fucosylation levels were determined from analysis of total sera. Combination of lectin extraction, electrophoresis, and matrix-assisted laser desorption/ionization mass spectrometry (MALDI-MS) allowed for the identification of glycoproteins with hyperfucosylation.[43] Changes in the glycosylation of human serum IgG was also found in rheumatoid arthritis patients. Particularly, site-specific glycosylations revealed different extents of glycosylation occuring at all sites and an increase in bisecting GlcNAc and core fucose in the Fab fragment.[44]

Glycosylation also plays a pivotal role in virus infection and contributes significantly to virus pathogenecity and tropism. Of great interest are the 20 *N*-linked glycosylations that are prevalent on human immunodeficiency virus (HIV-1) gp120 glycoprotein and its contribution to

the binding of the HIV virus to its receptor CD4.[45] It was found that the *N*-linked glycosylation participates in the binding by conferring the proper native conformation of the CD4 binding pocket rather than facilitating direct interaction of the virus to the receptor, such as in lectin–glycoprotein interactions. Hidden in this conclusion, and perhaps the more interesting information obtained from the study, is the fact that deglycosylation of the HIV-1 gp120 did not alter its avidity for CD4 binding, thus indicating that once the epitope binding site is properly folded—by allowing the conformation to mature following glycosylation of gp120—the *N*-linked glycans are unlikely participants in the interaction.

These examples clearly illustrate that glycoproteins can make for excellent biomarkers, with it being demonstrated that PSA and CA125 are currently used in clinical diagnostic tools. It is also evident that owing to the large sets of glycans in their corresponding glycoproteins that need to be accurately profiled—variations in human-to-human samples included—there is the need for powerful techniques that can provide high selectivity in a high-throughput fashion.

1.3 Overview of the Different Macroscale Methods of Glycoprotein/Glycopeptide Isolation, Enrichment, and Identification

Physiological fluids often contain minute quantities of glycoproteins, and taken that differential glycosylation occurs during pathogenesis, physiological fluids should contain even smaller quantities of pathologically-related glycoproteins with increased heterogeneity. In addition, the wide range of protein concentrations in serum or plasma spans 7–10 orders of magnitude,[46] and glycoproteins are often masked by highly-abundant proteins, such as serum albumins (55%).[47] These characteristics put high demands on approaches that can reduce the complexity of the protein pool and impart high selectivity and resolving power. This section will address the commonly practiced macroscale methodologies that are encountered in glycoprotein/glycopeptide isolation and enrichment.

1.3.1 Lectin Affinity

The vast majority of glycoprotein enrichment strategies rely on methods utilizing lectin affinity. This is perhaps a consequence of the fact that lectins are inexpensive, ubiquitous (i.e. their sources include animals, plants, and microorganisms), and well-characterized in terms of their specificities, although the last point is probably debatable—its characterization could also have been driven by the need for them. As illustrated in the previous section, lectin affinity chromatography is a very valuable tool in the identification of potential biomarkers from biological specimens. The discovery of lectins was made by Stillmark[48] in 1888 upon a chance encounter of a hemagglutinating activity of his castor bean extract (ricin). Lectins (from the Latin-derived word "*legere*" meaning "to select") are often defined in the literature as carbohydrate-binding proteins of non-immune origin capable of agglutinating cells or precipitating glycoconjugates.[49] However, Van Damme and co-authors[50] find this definition restrictive, as they do not include all lectins (e.g. some have carbohydrate-binding properties but do not exhibit agglutination activity). In particular, they have defined plant lectins as plant proteins that contain at least one non-catalytic epitope that exhibits reversible binding to a specific mono- or oligosaccharide. Currently, lectins are classified according to 7 saccharide-binding specificities (mannose-, mannose/maltose-, mannose/glucose-, GlcNAc/$(GlcNac)_n$-, Gal/GalNAc-, fucose-, and sialic acid-binding lectins) but a broader classification groups them according to the number of saccharide binding domains (merolectins or hololectins) and whether or not there exists in the same lectin another domain that participates in biological activity independent of the activity of the saccharide-binding domain (chimerolectins or superlectins).[50]

Hundreds of lectins are known as evidenced by the listing in the book *Lectins*[49] and the *Handbook of Plant Lectins*.[50] They are available commercially, and several vendors such as

Sigma, Vector Laboratories, Galab Technologies, Amersham Pharmacia, and Pierce offer unconjugated and conjugated lectins (agarose-bound, biotinylated, and fluorescently-labeled), lectin antibodies, and pre-made columns and kits. Typically, lectins are generally categorized as having specific or relatively broad saccharide specificities. This categorization is rather subjective and relies mostly on the commonness or uniqueness of the mono- or oligosaccharide structures and the intricate details featured in the glycans. A lectin that perhaps best illustrates very narrow (high) specificity is the *Macckia amurensis* lectin (MAL) that recognizes the terminal sialic acid residue that is linked $\alpha 2 \rightarrow 3$ to galactose residues but not sialic acid linked $\alpha 2 \rightarrow 6$ to galactose.[8] Alternatively, by having relatively broad saccharide specificity, the lectin recognizes a saccharide moiety that is common to many glycans. The most common ones of this category are concanavalin A (Con A) and wheat germ agglutinin (WGA) that have specificities towards D-mannose and GlcNac residues, two quite common residues in *N*-glycans. These two lectins are often employed to isolate a large set of glycoproteins[51-53] that purportedly provide a good representation of the glycoprotein pool. However, while it is possible to isolate a large set of glycoproteins using lectins with relatively broad saccharide specificities, inherent variations in the structure of the sugars bound to the protein have not allowed for isolation of *all* components of a given glycoprotein pool based on each lectin.[51]

To this end, enrichment of glycoproteins from physiological specimens is often performed by serial lectin affinity (S–LAC, lectin columns connected in series)[6-10] or multi-lectin affinity chromatography (M–LAC, multiple lectins in the same column).[11,46,54-55] Both methods employ several lectins of varying structural selectivity to target different populations of glycoprotein; hence, a more complete capture is realized. Hancock and co-workers[11,54] were the pioneers of M–LAC, and they employed three broad specificity lectins, Con A, WGA, and

jacalin (specific for GalNAc residues in *O*-glycans). In their work, they observed that indeed each lectin captured a subset of serum glycoproteome and some overlap in the lectin specificity (i.e. some glycoproteins captured by one lectin were also captured by another lectin); these outcomes highlight the fact that complete capture of glycoproteins cannot be achieved even with broad specificity lectins. The specificity and efficiency of the M–LAC was demonstrated when human serum was subjected to M–LAC.[11] The majority of the glycoproteins were found enriched in the bound fraction compared to the flow-through fraction (unbound). It can be said that although enrichment was observed, it was not 100% efficient. The selectivity was moderate, as a small amount of albumin was found in the bound fraction based on SDS–PAGE results. However, when a depletion step was performed on a plasma sample (i.e. underwent removal of high-abundance serum proteins) prior to M–LAC, the number of identified glycoproteins by mass spectrometry increased significantly, perhaps due to increased ionization of glycoproteins resulting from the absence of high-abundance proteins, such as albumin.[54] In general, M–LAC is perhaps more efficient and practical than S–LAC because it requires less sample handling. Perhaps S–LAC is more appropriate in cases where a general to specific isolation is deemed necessary.

Lectins are often utilized as immobilized materials on chromatographic support matrixes including, but not limited to, agarose, cellulose, silica, polymer beads, and monoliths.[56-57] The immobilization strategies depend highly on the type of matrix, and the lectin attachment is usually accomplished following matrix activation.[57] Lectin-affinity electrophoresis, on the other hand, is less common than the chromatographic techniques, but it has also proven useful in terms of qualitative assessment of changes in glycosylation of serum proteins. When serum from patients suffering from alcoholism were subjected to Con A– and *Datura stramonium* lectin

(DSL)–affinity electrophoresis, the serum proteins isolated were found to be lacking in terminal sialic acids and *N*-glycans.[58] Estimations of binding constant were also performed using lectin affinity electrophoresis.[59]

1.3.2 Enrichment by Hydrazide Chemistry

Zhang *et al*.[60] introduced a quantitative glycoproteome profiling that involved chemical manipulation of the glycoproteins by hydrazide chemistry. The "top down" approach involves the following sequence of steps: (1) periodate oxidation of cis-diol groups in the glycoprotein into aldehydes; (2) coupling of the aldehydes generated on the glycoproteins to a hydrazide-immobilized solid support; (3) removal/collection of non-glycosylated proteins by simple washing; (4) proteolysis of the glycoproteins into glycopeptides by trypsin while on the solid support; (5) removal/collection of tryptic peptides; (6) release of tryptic glycopeptides by the endoglycosidase PNGase F, or isotopic labeling of glycopeptides prior to tryptic release; and (7) analysis of tryptic glycopeptides by high-performance liquid chromatography and mass spectrometric techniques. Their initial results on human serum profiling identified 145 unique peptides that mapped to 57 unique proteins, while an isotope-coded affinity-tagged (ICAT) reagent method only identified 72 unique peptides that mapped to 23 unique proteins.[60] The outcomes from the study by Zhang demonstrated an increased efficiency for the hydrazide chemistry method; this is because the hydrazide route does not suffer from the presence of high-abundance proteins. When an LNCaP membrane fraction (human prostate adenocarcinoma cell line) was subjected to the hydrazide method, 104 unique peptides that mapped to 64 unique proteins were identified and contained the *N*-glycosylation consensus motif; these results highlight the selectivity of the method to *N*-glycosylations.

The same group later extended—or modified—the hydrazide method by first performing the tryptic digestion of the glycoproteins prior to oxidation of the cis-diol groups. This "bottom up" approach allowed for glycopeptide enrichment of over 90% of glycopeptides in serum.[61] Depletion of the abundant plasma and serum proteins was accomplished by the method and allowed the identification of low-abundance glycoproteins.[62] This method was successfully adapted by Hood *et al.*[63] for the comprehensive profiling of the microsomal fractions of the cisplatin-resistant ovarian cancer cell line IGROV-1/CP; a 91% selectivity for the *N*-linked consensus sequence was achieved. The authors[63] claimed increased sensitivity with minimized sample loss compared to the protocol from Zhang *et al.*[60,62] In the latter's work,[60,62] a solid-phase extraction step was employed to remove excess periodate following the oxidation reaction and before subjecting the tryptic products to hydrazide resin; the SPE step is a potential route for sample loss. Hood and co-workers[63] eliminated this step by instead quenching the periodate followed by subjecting the tryptic products to hydrazide chemistry. As a result, a three-fold increase in the number of identified proteins was realized compared to the method of Zhang *et al.* in the analysis of similar samples.

Improved sequence coverage was achieved by Chen *et al.*[64] when they integrated multiple enzyme digestion to the hydrazide enrichment protocol. By using three proteases of broad and complementary specificity—trypsin, pepsin, and thermolysin—939 *N*-glycosylation sites were identified, as opposed to 622 resulting from a shotgun approach (i.e. using trypsin alone) of human liver tissue. They argued that the use of trypsin alone results in missed tryptic cleavages—a prevalent occurrence in glycoprotein digestion due to steric hindrance posed by the glycans—and yields proteins that are outside the mass detection range typical for MS/MS

techniques (800–3500 Da). Hence, peptides outside the range are not likely detected, as they illustrated.

It is clear that hydrazide enrichment can target *N*-glycosylations with high selectivity and increased sensitivity. In addition, the potential of this method to determine the *N*-glycosylation site (or the lack thereof) is of tremendous importance, especially for diseases manifested by deficiencies in *N*-glycosylation (type 1 congenital disorders of glycosylation).[65-66] However, glycan information is lost in the process, because it remains attached to the solid support. This has a negative impact on biomarker discovery because differential glycosylation (i.e. changes in the glycan composition and structure) and its correlation with disease and cancer development, and metastatic potential, cannot be probed properly.

1.3.3 Hydrophilic Interaction Liquid Chromatography (HILIC)

Hydrophilic interaction liquid chromatography relies heavily on the interactions between a hydrophilic stationary phase and polar analytes, with the latter's subsequent elution by use of a relatively hydrophobic binary eluent. Where the line is drawn between HILIC and normal-phase chromatography (NPC) is somewhat unclear. However, Alpert's definition that the mechanism of HILIC is based on the partitioning of analyte between the water-rich layer of the stationary phase and the bulk eluent, as opposed to the NPC adsorption-based mechanism, is gaining acceptance and seems to be an accurate definition as seen in the literature.[67] Another important qualifier for HILIC is that water is the strongly eluting solvent.[67]

A variety of stationary phases is employed in HILIC and includes bare silica, aminopropyl-bonded silica, amide silica, polymer-based amino packing, poly(succinimide)-bonded silica and derivatives, cyano silica, cyanopropyl silica, diol silica, cyclodextrin-based columns, sulfonated SDVB, and more recently, sulfoalkylbetaine silica.[67-72] The emergence of

these different stationary phases is a consequence of the advantages that each brings—compared to the others—to the HILIC format and the separation. For example, polymer-based amino packings have greater stability compared to bare silica and aminopropyl-bonded silica, while amide silica prevents irreversible chemisorptions encountered in amino-based materials. Poly(succinimide)-bonded silica is capable of being further derivatized thereby increasing the potential of HILIC to cover different analyte types. Diol silica corrects for the cumbersome adsorption properties of bare silica. Cyclodextrin-based columns—with a high density of hydroxyl groups—increases the hydrophilic character of the stationary phase, and the sulfoalkylbetaine silica provides water-retaining properties and significantly less ionic retention than bare or amino-coated silica.[67-68] Hägglund and co-workers[69] packed GE-Loader tips with the neutral, zwitterionic HILIC material sulfobetaine-bound resin, thereafter referred to as ZIC–HILIC. Together with a Con A (lectin) pre-enrichment and endoglycosidase digestion, ZIC–HILIC bound glycopeptides were eluted with 99.5% H_2O, 0.5% formic acid. Analysis of human plasma using this method identified 62 glycosylation sites that mapped to 37 unique glycoproteins, indicating the effectiveness of ZIC–HILIC for glycopeptide enrichment. However, the authors admittedly used the lectin column as an initial glycoprotein enrichment step prior to ZIC–HILIC to decrease the complexity of the glycopeptide pool. Nevertheless, they were able to successfully identify even the glycopeptides from less abundant glycoproteins.

Using ZIC–HILIC in the absence of a lectin pre-treatment, Picariello *et al.*[70] demonstrated that while they were able to identify the *N*-glycoproteins and the glycan sites of the glycoproteins responsible for the antiviral and antimicrobial properties of human milk and even some weakly expressed glycoproteins such as breast tumor novel factor 1 and RING finger protein 134, their results raised some specificity issues. They observed that non-glycosylated

peptides bearing the amino acid sequence –EEE– or –EDE– were enriched in the ZIC–HILIC, along with non-glycosylated peptides from caseins, serum albumin, and lactoferrin of which sequences were not provided.

In a communication by Takegawa *et al.*,[71] the power of ZIC–HILIC in selectively resolving isomeric *N*-glycopeptides and recognizing structural differences among sialylated *N*-glycan isomers and neutral *N*-glycans was illustrated with tryptic glycopeptides and 2-aminopyridine–derivatized *N*-glycans of α-1 acid glycoprotein. For example, differential retention was achieved for *N*-glycopeptides having the same glycan structure but differing in the peptide that carries them. The retention of *N*-glycans with and without sialic acids can be finely tuned by electrolyte concentration, thereby resolving structurally-analogous *N*-glycans. A similar observation was provided by Wuhrer *et al.*[72] in their analysis of model glycoproteins using a nanoscale amide-80 column. They found that the retention of identical glycopeptide moieties having different *N*-glycan structures depended on the size of the glycan. They also observed that variation in peptide moieties changed the retention time of the glycopeptides, even though they all contain the same glycosylation.

Collectively, the results from Takegawa *et al.* and Wuhrer *et al.* point to the general conclusion that the interaction of glycopeptides and *N*-glycans with the stationary phase is mediated by hydrogen bonding, a mechanism that is not specific to glycopeptides as illustrated by the work of Cao *et al.*[73] In their analysis of secreted proteins of human hepatocellular carcinoma cells, they employed both hydrophilic interaction—or affinity as they referred to it—liquid chromatography (HA) and hydrazide chemistry method (HC) in the enrichment of *N*-glycopeptides.[73] A complementarity in terms of the number of glycosylation sites identified by a combination of both methods was observed, such that a more global enrichment of

glycopeptides was realized. Out of the 300 non-redundant glycosylation sites, there was only a 41% (124) overlap, while 12% (35) and 47% (141) were uniquely identified by HC and HA, respectively. The important outcomes of this study are two-fold: (1) HA proves to be more global in terms of its enrichment capability owing to the larger number of glycosylation sites it identified compared to HC; and (2) HC is a more specific enrichment protocol with a 93% specificity (based on the ratio of the number of *N*-glycopeptide versus total number of tryptic peptides), while HA has 51% specificity. This result highlights the lack of specificity of HA primarily because its enrichment mechanism is based on hydrogen bonding that is not exclusive to glycans.

In general, hydrophilic interaction liquid chromatography has the power to resolve structurally-similar *N*-glycopeptides and *N*-glycans and identify *N*-glycosylation sites upon MS investigation. Although it can deplete high-abundance glycopeptides, it suffers from low specificity, as demonstrated by the works presented above.

1.3.4 Size-Exclusion Chromatography

A survey by Alvarez-Manzanilla and co-workers[74] of the *in-silico* tryptic peptides of all the human protein sequences in the National Center for Biotechnology Information (NCBI) database revealed that over 90% of the peptides have masses below 2000 Da. They hypothesized that because the mass of the smallest *N*-glycan is over 1200 Da, *N*-glycopeptides would have masses that are well above the non-glycosylated peptides. Hence, they proposed that enrichment and separation of *N*-glycopeptides can be performed by size-exclusion chromatography. Analysis of the radiolabeled glycopeptides from Chinese hamster ovary cells revealed that 87% of the *N*-glycopeptides eluted first between the 17- and 22-min mark during the 40-min run. The enrichment capability of the method was illustrated with the tryptic digest of a mixture of the

model glycoproteins bovine thyroglobulin and human transferrin, where the number of identified glycopeptides increased substantially from four to twelve before and after SEC enrichment. Similarly, when the method was applied in the analysis of glycopeptides from human serum, they were able to identify low-abundance glycoproteins that were not observed in the absence of the SEC enrichment method. Although the authors presented some compelling results, the method has not been substantially investigated since its introduction. A survey of the literature results in just one study that referenced the work of Alvarez-Manzanilla and co-workers.[75] The investigation conducted by Jia *et al.*[75] involved an ultrafiltration method based on molecular weight cut-off technology. The tryptic peptide digests were introduced in a Microcon YM-3 centrifugal filter device with a nominal molecular weight cut-off of 3000 Da. The supposition is that core-fucosylated *N*-glycopeptides are preferentially-enriched, thereby composing the retentate, based on the larger molecular masses of *N*-glycopeptides. When a mixture of four glycoproteins was subjected to the enrichment method followed by mass spectrometric techniques, only seven out of the expected eight glycopeptides were identified in the retentate, one glycopeptide more than an un-enriched sample. The filtrate (i.e. it should contain low molecular weight peptides) unsurprisingly contained glycopeptides, albeit at decreased peak intensity in the mass spectrum than without enrichment. The studies conducted by these two research groups clearly provide evidence of enrichment of glycopeptides that enabled detection of even low-abundance glycoproteins. However, it was also illustrated that losses of glycopeptides are apparent, most likely the small fragment ones.

1.3.5 Enrichment by Boronic Acids

The characteristic of phenylboronic acids to form reversible complexes with diol-containing materials, such as sugars, has led to numerous developments for eventual application

in areas such as sensor technology,[76-81] drug delivery,[82] and affinity chromatography.[83-84] Current knowledge on the mechanism of the diol-boronic acid interaction is based on the equilibrium formation of a heterocylic diester from 1,2- or 1,3-diol groups and a tetrahedral boronate ion (Scheme 1.1);[15] this equilibrium is a function of the ionization constant K_a of the boronic acid moiety. Thus, the coordination of diol species is commonly performed at a pH that results in conversion of the trigonal planar boronic acid species into the tetrahedral boronate ion. Although it is generally accepted that the boronate ion is the active binding species, Ishihara and co-workers[85] are of the opinion that the neutral planar boronic acid has comparable or even

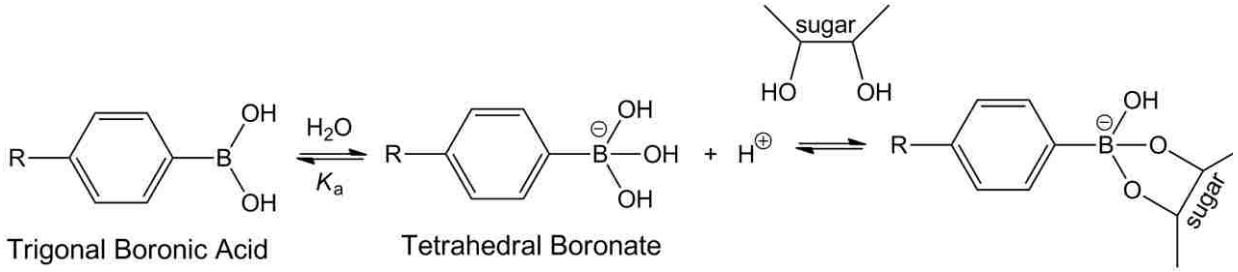

Scheme 1.1 Boronic acid equilibrium

higher reactivity toward diols than the boronate ion, regardless of solution pH. Because boronic acids recognize diol groups, they are expected to discrimate diol-containing materials from non-diol-containing ones; thus it has a more general specificity. Apart from the primary diol-boronate interaction, secondary interactions such as electrostatic, hydrophobic, hydrogen bonding, and coordination are known to participate in the recognition mechanism.[84] A variety of boronic acid-containing materials can be found both in the literature or obtained from commercial sources. Several suppliers provide them as 3-aminophenylboronic acid immobilized on polyacrylamide spherical gel beads (the Affi-gel from Biorad and the immobilized boronic acid gel from Pierce), on agarose beads (from Sigma or the Aminophenyl Boronate A6XL from

ProMetic Biosciences), on acrylic beads (from Sigma), on poly(methacrylate) beads (the TSKgel Boronate-5PW from Tosoh Bioscience), or as poly(methyl methacrylate)-bound boronic acid (the boric acid gel from Aldrich). Non-commercial preparations with 3-aminophenylboronic acid as recognition and/or enrichment element are found on silica beads,[13,86] silica capillaries,[87] magnetic particles,[88-90] polymer beads,[91-92] glassy carbon electrodes,[93] gold electrodes,[94] and gold[76-77,81,95] and glass surfaces.[96]

Xu *et al.*[13] prepared a novel boronic acid-modified mesoporous silica (bead-like) which features high surface area and large accessible three-dimensional porosity. The ordered mesoporous silica decorated with a large surface density of silanol groups was efficiently utilized to attach 3-aminophenylboronic acid–derivatized 3-glycidyloxypropyltrimethoxysilane via a condensation reaction. The merits of this novel material included a much shorter loading time (i.e. time to reach complete saturation) in the order of a few minutes, 15 min to be exact, compared to conventional methods, a consequence of increased mass transfer. The enrichment of glycopeptides on this material can be conveniently implemented by non-trained personnel because its bead-like nature allows for easy separation of the glycopeptide-enriched material from the mixture by centrifugation. The high specificity for glycopeptide binding was demonstrated by the absence of glycosylated peptides from a mixture of model glycoproteins in the supernatant. In addition, the presence of non-glycosylated peptides from BSA did not affect the specificity of the material for horseradish peroxidase, albeit the recovery was slightly compromised. More importantly, the limit of detection of glycopeptides was improved by two orders of magnitude.

A recent improvement in the utility of boronic acid is its integration into MALDI plates for direct determination of glycoproteins by MS. Xu *et al.*[97] and Lee *et al.*[89] both demonstrated

direct identification of glycopeptides/glycoproteins by MALDI-MS while enriched on the boronic acid–gold-coated Si wafer and magnetic beads, respectively. No elution was required, and sample handling was minimal, thereby resulting in reduced losses of enriched glycopeptides and glycoproteins. When Sparbier *et al.*[90] compared the enrichment capability of four magnetic beads each modified with the lectins Con A, *Lens culinaris* agglutinin, WGA, and boronic acid, the largest number of unique glycoproteins were identified from the boronic acid beads, a likely outcome because boronic acids are less restrictive in terms of their specificity.

1.4 Microfluidic Device-based Analysis of Glycoproteins and Glycopeptides

The whole idea of downscaling or miniaturization of analytical processes is to impart improvement in the analytical performance.[98] Consequently, a quadratic decrease in equilibration time, which reduces the time-scale of the process, is realized. More importantly, better separation is achieved because the separation efficiency per unit time (i.e. number of theoretical plates per unit time) is inversely related to the square of the capillary diameter.[99] Recently, microscale and microchip devices are employed for glycoprotein/glycopeptide analysis. Because of their inherent heterogeneity and the complexity of the biological fluid in which they are found, their analysis is challenging. In addition, the demand for high-throughput analysis is growing because of the immense potential of glycoproteins as biomarkers. Therefore, glycoprotein analysis will greatly benefit from the features offered by microscale and miniaturized methods.

1.4.1 Literature Review of Microscale and Nanoscale Methods for Analysis of Glycoproteins and Glycopeptides

A lectin microcolumn (5-cm long × 500 μm or 1 mm i.d.) packed with either Con A- or *Sambucus nigra*-derivatized silica was prepared by Madera *et al.*[100] and integrated into a high

performance affinity chromatography/MS system. Using model glycoproteins, a shorter analysis time was achieved using the silica-based column compared to a sepharose-based material under identical conditions. The Con A microcolumn was observed to be selective toward RNAse B, as addition of BSA to the mixture prior the analysis did not diminish the capacity of the microcolumn to bind RNAse B. In addition, efficient capture of RNAse B and and its subsequent elution was also observed. The presence of other peptides normally suppresses the ionization of weakly-ionized glycopeptides; hence, a pre-enrichment is often required prior to MS analysis. By using the on-line lectin microcolumn prior to MS, peak intensities of low-abundance *N*-glycopeptides from bovine fetuin were found to be ~20-fold higher than in the absence of the on-line lectin preconcentration.

Monoliths, particularly polymer monoliths, are gaining increasing attention as matrices for separation systems, because they can provide fast mass transfer, high loading capacity, high flow rates, and an *in situ* preparation with controllable surface properties. These are features from which micro- or nanoscale separations can greatly benefit. In fact, a number of literature reports use monoliths in microscale formats as an on-line or off-line preconcentration platform[101-102] and also as nanoelectrospray emitters.[103] Feng and co-workers[101] fabricated a nanoscale Con A chelating monolithic capillary (10 cm × 200 μm i.d.) by immobilizing Con A on an iminodiacetic acid-derivatized poly(glycidyl methacrylate-*co*-ethylene dimethacrylate) or [poly(GMA-co-EDMA)] through chelation by Cu^{2+}. One attractive feature of this format is that elution of bound glycoproteins can result with either the conventional sugar-based elution buffer or an ammoniated water eluent wherein Con A co-elutes with the glycoprotein; the latter allows for direct analysis of eluate by MS. Comparison of the number of identified *N*-glycoproteins from urine samples of normal or bladder cancer patients, with either the nanoscale Con A

chelating lectin affinity or conventional Con A lectin affinity chromatography columns, revealed that there is at least three-fold more glycoproteins identified with the former using the same initial sample loading of 10 μg. In addition, the reproducibility (i.e. percentage of commonly identified proteins of replicate samples) is higher for the monolithic format (61%) compared to that for the conventional format (25%), for urine samples from bladder cancer patients.

These preconcentration monolithic columns can be further utilized as nanoelectrospray emitters for MS analysis. Bedair and Oleschuk[103] fabricated a monolithic [poly(GMA-*co*-EDMA)] capillary column (10 cm × 75 μm i.d.) with immobilized Con A and initially used the column for off-line preconcentration of 20-μL tryptic digests from RNAse B. Subsequently, the column was mounted to a mass spectrometer, and the tryptic glycopeptides were then eluted and directly infused into the nano-electrospray mass spectrometer. The resulting enrichment of glycopeptides allowed the detection of the five glycoforms of RNAse B, as opposed to an inability to detect the glycopeptides using a direct infusion of the tryptic digest without preconcentration. These results provide evidence for the value of integrating microfluidic devices to nano-ESI MS, which will most likely revolutionize glycoproteomic studies.

Potter *et al.*[102] demonstrated that boronate affinity monoliths allow separation of ribonucleosides from 2-deoxyribonucleosides using a micro-liquid chromatography separation. The capillary column (33 cm × 100 μm i.d.) was initially modified with a poly(glycidyl methacrylate-*co*-ethyleneglycol dimethacrylate) or [poly(GMA-*co*-EDMA)]. *p*-hydroxyphenyl-boronic acid was then subsequently attached to the oxirane rings of the polymer to yield an 8-cm modified surface. However, the analytical merits of the micro-liquid chromatography method in their study were not addressed. Nevertheless, the authors hope to integrate their boronic acid

micro-affinity system into microfluidic devices to create a micro-total analytical system (μTAS) for glycoconjugates.

1.4.2 Microanalytical Devices

Any advancement in glycoanalysis would aid in clinical diagnostics and therapeutics where applications can be realized toward point-of-care testing that is becoming increasingly important for the early and cost-effective detection of cancers and diseases. An area that is helping advance efforts to achieve these goals is that focused on biomicroelectromechanical sytems (bioMEMS)—or micrototal analysis systems (μTAS), lab-on-a-chip, or microanalytical devices—a rapidly growing field introduced about 18 years ago through the pioneering work of Harrison and Manz.[104-106] In general, these miniaturized devices are designed as integrated systems that address sample preparation and pretreatment, and analyte separation, detection, and analysis; thus, they are touted as being capable of performing complex analyses in a single device, thereby drastically reducing processing times (i.e. from sample preparation to data analysis) and human-associated errors. The active elements are typically microns in size, and the device is no more than several inches in dimension. These systems hold the promise of minimal sample and reagent consumption, fast analysis time, portable format, component integration and automation, multiplexing, and economically-sound devices. These are precisely the advantages that are required if glycoprotein analysis is to advance at a level where physiological fluids can be easily processed. To date, applications of μTAS are widespread which includes drug delivery, protein and DNA separation and analysis, immunoassays, pharmaceutical analysis, forensics, and environmental monitoring.[105,107-108]

Plastics or polymers, such as poly(methyl methacrylate) (PMMA), poly(dimethyl siloxane) (PDMS), polystyrene (PS), and polycarbonate (PC), are established substrates for the

fabrication of microanalytical devices, and they offer several advantages over their silica, glass or quartz counterparts that have led to their gain in popularity.[99,109-113] A few of the notable advantages that can be translated into superior qualities and capabilities for microanalytical devices include the capability to produce both typical-dimension and high-aspect-ratio microstructures (HARMS) from relatively inexpensive materials, the use of a variety of micromachining methods that are relatively easy to implement using polymers as the fabrication substrate because of their low glass transition temperatures (T_g) and physical/optical properties.[105,113-114]

Perhaps one of the initially-encountered major disadvantages of polymeric substrates during the early days of their use as substrates for fabricating microanalysis devices—that made them somewhat inferior to glass—was the lack of established surface chemical modification routes for tailoring the properties of the polymer devices. Unlike glass for which silane-based derivatization methods were well-established, many polymeric substrates lacked (and some still do lack) the functional handle to accommodate various ligands on their surfaces that are suitable for a variety of applications.

However, polymeric substrates have seen a boost in the area of chemical modification over the years. For PMMA in particular, carboxylic acids were introduced by UV irradiation[111] and oxygen plasma treatment.[110] Amine-terminated surfaces were prepared by aminolysis reactions.[112,115] PMMA sheets with integrated and exposed glycidyl methacrylate groups (PGMAMMA) were prepared by thermally-induced, free-radical polymerization, and further elaboration of the reactive glycidyl groups was performed via amination.[116]

Since the introduction of atom transfer radical polymerization (ATRP) by the independent investigations of Matyjaszewski[117] and Sawamoto,[118] the field of microfluidics has

seen great benefits from it. ATRP is a controlled free-radical polymerization that is catalyzed by transition metal complexes. Matyjaszewski and co-worker's ATRP protocol involved Cu as the catalyst; the protocol that is in widespread implementation nowadays. In fact as of 2008, he has published over 500 papers on the topic of ATRP with those works being cited over 30,000 times, making him one of the most-highly cited researchers in the field of chemistry. The popularity of ATRP versus conventional free-radical polymerization is mainly associated with the uniform polymer chain length (i.e. narrow molecular weight distribution) obtained in high yield (i.e. high grafting density) as a consequence of the equilibrium between dormant and actively propagating species. The implementation is simple and can tolerate a wide variety of monomers, and polymerization is fast (i.e. minutes) and can be performed at room temperature and in aqueous media. More importantly, polymerization can be made to be surface confined, thus eliminating non-specific adsorptions of solution-formed polymers just as in AIBN-based free radical polymerization; this greatly reduces the steps in modifying the surfaces.

Wirth and co-workers[119] passivated the surface of a PDMS channel with poly(acrylamide) through surface-initiated ATRP (SI–ATRP). The high grafting density of polyacrylamide allowed the baseline electrophoretic separation of a mixture of lysozyme and cytochrome C in under 35 sec due to the elimination of reversible and irreversible hydrophobic interactions of the proteins toward the surface. Lee *et al.*[110] ATRP-grafted poly(ethylene glycol) (PEG) on PMMA channel which resulted in substantial reduction of electroosmotic flow and non-specific adsorptions. Later on, they fabricated a microfluidic device from poly(glycidyl methacrylate-*co*-methyl acrylate) sheet[116] to which poly(ethylene glycol) was grafted by SI–ATRP.[116,120] These works demonstrate the applicability of ATRP in the modification of polymeric microfluidic substrates.

1.4.3 Literature Review on Microfluidic Device-based Analysis of Glycoproteins and Glycopeptides

Mao *et al.*[121] are perhaps the very first individuals who invoked microdevice-based separation of glycopeptides. Using a commercially available Micralyne standard simple glass cross device with a 1.0-cm injection channel and 8.5-cm separation channel with a dimension of 50 μm × 20 μm, the separation of the tryptic digests of chicken ovalbumin and turkey ovalbumin were accomplished by microdevice zone electrophoresis in 10 min. Importantly, the peak capacity obtained in the microdevice electrophoresis format was similar to that from capillary electrochromatography and HPLC.

The same group[122] fabricated a miniaturized format of lectin affinity chromatography that integrated a lectin affinity monolith column into a microchannel (70 μm × 20 μm) of a glass microfluidic device. Along with the chromatography channel, the microfluidic device contained the running buffer, eluent buffer, sample, sample waste, washing, and waste reservoirs. The monolith (500 μm of the channel length) was prepared *in situ* in the microchannel by UV polymerization of glycidyl methacrylate and ethylene dimethacrylate, to which the lectin *Pisum sativum* agglutinin was immobilized via reaction between the epoxy groups in the monolith and the ε-amino groups in the lectin. By electrokinetic driving force, glycoforms from chicken ovalbumin, chicken ovomucoid, and turkey ovalbumin were separated into several fractions (e.g. non-bound, weakly-bound, and strongly-bound) which reflected the affinity specificity of the glycoforms toward *Pisum sativum* agglutinin. Other notable merits of this lectin affinity microfluidic device include significant reduction in analysis time compared to conventional lectin affinity chromatography (i.e. 400 s compared to 4 h), small sample volume (~98 pL that translates into < 300 pg glycoprotein injected), and resistance to non-specific adsorption as

demonstrated by the absence of human serum albumin binding. They later fabricated a microfluidic device with a nanoelectrospray interface for glycopeptide separation by microfluidic device/MS system.[123] The analysis of the tryptic glycoforms from RNAse B was performed on a 3-aminopropyltriethoxysilane–derivatized glass microchannel followed by subsequent identification of the eluted compounds with quadrupole ion trap mass spectrometer. A review on microdevice hyphenation to MS for glycoproteomic investigation is provided by Bindila and Peter-Katilinic.[124]

The work of Bynum *et al*.[125] is also worthy of attention even though its main focus is the purification and separation of released *N*-glycans from glycosylated recombinant monoclonal antibodies. A three-layer integrated microfluidic liquid chromatography-mass spectrometry (LC-MS) device was fabricated by utilizing three devices that were fixed on an Agilent HPLC-chip cube MS. The workflow on this microfluidic device involves glycan cleavage on the first device (top) that is packed with PNGase F-immobilized silica beads, followed by capture of deglycosylated proteins on the second device (middle) that is packed with reversed-phase C8 beads, and finally enrichment and separation of *N*-glycans on the third device (bottom) with a column packed with porous graphitized carbon. The eluted *N*-glycans were directly sprayed through the nanoelectrospray tip into the time-of-flight mass spectrometer. The performance of this automated and integrated system was demonstrated with Chinese hamster ovary cell-derived monoclonal antibody A1 and Ab2 and mouse NS0 cell-derived Ab3, wherein the analysis was completed in only 10 min, as opposed to hours to days using the traditional methodologies. In addition, due to the fast deglycosylation step (~3 s), β-glycosylamines (that immediately undergo conversion to the free-reducing end forms) were measurable. Another feature of this integrated device is the ability to rapidly analyze intact and deglycosylated antibodies by changing the

device configuration (e.g. removal of the third, bottom, device). These outcomes demonstrate how glycoprotein analysis benefits from integration into microfluidic devices.

1.5 References

(1) Peracaula, R.; Tabarés, G.; Royle, L.; Harvey, D. J.; Dwek, R. A.; Rudd, P. M.; de Llorens, R. Altered glycosylation pattern allows the distinction between prostate-specific antigen (PSA) from normal and tumor origins. *Glycobiology* **2003**, *13*, 457-470.

(2) Tabarés, G.; Radcliffe, C. M.; Barrabés, S.; Ramírez, M.; Aleixandre, R. N.; Hoesel, W.; Dwek, R. A.; Rudd, P. M.; Peracaula, R.; de Llorens, R. Different glycan structures in prostate-specific antigen from prostate cancer sera in relation to seminal plasma PSA. *Glycobiology* **2006**, *16*, 132-145.

(3) Dwek, M. V.; Ross, H. A.; Leathem, A. J. C. Proteome and glycosylation mapping identifies post-translational modifications associated with aggressive breast cancer. *Proteomics* **2001**, *1*, 756-762.

(4) Saldova, R.; Royle, L.; Radcliffe, C. M.; Abd Hamid, U. M.; Evans, R.; Arnold, J. N.; Banks, R. E.; Hutson, R.; Harvey, D. J.; Antrobus, R.; Petrescu, S. M.; Dwek, R. A.; Rudd, P. M. Ovarian cancer is associated with changes in glycosylation in both acute-phase proteins and IgG. *Glycobiology* **2007**, *17*, 1344-1356.

(5) Tian, Y.; Zhang, H. Glycoproteomics and clinical applications. *Proteomics: Clin. Appl.* **2010**, *4*, 124-132.

(6) Cummings, R. D.; Kornfeld, S. Fractionation of asparagine-linked oligosaccharides by serial lectin-agarose affinity-chromatography - a rapid, sensitive, and specific technique. *J. Biol. Chem.* **1982**, *257*, 1235-1240.

(7) Qiu, R.; Regnier, F. E. Comparative glycoproteomics of *N*-linked complex-type glycoforms containing sialic acid in human serum. *Anal. Chem.* **2005**, *77*, 7225-7231.

(8) Endo, T. Fractionation of glycoprotein-derived oligosaccharides by affinity chromatography using immobilized lectin columns. *J. Chromatogr. A* **1996**, *720*, 251-261.

(9) Schwientek, T.; Mandel, U.; Roth, U.; Müller, S.; Hanisch, F.-G. A serial lectin approach to the mucin-type *O*-glycoproteome of *Drosophila melanogaster* S2 cells. *Proteomics* **2007**, *7*, 3264-3277.

(10) Sumi, S.; Arai, K.; Kitahara, S.; Yoshida, K.-I. Serial lectin affinity chromatography demonstrates altered asparagine-linked sugar-chain structures of prostate-specific antigen in human prostate carcinoma. *J. Chromatogr. B* **1999**, *727*, 9-14.

(11) Yang, Z. P.; Hancock, W. S. Approach to the comprehensive analysis of glycoproteins isolated from human serum using a multi-lectin affinity column. *J. Chromatogr. A* **2004**, *1053*, 79-88.

(12) Whelan, S. A.; Lu, M.; He, J.; Yan, W.; Saxton, R. E.; Faull, K. F.; Whitelegge, J. P.; Chang, H. R. Mass spectrometry (LC/MS-MS) site-mapping of *N*-glycosylated membrane proteins for breast cancer biomarkers. *J. Proteome Res.* **2009**, *8*, 4151-4160.

(13) Xu, Y.; Wu, Z.; Zhang, L.; Lu, H.; Yang, P.; Webley, P. A.; Zhao, D. Highly specific enrichment of glycopeptides using boronic acid-functionalized mesoporous silica. *Anal. Chem.* **2009**, *81*, 503-508.

(14) Björhall, K.; Miliotis, T.; Davidsson, P. Comparison of different depletion strategies for improved resolution in proteomic analysis of human serum samples. *Proteomics* **2005**, *5*, 307-317.

(15) Lorand, J. P.; Edwards, J. O. Polyol complexes and structure of the benzeneboronate ion. *J. Org. Chem.* **1959**, *24*, 769-774.

(16) Yamanaka, H.; Yoshizako, K.; Akiyama, Y.; Sota, H.; Hasegawa, Y.; Shinohara, Y.; Kikuchi, A.; Okano, T. Affinity chromatography with collapsibly tethered ligands. *Anal. Chem.* **2003**, *75*, 1658-1663.

(17) Schachter, H.; Roseman, S. Mammalian glycosyltransferases: Their role in the synthesis and function of complex carbohydrates and glycolipids. In *The biochemistry of glycoproteins and proteoglycans*; Lennarz, W. J., Ed.; Plenum Press: New York, 1980, p 85-160.

(18) Axford, J. Glycobiology and medicine: An introduction. *J. R. Soc. Med.* **1997**, *90*, 260-264.

(19) Struck, D. K.; Lennarz, W. J. The function of saccharide-lipids in synthesis of glycoproteins. In *The biochemistry of glycoproteins and proteoglycans*; Lennarz, W. J., Ed.; Plenum Press: New York, 1980, p 35-84.

(20) Julenius, K.; Mølgaard, A.; Gupta, R.; Brunak, S. Prediction, conservation analysis, and structural characterization of mammalian mucin-type *O*-glycosylation sites. *Glycobiology* **2005**, *15*, 153-164.

(21) Brooks, S. A. Strategies for analysis of the glycosylation of proteins: Current status and future perspectives. *Mol. Biotechnol.* **2009**, *43*, 76-88.

(22) Apweiler, R.; Hermjakob, H.; Sharon, N. On the frequency of protein glycosylation, as deduced from analysis of the Swiss-Prot database. *Biochim. Biophys. Acta, Gen. Subj.* **1999**, *1473*, 4-8.

(23) Plummer, T. H., Jr.; Hirs, C. H. W. The isolation of ribonuclease B, a glycoprotein, from bovine pancreatic juice. *J. Biol. Chem.* **1963**, *238*, 1396-1401.

(24) Fu, D. T.; Chen, L.; Oneill, R. A. A detailed structural characterization of ribonuclease B oligosaccharides by H-NMR spectroscopy and mass-spectrometry. *Carbohydr. Res.* **1994**, *261*, 173-186.

(25) Seligman, P. A.; Schleicher, R. B.; Allen, R. H. Isolation and characterization of the transferrin receptor from human-placenta. *J. Biol. Chem.* **1979**, *254*, 9943-9946.

(26) Satomi, Y.; Shimonishi, Y.; Hase, T.; Takao, T. Site-specific carbohydrate profiling of human transferrin by nano-flow liquid chromatography/electrospray ionization mass spectrometry. *Rapid Commun. Mass Spectrom.* **2004**, *18*, 2983-2988.

(27) Irimura, T.; Nicolson, G. L. Carbohydrate-chain analysis by lectin binding to mixtures of glycoproteins, separated by polyacrylamide slab-gel electrophoresis, with *in situ* chemical modifications. *Carbohydr. Res.* **1983**, *115*, 209-220.

(28) Neuberger, A. Carbohydrates in proteins i. The carbohydrate component of crystalline egg albumin. *Biochem. J* **1938**, *32*, 1435-1451.

(29) Harvey, D. J.; Wing, D. R.; Küster, B.; Wilson, I. B. H. Composition of *N*-linked carbohydrates from ovalbumin and co-purified glycoproteins. *J. Am. Soc. Mass. Spectrom.* **2000**, *11*, 564-571.

(30) Dekker, J.; Rossen, J. W. A.; Büller, H. A.; Einerhand, A. W. C. The MUC family: An obituary. *Trends Biochem. Sci* **2002**, *27*, 126-131.

(31) Muramatsu, T. Carbohydrate signals in metastasis and prognosis of human carcinomas. *Glycobiology* **1993**, *3*, 291-296.

(32) Kufe, D. W. Mucins in cancer: Function, prognosis and therapy. *Nat. Rev. Cancer* **2009**, *9*, 874-885.

(33) Kornfeld, R.; Kornfeld, S. Structure of glycoprotein oligosaccharides. In *The biochemistry of glycoproteins and proteoglycans*; Lennarz, W. J., Ed.; Plenum Press: New York, 1980, p 1-34.

(34) Hanisch, F.-G. *O*-glycosylation of the mucin type. *Biol. Chem.* **2005**, *382*, 143-149.

(35) Spiro, R. G.; Bhoyroo, V. D. Structure of the *O*-glycosidically linked carbohydrate units of fetuin. *J. Biol. Chem.* **1974**, *249*, 5704-5717.

(36) Wang, Z.; Hart, G. Glycomic approaches to study GlcNacylation: Protein identification, site-mapping, and site-specific *O*-GlcNAc quantitation. *Clin. Proteomics* **2008**, *4*, 5-13.

(37) Varki, A. Biological roles of oligosaccharides: All of the theories are correct. *Glycobiology* **1993**, *3*, 97-130.

(38) Drake, R. R.; Schwegler, E. E.; Malik, G.; Diaz, J.; Block, T.; Mehta, A.; Semmes, O. J. Lectin capture strategies combined with mass spectrometry for the discovery of serum glycoprotein biomarkers. *Mol. Cell Proteomics* **2006**, *5*, 1957-1967.

(39) Ohtsubo, K.; Marth, J. D. Glycosylation in cellular mechanisms of health and disease. *Cell* **2006**, *126*, 855-867.

(40) Hakomori, S.-i. Tumor malignancy defined by aberrant glycosylation and sphingo(glyco)lipid metabolism. *Cancer Res.* **1996**, *56*, 5309-5318.

(41) Orntoft, T. F.; Vestergaard, E. M. Clinical aspects of altered glycosylation of glycoproteins in cancer. *Electrophoresis* **1999**, *20*, 362-371.

(42) Handerson, T.; Camp, R.; Harigopal, M.; Rimm, D.; Pawelek, J. β1,6-branched oligosaccharides are increased in lymph node metastases and predict poor outcome in breast carcinoma. *Clin. Cancer Res.* **2005**, *11*, 2969-2973.

(43) Comunale, M. A.; Lowman, M.; Long, R. E.; Krakover, J.; Philip, R.; Seeholzer, S.; Evans, A. A.; Hann, H.-W. L.; Block, T. M.; Mehta, A. S. Proteomic analysis of serum associated fucosylated glycoproteins in the development of primary hepatocellular carcinoma. *J. Proteome Res.* **2006**, *5*, 308-315.

(44) Youings, A.; Chang, S. C.; Dwek, R. A.; Scragg, I. G. Site-specific glycosylation of human immunoglobulin G is altered in four rheumatoid arthritis patients. *Biochem. J* **1996**, *314*, 621-630.

(45) Li, Y.; Luo, L.; Rasool, N.; Kang, C. Y. Glycosylation is necessary for the correct folding of human immunodeficiency virus gp120 in CD4 binding. *J. Virol.* **1993**, *67*, 584-588.

(46) Madera, M.; Mechref, Y.; Klouckova, I.; Novotny, M. V. High-sensitivity profiling of glycoproteins from human blood serum through multiple-lectin affinity chromatography and liquid chromatography/tandem mass spectrometry. *J. Chromatogr. B* **2007**, *845*, 121-137.

(47) Anderson, N. L.; Anderson, N. G. The human plasma proteome. *Mol. Cell Proteomics* **2002**, *1*, 845-867.

(48) Stillmark, H. Ricin, a toxic enzyme from seeds of *Ricinus communis* and other *euphorbiaceae*. Ph.D. Thesis, Medical School of Dorpat, 1888.

(49) Sharon, N.; Lis, H. *Lectins*; 2nd ed.; Springer: Dordrecht, The Netherlands, 2007.

(50) Van Damme, E. J. M.; Peumans, W. J.; Pusztai, A.; Bardocz, S. *Handbook of plant lectins: Properties and biomedical applications*; John Wiley & Sons: Chichester, 1998.

(51) Ghosh, D.; Krokhin, O.; Antonovici, M.; Ens, W.; Standing, K. G.; Beavis, R. C.; Wilkins, J. A. Lectin affinity as an approach to the proteomic analysis of membrane glycoproteins. *J. Proteome Res.* **2004**, *3*, 841-850.

(52) Bedair, M.; El Rassi, Z. Affinity chromatography with monolithic capillary columns - II. Polymethacrylate monoliths with immobilized lectins for the separation of glycoconjugates by nano-liquid affinity chromatography. *J. Chromatogr. A* **2005**, *1079*, 236-245.

(53) Nawarak, J.; Phutrakul, S.; Chen, S.-T. Analysis of lectin-bound glycoproteins in snake venom from the *elapidae* and *viperidae* families. *J. Proteome Res.* **2004**, *3*, 383-392.

(54) Plavina, T.; Wakshull, E.; Hancock, W. S.; Hincapie, M. Combination of abundant protein depletion and multi-lectin affinity chromatography (M-LAC) for plasma protein biomarker discovery. *J. Proteome Res.* **2006**, *6*, 662-671.

(55) Qiu, R.; Regnier, F. E. Use of multidimensional lectin affinity chromatography in differential glycoproteomics. *Anal. Chem.* **2005**, *77*, 2802-2809.

(56) Mechref, Y.; Madera, M.; Novotny, M. V. Glycoprotein enrichment through lectin affinity techniques. *Methods Mol. Biol.* **2008**, *424*, 373-396.

(57) Monzo, A.; Bonn, G. K.; Guttman, A. Lectin-immobilization strategies for affinity purification and separation of glycoconjugates. *Trends Anal. Chem.* **2007**, *26*, 423-432.

(58) Inoue, T.; Yamauchi, M.; Ohkawa, K. Structural studies on sugar chains of carbohydrate-deficient transferrin from patients with alcoholic liver disease using lectin affinity electrophoresis. *Electrophoresis* **1999**, *20*, 452-457.

(59) Heegaard, N. H. H. Affinity in electrophoresis. *Electrophoresis* **2009**, *30*, S229-S239.

(60) Zhang, H.; Li, X.-J.; Martin, D. B.; Aebersold, R. Identification and quantification of *N*-linked glycoproteins using hydrazide chemistry, stable isotope labeling and mass spectrometry. *Nat. Biotechnol.* **2003**, *21*, 660-666.

(61) Zhang, H.; Yi, E. C.; Li, X.-j.; Mallick, P.; Kelly-Spratt, K. S.; Masselon, C. D.; Camp, D. G.; Smith, R. D.; Kemp, C. J.; Aebersold, R. High throughput quantitative analysis of serum proteins using glycopeptide capture and liquid chromatography mass spectrometry. *Mol. Cell Proteomics* **2005**, *4*, 144-155.

(62) Tian, Y.; Zhou, Y.; Elliott, S.; Aebersold, R.; Zhang, H. Solid-phase extraction of *N*-linked glycopeptides. *Nat. Protoc.* **2007**, *2*, 334-339.

(63) Sun, B.; Ranish, J. A.; Utleg, A. G.; White, J. T.; Yan, X.; Lin, B.; Hood, L. Shotgun glycopeptide capture approach coupled with mass spectrometry for comprehensive glycoproteomics. *Mol. Cell Proteomics* **2007**, *6*, 141-149.

(64) Chen, R.; Jiang, X.; Sun, D.; Han, G.; Wang, F.; Ye, M.; Wang, L.; Zou, H. Glycoproteomics analysis of human liver tissue by combination of multiple enzyme digestion and hydrazide chemistry. *J. Proteome Res.* **2009**, *8*, 651-661.

(65) Schenk, B.; Imbach, T.; Frank, C.; Grubenmann, C.; Helenius, J.; Jaeken, J.; Matthijs, G.; Hennet, T.; Aebi, M. Congenital disorders of glycosylation: Deficiencies in the ER pathway. *Glycobiology* **2001**, *11*, 863-863.

(66) Aebi, M.; Hennet, T. Congenital disorders of glycosylation: Genetic model systems lead the way. *Trends Cell Biol.* **2001**, *11*, 136-141.

(67) Hemstrom, P.; Irgum, K. Hydrophilic interaction chromatography. *J. Sep. Sci.* **2006**, *29*, 1784-1821.

(68) Ikegami, T.; Tomomatsu, K.; Takubo, H.; Horie, K.; Tanaka, N. Separation efficiencies in hydrophilic interaction chromatography. *J. Chromatogr. A* **2008**, *1184*, 474-503.

(69) Hägglund, P.; Bunkenborg, J.; Elortza, F.; Jensen, O. N.; Roepstorff, P. A new strategy for identification of *N*-glycosylated proteins and unambiguous assignment of their glycosylation sites using HILIC enrichment and partial deglycosylation. *J. Proteome Res.* **2004**, *3*, 556-566.

(70) Picariello, G.; Ferranti, P.; Mamone, G.; Roepstorff, P.; Addeo, F. Identification of *N*-linked glycoproteins in human milk by hydrophilic interaction liquid chromatography and mass spectrometry. *Proteomics* **2008**, *8*, 3833-3847.

(71) Takegawa, Y.; Deguchi, K.; Ito, H.; Keira, T.; Nakagawa, H.; Nishimura, S. I. Simple separation of isomeric sialylated *N*-glycopeptides by a zwitterionic type of hydrophilic interaction chromatography. *J. Sep. Sci.* **2006**, *29*, 2533-2540.

(72) Wuhrer, M.; Koeleman, C. A. M.; Hokke, C. H.; Deelder, A. M. Protein glycosylation analyzed by normal-phase nano-liquid chromatography-mass spectrometry of glycopeptides. *Anal. Chem.* **2005**, *77*, 886-894.

(73) Cao, J.; Shen, C.; Wang, H.; Shen, H.; Chen, Y.; Nie, A.; Yan, G.; Lu, H.; Liu, Y.; Yang, P. Identification of *N*-glycosylation sites on secreted proteins of human hepatocellular carcinoma cells with a complementary proteomics approach. *J. Proteome Res.* **2009**, *8*, 662-672.

(74) Alvarez-Manilla, G.; Atwood; Guo, Y.; Warren, N. L.; Orlando, R.; Pierce, M. Tools for glycoproteomic analysis: Size exclusion chromatography facilitates identification of

tryptic glycopeptides with *N*-linked glycosylation sites. *J. Proteome Res.* **2006**, *5*, 701-708.

(75) Jia, W.; Lu, Z.; Fu, Y.; Wang, H. P.; Wang, L. H.; Chi, H.; Yuan, Z. F.; Zheng, Z. B.; Song, L. N.; Han, H. H.; Liang, Y. M.; Wang, J. L.; Cai, Y.; Zhang, Y. K.; Deng, Y. L.; Ying, W. T.; He, S. M.; Qian, X. H. A strategy for precise and large scale identification of core fucosylated glycoproteins. *Mol. Cell Proteomics* **2009**, *8*, 913-923.

(76) Kitano, H.; Anraku, Y.; Shinohara, H. Sensing capabilities of colloidal gold monolayer modified with a phenylboronic acid-carrying polymer brush. *Biomacromolecules* **2006**, *7*, 1065-1071.

(77) Anraku, Y.; Takahashi, Y.; Kitano, H.; Hakari, M. Recognition of sugars on surface-bound cap-shaped gold particles modified with a polymer brush. *Colloids Surf., B* **2007**, *57*, 61-68.

(78) Soh, N.; Sonezaki, M.; Imato, T. Modification of a thin gold film with boronic acid membrane and its application to a saccharide sensor based on surface plasmon resonance. *Electroanalysis* **2003**, *15*, 1281-1290.

(79) Liu, J. T.; Chen, L. Y.; Shih, M. C.; Chang, Y.; Chen, W. Y. The investigation of recognition interaction between phenylboronate monolayer and glycated hemoglobin using surface plasmon resonance. *Anal. Biochem.* **2008**, *375*, 90-96.

(80) Gabai, R.; Sallacan, N.; Chegel, V.; Bourenko, T.; Katz, E.; Willner, I. Characterization of the swelling of acrylamidophenylboronic acid-acrylamide hydrogels upon interaction with glucose by faradaic impedance spectroscopy, chronopotentiometry, quartz-crystal microbalance (QCM), and surface plasmon resonance (SPR) experiments. *J. Phys. Chem. B* **2001**, *105*, 8196-8202.

(81) Chen, H. X.; Lee, M.; Lee, J.; Kim, J. H.; Gal, Y. S.; Hwang, Y. H.; An, W. G.; Koh, K. Formation and characterization of self-assembled phenylboronic acid derivative monolayers toward developing monosaccharide sensing-interface. *Sensors* **2007**, *7*, 1480-1495.

(82) Matsumoto, A.; Ikeda, S.; Harada, A.; Kataoka, K. Glucose-responsive polymer bearing a novel phenylborate derivative as a glucose-sensing moiety operating at physiological pH conditions. *Biomacromolecules* **2003**, *4*, 1410-1416.

(83) Singhal, R. P.; Desilva, S. S. M. Boronate affinity-chromatography. *Adv. Chromatogr.* **1992**, *31*, 293-335.

(84) Liu, X.-C. Boronic acids as ligands for affinity chromatography. *Chin. J. Chromatogr.* **2006**, *24*, 73-80.

(85) Iwatsuki, S.; Nakajima, S.; Inamo, M.; Takagi, H. D.; Ishihara, K. Which is reactive in alkaline solution, boronate ion or boronic acid? Kinetic evidence for reactive trigonal boronic acid in an alkaline solution. *Inorg. Chem.* **2007**, *46*, 354-356.

(86) Hagemeier, E.; Boos, K. S.; Schlimme, E.; Lechtenborger, K.; Kettrup, A. Synthesis and application of a boronic acid substituted silica for high-performance liquid affinity-chromatography. *J. Chromatogr.* **1983**, *268*, 291-295.

(87) Bossi, A.; Castelletti, L.; Piletsky, S. A.; Turner, A. P. F.; Righetti, P. G. Properties of poly-aminophenylboronate coatings in capillary electrophoresis for the selective separation of diastereoisomers and glycoproteins. *J. Chromatogr. A* **2004**, *1023*, 297-303.

(88) Zhou, W.; Yao, N.; Yao, G. P.; Deng, C. H.; Zhang, X. M.; Yang, P. Y. Facile synthesis of aminophenylboronic acid-functionalized magnetic nanoparticles for selective separation of glycopeptides and glycoproteins. *Chem. Commun.* **2008**, 5577-5579.

(89) Lee, J. H.; Kim, Y. S.; Ha, M. Y.; Lee, E. K.; Choo, J. B. Immobilization of aminophenylboronic acid on magnetic beads for the direct determination of glycoproteins by matrix assisted laser desorption ionization mass spectrometry. *J. Am. Soc. Mass. Spectrom.* **2005**, *16*, 1456-1460.

(90) Sparbier, K.; Asperger, A.; Resemann, A.; Kessler, I.; Koch, S.; Wenzel, T.; Stein, G.; Vorwerg, L.; Suckau, D.; Kostrzewa, M. Identification and characterization of glycoproteins in human serum by means of glyco-specific magnetic bead separation and LC-MALDI analysis. *Journal of Biomolecular Techniques* **2007**, *18*, 252-258.

(91) Khavkin, J. A.; Roytman, M. J.; Khavkine, M. J. Accumulative solid-phase sorption of pollutants as a method for hygienic and environmental inspection. III. Detection of biowaste using boronylated carrier. *Anal. Lett.* **2004**, *37*, 781-788.

(92) Koyama, T.; Terauchi, K. Synthesis and application of boronic acid-immobilized porous polymer particles: A novel packing for high-performance liquid affinity chromatography. *J. Chromatogr. B* **1996**, *679*, 31-40.

(93) Liu, S. Q.; Miller, B.; Chen, A. C. Phenylboronic acid self-assembled layer on glassy carbon electrode for recognition of glycoprotein peroxidase. *Electrochem. Commun.* **2005**, *7*, 1232-1236.

(94) Zayats, M.; Katz, E.; Willner, I. Electrical contacting of glucose oxidase by surface-reconstitution of the apo-protein on a relay-boronic acid-FAD cofactor monolayer. *J. Am. Chem. Soc.* **2002**, *124*, 2120-2121.

(95) Kanayama, N.; Kitano, H. Interfacial recognition of sugars by boronic acid-carrying self-assembled monolayer. *Langmuir* **1999**, *16*, 577-583.

(96) Ivanov, A. E.; Eccles, J.; Panahi, H. A.; Kumar, A.; Kuzimenkova, M. V.; Nilsson, L.; Bergenstahl, B.; Long, N.; Phillips, G. J.; Mikhalovsky, S. V.; Galaev, I. Y.; Mattiasson, B. Boronate-containing polymer brushes: Characterization, interaction with saccharides and mammalian cancer cells. *J. Biomed. Mater. Res., Part A* **2009**, *88A*, 213-225.

(97) Xu, Y. W.; Zhang, L. J.; Lu, H. J.; Yang, P. Y. On-plate enrichment of glycopeptides by using boronic acid functionalized gold-coated Si wafer. *Proteomics* **2010**, *10*, 1079-1086.

(98) Reyes, D. R.; Iossifidis, D.; Auroux, P.-A.; Manz, A. Micro total analysis systems. 1. Introduction, theory, and technology. *Anal. Chem.* **2002**, *74*, 2623-2636.

(99) Becker, H.; Locascio, L. E. Polymer microfluidic devices. *Talanta* **2002**, *56*, 267-287.

(100) Madera, M.; Mechref, Y.; Novotny, M. V. Combining lectin microcolumns with high-resolution separation techniques for enrichment of glycoproteins and glycopeptides. *Anal. Chem.* **2005**, *77*, 4081-4090.

(101) Feng, S.; Yang, N.; Pennathur, S.; Goodison, S.; Lubman, D. M. Enrichment of glycoproteins using nanoscale chelating Concanavalin A monolithic capillary chromatography. *Anal. Chem.* **2009**, *81*, 3776-3783.

(102) Potter, O. G.; Breadmore, M. C.; Hilder, E. F. Boronate functionalised polymer monoliths for microscale affinity chromatography. *Analyst* **2006**, *131*, 1094-1096.

(103) Bedair, M.; Oleschuk, R. D. Lectin affinity chromatography using porous polymer monolith assisted nanoelectrospray MS/MS. *Analyst* **2006**, *131*, 1316-1321.

(104) Manz, A.; Harrison, D. J.; Verpoorte, E. M. J.; Fettinger, J. C.; Paulus, A.; Lüdi, H.; Widmer, H. M. Planar chips technology for miniaturization and integration of separation techniques into monitoring systems: Capillary electrophoresis on a chip. *J. Chromatogr. A* **1992**, *593*, 253-258.

(105) Arora, A.; Simone, G.; Salieb-Beugelaar, G. B.; Kim, J. T.; Manz, A. Latest developments in micro total analysis systems. *Anal. Chem.* **2010**, *82*, 4830-4847.

(106) Harrison, D. J.; Fluri, K.; Seiler, K.; Fan, Z.; Effenhauser, C. S.; Manz, A. Micromachining a miniaturized capillary electrophoresis-based chemical analysis system on a chip. *Science* **1993**, *261*, 895-897.

(107) *Bio-mems: Technologies and applications*; Wang, W.; Soper, S. A., Eds.; CRC Press: Boca Raton, 2007.

(108) Sinville, R.; Soper, S. A. High resolution DNA separations using microchip electrophoresis. *J. Sep. Sci.* **2007**, *30*, 1714-1728.

(109) McDonald, J. C.; Whitesides, G. M. Poly(dimethyl siloxane) as a material for fabricating microfluidic devices. *Acc. Chem. Res.* **2002**, *35*, 491-499.

(110) Liu, J.; Pan, T.; Woolley, A. T.; Lee, M. L. Surface-modified poly(methyl methacrylate) capillary electrophoresis microchips for protein and peptide analysis. *Anal. Chem.* **2004**, *76*, 6948-6955.

(111) Wei, S.; Vaidya, B.; Patel, A. B.; Soper, S. A.; McCarley, R. L. Photochemically patterned poly(methyl methacrylate) surfaces used in the fabrication of microanalytical devices. *J. Phys. Chem. B* **2005**, *109*, 16988-16996.

(112) Soper, S. A.; Henry, A. C.; Vaidya, B.; Galloway, M.; Wabuyele, M.; McCarley, R. L. Surface modification of polymer-based microfluidic devices. *Anal. Chim. Acta* **2002**, *470*, 87-99.

(113) Soper, S. A.; Ford, S. M.; Qi, S.; McCarley, R. L.; Kelly, K.; Murphy, M. C. Peer reviewed: Polymeric microelectromechanical systems. *Anal. Chem.* **2000**, *72*, 642 A-651 A.

(114) Kelly, R. T.; Woolley, A. T. Thermal bonding of polymeric capillary electrophoresis microdevices in water. *Anal. Chem.* **2003**, *75*, 1941-1945.

(115) Henry, A. C.; Tutt, T. J.; Galloway, M.; Davidson, Y. Y.; McWhorter, C. S.; Soper, S. A.; McCarley, R. L. Surface modification of poly(methyl methacrylate) used in the fabrication of microanalytical devices. *Anal. Chem.* **2000**, *72*, 5331-5337.

(116) Liu, J.; Sun, X.; Lee, M. L. Surface-reactive acrylic copolymer for fabrication of microfluidic devices. *Anal. Chem.* **2005**, *77*, 6280-6287.

(117) Wang, J. S.; Matyjaszewski, K. Controlled living radical polymerization - atom transfer radical polymerization in the presence of transition metal complexes. *J. Am. Chem. Soc.* **1995**, *117*, 5614-5615.

(118) Kato, M.; Kamigaito, M.; Sawamoto, M.; Higashimura, T. Polymerization of methyl methacrylate with the carbon tetrachloride dichlorotris(triphenylphosphine)ruthenium(II) methylaluminum bis(2,6-di-*tert*-butylphenoxide) initiating system - possibility of living radical polymerization. *Macromolecules* **1995**, *28*, 1721-1723.

(119) Xiao, D. Q.; Van Le, T.; Wirth, M. J. Surface modification of the channels of poly(dimethyl siloxane) microfluidic chips with polyacrylamide for fast electrophoretic separations of proteins. *Anal. Chem.* **2004**, *76*, 2055-2061.

(120) Sun, X. F.; Liu, J. K.; Lee, M. L. Surface modification of polymer microfluidic devices using in-channel atom transfer radical polymerization. *Electrophoresis* **2008**, *29*, 2760-2767.

(121) Mao, X.; Wang, K.; Du, Y.; Lin, B. Analysis of chicken and turkey ovalbumins by microchip electrophoresis combined with exoglycosidase digestion. *Electrophoresis* **2003**, *24*, 3273-3278.

(122) Mao, X.; Luo, Y.; Dai, Z.; Wang, K.; Du, Y.; Lin, B. Integrated lectin affinity microfluidic chip for glycoform separation. *Anal. Chem.* **2004**, *76*, 6941-6947.

(123) Mao, X.; Chu, I. K.; Lin, B. A sheath-flow nanoelectrospray interface of microchip electrophoresis MS for glycoprotein and glycopeptide analysis. *Electrophoresis* **2006**, *27*, 5059-5067.

(124) Bindila, L.; Peter-Katalinić, J. Chip-mass spectrometry for glycomic studies. *Mass Spectrom. Rev.* **2009**, *28*, 223-253.

(125) Bynum, M.; Baginski, T.; Killeen, K.; Keck, R. Integrated microfluidic LC-MS. *Pharm. Technol.* **2010**, *34*, s32-s39.

CHAPTER 2

ASSESSMENT OF GLYCOPROTEIN INTERACTIONS WITH 4-[(2-AMINOETHYL)CARBAMOYL]PHENYLBORONIC ACID SURFACES USING SURFACE PLASMON RESONANCE SPECTROSCOPY*

2.1 Introduction

Glycosylation renders particular functions that are reflected in most of the physico-chemical and biological properties of proteins. Some of the key roles in which glycosylated proteins participate include cellular recognition, protein folding, and protein trafficking.[1] On the other hand, aberrant glycosylations—as manifested by changes in glycosylation levels and alterations in glycan structures—have been associated with the development and progression of cancer and other diseases.[2-3] As a result, glycosylated proteins have been the subject of many research efforts targeting the elucidation of structure-function relationships.

The characteristic of phenylboronic acids to form reversible complexes with diol-containing materials, such as sugars, has led to numerous developments for eventual application in areas such as sensor technology,[3-8] drug delivery,[9] and affinity chromatography.[10-11] Current knowledge on the mechanism of the diol-boronic acid interaction is based on the equilibrium formation of a heterocylic diester from 1,2- or 1,3-diol groups and a tetrahedral boronate ion (Scheme 2.1);[12] this equilibrium is a function of the ionization constant K_a of the boronic acid moiety. Thus, the coordination of diol species is commonly performed at a pH that results in conversion of the trigonal planar boronic acid species into the tetrahedral boronate ion. Although it is generally accepted that the boronate ion is the active binding species, Ishihara and co-workers[13] are of the opinion that the neutral planar boronic acid has comparable or even higher reactivity toward diols than the boronate ion, regardless of solution pH.

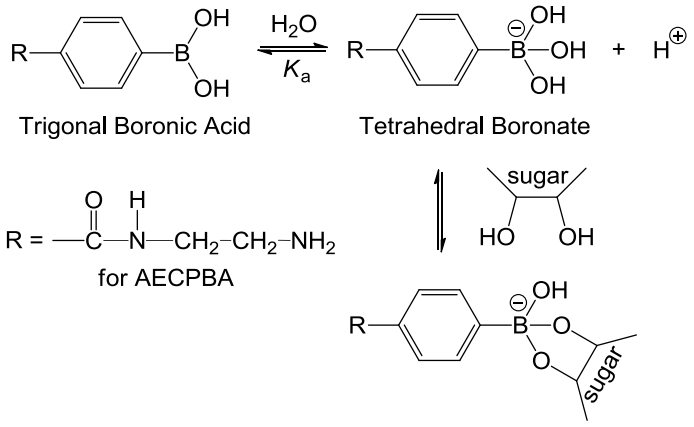

Scheme 2.1. Depiction of phenylboronic acid–sugar equilibrium for 4-[(2-aminoethyl)carbamoyl]phenylboronic acid, AECPBA.

The ability to select, from a diverse protein population, a given subset of glycosylated proteins (enrichment) using surface-attached capture agents is of great importance in the systematic identification and quantification of disease-related biomarkers obtained from tissues and circulating cells.[1,14] Although interaction analysis between surface-attached boronic acid derivatives and simple saccharides (non-protein-containing) is quite common in the literature,[6,15-17] it is surprising to find from an exhaustive survey of the literature that reports on the interaction analysis of surface-immobilized boronic acids with solution-phase proteins—glycosylated and non-glycosylated alike—are limited, at best.[3-5,18-19] In two of the extent studies, investigations were performed on colloidal gold possessing a polymer brush of 3-acrylamidophenylboronic acid for determination of glycoprotein presence.[4-5] However, the limited number and variety of proteins used did not allow for a thorough probing of protein properties that might have an impact on the feasibility of the Au colloid system in the development of sensors for analysis of glycoproteins. In two other studies, single glycoprotein binding (glycated hemoglobin[3] and glycosylated albumin[18]) on alkanethiol/Au surfaces was investigated, but the elution (regeneration) of the surfaces was not addressed. In the only other study of which I am aware, electrochemical methods were used to study the affinity interactions between electropolymerized

boronic acid films on electrodes and a select group of glycoproteins having limited glycan variety.[19] Thus, it would be of great benefit to develop surface immobilization chemistries for attachment of a diverse collection of phenylboronic acids and gain knowledge regarding their ability to capture and release different and closely-related glycosylated proteins under a variety of solution conditions.

This chapter reports on the evaluation of glycoprotein–surface-attached boronic acid interactions by surface plasmon resonance spectroscopy (SPR). To the best of my knowledge, this is the first time that a boronic acid derivative has been successfully immobilized onto SPR sensor surfaces and then subsequently used to study the interactions between surface boronic acids and solution-phase glycoproteins. It is shown that SPR can be used to readily follow interactions between surface boronic acids and glycoproteins without complex and laborious surface preparation. In particular, the novel boronic acid derivative 4-[(2-aminoethyl)carbamoyl]phenylboronic acid, AECPBA, is immobilized on carboxymethyl dextran hydrogels using carbodiimide coupling, Scheme 2.2, and is subsequently employed as the capture element in an SPR device, Scheme 2.1. AECPBA is chosen because a soluble polymer bearing this boronic acid derivative exhibits increased sensitivity to glucose binding under physiological conditions, and the pK_a of the boronic acid/boronate pair of AECPBA is lower than other phenylboronic acids, making it attractive for capture of proteins in biological milieu.[9] In the work here, a variety of glycosylated and non-glycosylated proteins having various properties was investigated to provide insight into the nature of the interaction between the boronic acid-modified sensor surface and the proteins. Furthermore, the use of immobilized AECPBA as a reversible capture-and-release agent is demonstrated by the quantitative elution of glycoproteins

from AECPBA surfaces by borate buffer. Secondary interactions are also discussed in the context of non-specific adsorption to the carboxymethyl dextran matrix and the boronic acid ligand.

2.2 Experimental Section

2.2.1 Materials

AECPBA was prepared as previously reported.[9] CM5 sensor chips (carboxymethyl dextran on Au) were obtained from Biacore (Uppsala, Sweden). Avidin, ExtrAvidin, fetuin, asialofetuin, RNAse A, RNase B, and human transferrin were purchased from Sigma and were used as received. Other chemicals obtained from Sigma (St. Louis, MO) include 1-ethyl-3-[3-dimethylaminopropyl]carbodiimide hydrochloride (EDC), 2-(*N*-morpholino)ethanesulfonic acid (MES), tris(hydroxymethyl)aminomethane (Tris), 4-(2-hydroxyethyl)-1-piperazineethanesulfonic acid (HEPES), EDTA, glycine, Tween-20, and ethanolamine. *N*-hydroxysuccinimide (NHS) was obtained from Pierce Biotechnology (Rockford, IL). Boric acid was obtained from EM Science (Gibbstown, NJ). NaOH and NaCl were purchased from Fisher Scientific. HCl was obtained from VWR (West Chester, PA). All solutions were prepared in Nanopure water (Barnstead, >18 MΩ·cm). pH 7.40 HBS-EP consisted of 0.01 M HEPES, 0.15 M NaCl, 3.0×10^{-3} M EDTA, and 0.0050% (v/v) Tween-20. All buffers and reagents used were degassed and filtered prior to use in SPR experiments.

2.2.2 Potentiometric Titration

To determine the pK_a of AECPBA, 1.5×10^{-2} g of AECPBA was dissolved in 20.00 mL of 0.010 N NaOH. To this solution was added 0.50-mL portions of the titrant (0.010 N HCl containing 0.150 M NaCl) and the pH at each interval was determined using a calibrated glass pH electrode (Denver Instrument). A pK_a value of 8.0 was found using this method.

2.2.3 Surface Plasmon Resonance Measurements

Investigations of the interaction of select proteins with AECPBA- and hydroxyl-terminated control surfaces were performed with a Biacore X SPR instrument (Uppsala, Sweden). To prepare the sensor surface, the commercially-available CM5 sensor surface (Biacore) was functionalized with AECPBA either by direct EDC coupling or through EDC/NHS activation, Scheme 2.2. For direct EDC coupling, 65 μL of a mixture composed of 0.010 M AECPBA and 0.20 M EDC prepared in pH 6.00, 0.025 M MES was injected at a flow rate of 2 μL min^{-1} after achieving baseline with the same buffer. The unreacted, NHS-activated carboxyl groups were capped by injecting 65 μL of pH 8.50, 1.0 M aqueous ethanolamine, at a flow rate of 10 μL min^{-1}. For the sensor surface modification via EDC/NHS activation, pH 7.40 HBS-EP was used as the running buffer. The surface was activated by injecting 70 μL of a freshly prepared mixture consisting of 0.070 M NHS and 0.20 M EDC at a flow rate of 10 μL min^{-1}.

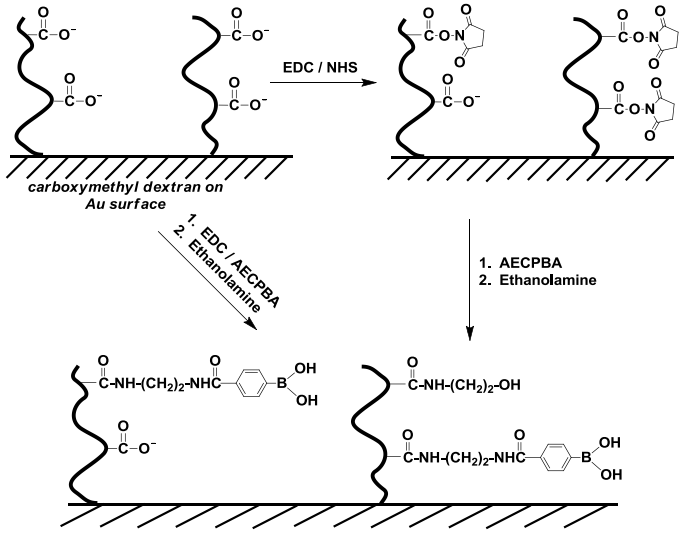

Scheme 2.2. Preparation of the AECPBA-functionalized carboxymethyl dextran (CM5) on Au sensor surface.

At the same flow rate, several 70 μL-injections of 0.020 M AECPBA prepared in pH 8.50, 0.10 M borate were performed. Finally, the remaining activated esters on the surface were deactivated by injecting 40 μL of pH 8.50, 1.0 M ethanolamine. To examine the binding of select proteins, either 0.050 M Tris buffer or 0.050 M glycine buffer (pH 8.00 and 9.00) containing 0.15 M NaCl were used as running and sample buffers. Protein solutions were passed over the AECPBA-functionalized surfaces at defined concentrations and flow rates. Values reported for the amount of protein bound are the average ± one standard deviation from replicate measurements. The AECPBA surface was regenerated following each protein injection with either single or multiple injections of pH 10.00, 0.10 M borate-buffer containing 0.30 M NaCl or a short pulse of 0.050 M NaOH at 10 μL min^{-1}.

2.3 Results and Discussion

2.3.1 Preparation of the AECPBA (Boronic Acid) Sensor Surface

The covalent attachment of AECPBA as followed by SPR, is shown in Figure 2.1. Activation of the carboxymethyl dextran surface was achieved through injections of EDC and NHS solutions, thereby transforming the carboxylic acid groups into NHS-activated esters. Alternatively, the carboxymethyl dextran surface can be activated directly by the use of EDC only (Figure 2.2). Subsequently, solutions of AECPBA in pH 8.50 borate buffer were passed over the surface several times (4× of 70 μL of 0.025 M AECPBA) to maximize the degree of AECPBA attachment. Removal of any non-covalently bound AECPBA and capping of any remaining NHS esters (formation of amide-linked, hydroxyl-terminated regions) was carried out using a solution of ethanolamine. SPR measures the resonance angle at which a minimum of reflected light occurs as a result of a change in the refractive index of the medium near a thin film of the metal (Au in this case)—for example, during analyte adsorption. This change in angle is

reported in Resonance Units (RU) such that a change of 0.1° is equivalent to 1000 RU.[20] The change in SPR response, measured in Resonance Units (RU), for the AECPBA surface was 1200, while hydroxyl-terminated control surfaces resulted in a change of 300 RU. Thus, it can be concluded that the SPR response (~1200 RU) is the result of covalent attachment of AECPBA, a small molecule, throughout the 200-nm thick carboxymethyl dextran hydrogel matrix. Although two methods were used to create the AECPBA surfaces, the difference in their performance (in terms of protein binding) was not directly compared and evaluated. Eventhough this is the case, any observations that were compared against each other were obtained under identical conditions (e.g. surface is obtained from one method only). Although it is desirable to determine the surface density of immobilized AECPBA ligand, this is not possible using the SPR response values. The published conversion factor of 10 RU = 1.0 $ng \cdot cm^{-2}$ used for proteins[20-21] should not be employed, because the refractive index of small molecules can be significantly different from that of proteins.[22]

2.3.2 Model Glycosylated Protein Binding on and Subsequent Elution from AECPBA Surfaces

Initial investigation of the binding capabilities of the AECPBA sensor surface was performed by flowing a solution of the model protein avidin in pH 9.00 glycine-buffered saline. Avidin is a 68 kDa tetrameric protein that consists of four identical subunits and contains 10% glycosylation.[23] Each subunit contains one glycosylation site at Asn 17;[24-25] glycans at this site have been shown by NMR to be heterogeneous in both composition and structure.[26] Evidence from that study[26] suggests that high mannose and hybrid types make up the oligosaccharide composition, with the latter hybrid type terminated with *N*-acetylglucosamine and/or galactose.

In Figure 2.3 is shown the SPR response for the AECPBA surface upon exposure to the glycoprotein avidin. The observed interaction beginning at roughly 250 s on the time axis is

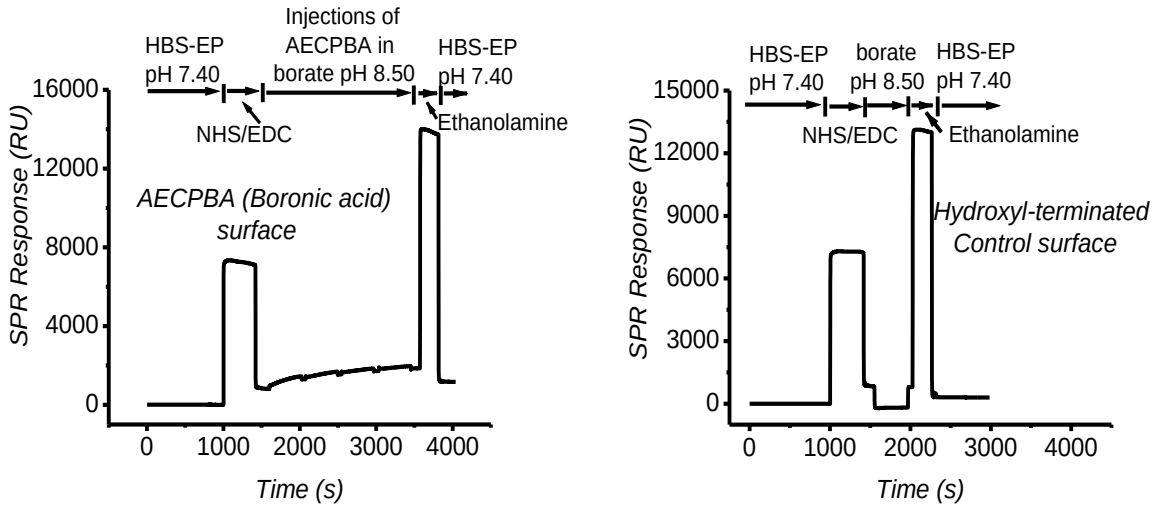

Figure 2.1. SPR sensorgrams from the preparation of AECPBA (left) and hydroxyl-terminated control (right) surfaces. In each case, the carboxymethyl dextran surfaces were first treated with pH 7.40 HBS-EP (0.010 M HEPES, 0.15 M NaCl, 3.0×10^{-3} M EDTA, 0.0050% v/v Tween-20), then 70 μL of 0.070 M NHS/0.20 M EDC was injected, followed by a minimum of 4 injections of 70 μL of 0.025 M AECPBA in pH 8.50 borate buffer for the AECPBA surface or 70 μL of pH 8.50 borate buffer followed by 40 μL of 1.0 M ethanolamine (pH 8.50) for the hydroxyl-terminated control surface. Capping of any remaining NHS sites on the AECPBA surface was achieved by injecting 40 μL of pH 8.50, 1.0 M ethanolamine.

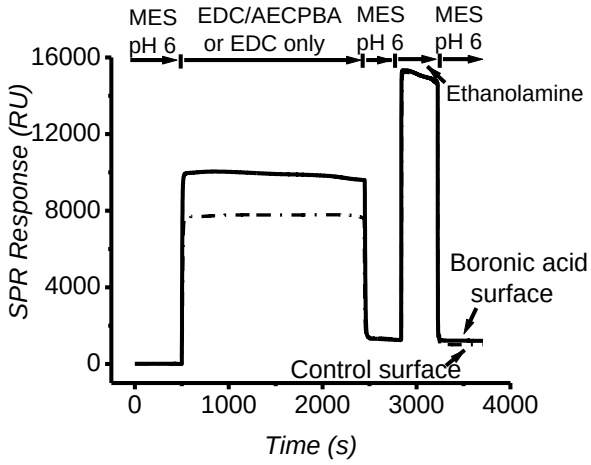

Figure 2.2. SPR sensograms during the preparation of AECPBA- (solid line) and hydroxyl-terminated control (dash-dot line) surfaces. In each case, the carboxymethyl dextran surfaces were first equilibrated with pH 6.00, 0.025 M MES buffer, followed by injection of a 65 μL solution of 0.20 M EDC/0.010 M AECPBA in pH 6.00 MES buffer for the AECPBA surface and 65 μL of 0.20 M EDC in pH 6.00 MES buffer for the hydroxyl-terminated control surface. Capping of any remaining carboxyl-activated sites was achieved using 65 μL of pH 8.50, 1.0 M ethanolamine solution. The AECPBA surface and hydroxyl-terminated control surface yielded an SPR response of 1200 RU and 1000 RU, respectively.

presumed to result from the specific weak covalent interaction between the active tetrahedral boronate ion and the sugar residues in the glycoprotein, Scheme 2.1. Although it is tempting to report the association/dissociation constants, the unknown stoichiometry of binding between avidin and AECPBA would render such values suspect.[27] However, the amount of surface-bound avidin at $[\text{avidin}]_{\text{solution}} = 5.16 \times 10^{-6}$ M can be determined. Based on the difference in RU responses of avidin prior to and after its injection, we calculate that roughly 13.1 ± 0.4 ng·cm^{-2} of avidin is bound to the AECPBA surface, a value that is ~3% of a close-packed avidin monolayer.[28] This value did not change upon increasing the number of EDC/NHS or AECPBA injections. The obtained value of 13.1 ± 0.4 ng·cm^{-2} of avidin was calculated using the established conversion factor of 10 RU = 1.0 ng·cm^{-2} for proteins from the average SPR response of ~130 RU. The response is measured between the baseline and the RU level after subtraction of the contribution of the bulk refractive index (as caused by any refractive index change due to some differences in the sample and running buffer used). Assuming a Langmuir adsorption process with a close-packed avidin monolayer (440 ng·cm^{-2}),[28] and using a typical boronic acid-glycoprotein association constant, such as that found for 3-acrylamidophenylboronic acid–avidin complexation ($K_{\text{assoc}} = 5.05 \times 10^{-3}$ M),[4] the expected amount of avidin bound to the AECPBA surface with $[\text{avidin}]_{\text{solution}} = 5.16 \times 10^{-6}$ M is calculated to be 11.2 ng·cm^{-2}, in good agreement with the observed 13.1 ± 0.4 ng·cm^{-2} value. The limit of detection was not determined in this case. It should be noted that this would be highly dependent upon several factors such as the molecular weight of the analyte, the ligand surface coverage, and the thermodynamic properties elicited by the interaction. However, a similar instrument—Biacore 1000—is reported to detect as low as less than 1% complete monolayer of protein bound.[28] Based on this, the monolayer coverage I obtained is derived from the weak interaction of avidin with the boronic acid groups.

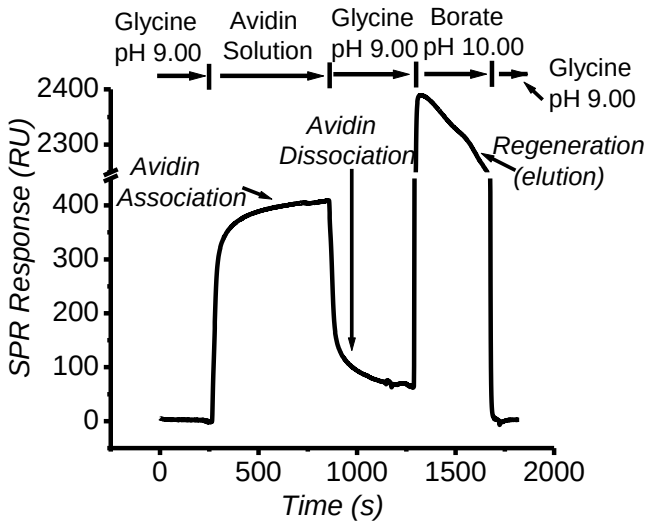

Figure 2.3. Representative SPR sensorgram for avidin binding on and elution from the AECPBA surface. The binding experiment was performed with 20 μL of 5.16×10^{-6} M avidin in pH 9.00 glycine-buffered saline (0.050 M glycine, 0.15 M NaCl) at a flowrate of 2 μL min^{-1}, while the elution (regeneration) experiment was performed with 65 μL of pH 10.00 borate-buffered saline (0.10 M borate, 0.30 M NaCl) at a flowrate of 10 μL min^{-1}. The flowrate during the buffer run is kept at 2 μL min^{-1}. The AECPBA surface was prepared through direct EDC coupling.

The covalent interaction between boronate and sugar is a reversible process, and dissociation of the sugar-boronate complex is usually facilitated using an acidic buffer[29] or a competing molecule, such as sorbitol.[30] However, experiments revealed that an appreciably low pH (e.g. $\leq$ pH 2.00, data not shown) was required to yield effective elution, but with use of such a low pH eluent, SPR responses were found to be inconsistent in-between binding experiments. I attribute this to AECPBA ligand loss from the sensor surface during use of the highly acidic eluent (amide hydrolysis). Similar outcomes have been observed for boronic acids attached via amides on chromatographic supports.[29] In the case of sorbitol, its ability to displace diols from the diol-boronate complex is based on its strong interaction with boronate ions.[31] Thus, use of sorbitol as an eluent is inappropriate in SPR analyses, because sorbitol binding to the boronate surface would result in misleading interpretation of the SPR baseline following regeneration with sorbitol (inability to establish pre-protein-exposure baseline). In general, sorbitol is a powerful

and appropriate eluting agent for select boronic acid sensing systems like those based on electrochemical sensing[32] wherein the baseline response is not affected by sorbitol binding on the electrode surface; however, sorbitol should be avoided as an eluent for boronic acid sensing applications possessing a transduction mechanism based on surface mass change, such as SPR and microbalance methods.[17]

I turned to borate as an eluent[33] for the AECPBA-bound glycoprotein avidin (regeneration of the AECPBA surface/release of captured avidin), as the borate acts as a competing molecule for covalent bond formation with the sugar chains of the glycoprotein, resulting in glycoprotein elution from the AECPBA surface. As shown in Figure 2.3, use of pH 10.00 borate-buffered saline resulted in the apparent complete removal of avidin after the dissociation phase of the experiment (at ~1300 s), as noted by the experimentally observed identical SPR reading before avidin injection (RU = 2) and after borate regeneration of the AECPBA surface (RU = 2). In addition, the AECBPBA surfaces could be treated numerous times (12 times, the maximum attempted) without any measurable impact on the ability of the boronic acid surfaces to bind avidin in subsequent association experiments. In other experiments, multiple injections of borate or a short pulse of NaOH solution[34-35] effected regeneration (*vide infra*). Overall, these outcomes demonstrate the capacity of the AECPBA surface to effectively bind glycoprotein analyte and the ability of borate to act as a mild and simple eluent for AECPBA-bound glycoprotein, thereby providing an avenue for comparative analysis of the binding of chemically distinct glycoproteins to AECPBA surfaces.

2.3.3 Impact of Glycosylated Protein Nature on Binding to AECPBA Surfaces

The relative affinity, measured as surface protein concentration, of several glycosylated proteins examined on the AECPBA surface prepared through the EDC/NHS activation method is

summarized in Table 2.1. The proteins are appropriately chosen so as to exhibit variation in molecular weights, degree of glycosylation, composition of heteroglycan chain and isoelectric points (p*I*),[36-40] to facilitate the determination of the nature of glycoprotein interaction with surface boronic acids. In general, the amount of glycosylated protein bound to the AECPBA surface is significantly greater than for the hydroxyl-terminated control surface. There is no observable general trend in the amount of protein bound with the p*I*, molecular weight, or degree of glycosylation for this set of proteins. Regeneration (i.e. removal of bound proteins and subsequent achievement of virtually identical baseline before protein injection and after regeneration) was routinely observed on the AECPBA- and hydroxyl-terminated control surfaces for this set of proteins.

Interestingly, a striking difference in SPR response was observed for fetuin and its desialylated analogue, asialofetuin. The amount of bound fetuin was found to be significantly lower compared to asialofetuin (~25%, Table 2.1), indicating that the binding constant for asialofetuin, K_{assoc}, on the AECPBA surface is significantly higher. Structurally, the only difference between the two proteins is the presence of the terminal *N*-acetylneuraminic acid (a.k.a. sialic acid) group in the six glycan chains of fetuin.[36] In a recent investigation of a colloidal gold-carrying, boronic acid polymer brush, the assumption was made that the higher K_{assoc} observed for ovalbumin compared to avidin was a result of the larger population of hydroxyl groups presented by the mannose-rich ovalbumin over the *N*-acetylglucosamine–rich avidin.[4] If the same case were to hold for fetuin and asialofetuin, the higher number of sugar constituents in fetuin (terminated with six sialic acid residues) should result in binding of more fetuin versus asialofetuin on the AECPBA surface; the converse is observed. We propose that the more sugar-rich fetuin (compared to asialofetuin) does not behave similarly to ovalbumin for

the following reasons: 1) not all hydroxyl groups will be available to participate in complex formation because some hydroxyl groups are involved in glycosidic linkages between saccharide units; 2) not all hydroxyl groups are oriented in the synperiplanar formation that is a requisite for boronate complexation;[41] and 3) steric hindrance[42] in the underlying sugars of the glycan chains will preclude binding. It was in fact demonstrated by ^{11}B NMR that the complexation of borates to galactomannan is only through the galactose units attached to and "hanging from" the mannan polymer backbone.[43] Evidence from that study[43] does not suggest any complexation of borate with the mannose units that are glycosidically-linked together to make up the oligosaccharide

Table 2.1. Comparison of the amount of proteins bound on the AECPBA surface and the hydroxyl-terminated (ethanolamine-capped) control surface.

protein properties				amount protein bound ($\times 10^2$ fmol·cm^{-2})	
protein [p*I*]	molecular weight (kDa)	glycosylated?	degree of glycosylation	AECPBA surface	hydroxyl-terminated control surface
fetuin [3.3]	48.4	yes	22%	4.6	2.6
asialofetuin [5.2]	<48.4	yes	14%	16	6.0
transferrin [5.6]	76–81	yes	6%	5.4	2.6
RNAse B [9.4]	14.7	yes	9%	17	4.1
RNAse A [9.4]	13.7	no	Not applicable	14	4.1

Protein concentrations ($\times 10^{-4}$ M) flowed over the AECPBA surfaces were: fetuin, 3.88; asialofetuin, 4.27; transferrin, 4.03; RNAse B, 4.19; and RNAse A, 3.97. 60 μL of protein solution (pH 8.00 glycine-buffered saline) was injected at 15 μL min^{-1}. The AECPBA surface was prepared through EDC/NHS activation. Regeneration was performed with pH 10.00, 0.10 M borate-buffered saline or 0.050 M NaOH solution. The values obtained are within 5% experimental error. Information on molecular weight, p*I*, and degree of glycosylation are provided in references 36-40.

backbone. Therefore, based on this, the degree of complex formation is not necessarily dependent on the number of sugar constituents of the glycan chains (% glycosylation) present in the glycoprotein.

With this knowledge in hand, the results with fetuin, asialofetuin, and human transferrin suggest that the identity of the sugar terminus plays a key role in determining the extent of binding of glycoproteins to the AECPBA surface. The six oligosaccharide chains of fetuin are terminated with *N*-acetylneuraminic acid units (sialic acid), while asialofetuin is essentially fetuin with its oligosaccharide chains terminated with galactose units (resulting from the desialylation procedure used to make it). Although it might be tempting to state that the lower observed AECPBA binding of fetuin is due to the negative charge of the *N*-acetylneuraminic acid residue (electrostatic repulsion by the boronate ion), this is not necessarily the case. Detailed investigations of *N*-acetylneuraminic acid binding to boronic/boronate systems revealed that *N*-acetylneuraminic acid binds more strongly at acidic to neutral pH, contrary to the generally accepted binding of neutral sugars at alkaline pHs.[42] It was rationalized that, unlike neutral sugars wherein strong complex formation with boronic acid systems occurs with the tetrahedral boronate ion to create a tetrahedral-formed complex, *N*-acetylneuraminic acid complexation with boronic acids results from interactions between the glycerin moiety of *N*-acetylneuraminic acid and the uncharged trigonal boronic acid, resulting in a trigonal complex. The observed increased stability of this trigonal complex at acidic to neutral pH is derived from the intramolecular B–O or B–N interaction created with the neighboring *N*-acetyl group. Because the boronic acid derivative used here has a pK_a of 8.0, and the binding was performed at pH 8.00, complex formation between fetuin and the boronic acid system through the glycerin group is unstable. This is because the larger proportion of tetrahedral boronate ion existing in solution results in

tetrahedral-formed complex between the boronate ion and the glycerin moiety without the stabilization from the B–O or B–N interaction, giving way to a weaker binding. This weaker interaction translates into a decreased amount of bound fetuin.

Importantly, we have observed that the amount of human transferrin bound to the AECPBA surface is roughly the same as for fetuin, further suggesting that the degree of glycoprotein binding to the boronic acid surface is heavily influenced by the identity of the terminal sugar of the glycan chains of the glycoprotein. Human transferrin has only two glycan chains, both of which are terminated with *N*-acetylneuraminic (sialic) acid,[37,44] as is the case for the glycan chains of fetuin. In addition, both transferrin and fetuin have galactose units immediately before the sialic acid terminus; the final five sugars of their terminal sequences are *N*-acetylneuraminic acid→galactose→*N*-acetylglucosamine→ mannose→ mannose.[44-46] From Table 2.1, it can be observed that the amount of fetuin and transferrin bound on the AECPBA surface is the same within experimental error (~5 × 10^2 fmol·cm^{-2}). This similarity in the amount of these two proteins bound on the AECPBA surface is striking, as there is a large difference in their degree of glycosylation (fetuin, 22%; transferrin, 6%) and molecular weight (fetuin, 48 kDa; transferrin, ~76 kDa). Thus, these results strongly support the hypothesis that the identity of the sugar terminus plays a key role in determining the extent of binding of glycoproteins to the AECPBA surface. These observations with fetuin, asialofetuin, and transferrin will be important during the design of systems for the enrichment of glycoproteins from a diverse protein pool.

2.3.4 Non-specific Protein Adsorption on Carboxymethyl Dextran Surfaces

It is interesting to note that SPR responses are evident on the hydroxyl-terminated control surface after glycoprotein solutions were presented to it, albeit the responses are significantly

lower than that found on the AECPBA surface for each protein. This hydroxyl-terminated control surface possesses ethanolamine-capped carboxylic acid groups that should result in diminished non-specific binding of proteins.[47] I attribute the observed SPR response to non-specific adsorption of proteins on the carboxymethyl dextran surface, similar to what has been observed for some proteins in a previous study.[28] Thus, it is hypothesized that the observed protein adsorption on the hydroxyl-terminated control surface is electrostatic in nature and may likely be due to the interaction between regions of underivatized surface carboxylic acids and a given protein, as dictated by protein isoelectric point (p*I*). Alternatively, it can be argued for proteins whose p*I*s render them negatively charged during the association phase of the experiment, such as fetuin (p*I* = 3.3) and asialofetuin (p*I* = 5.2), hydrogen-bonding to the dextran matrix[48] is a possible explanation of the observed non-specific adsorption. No matter the cause of the non-specific interactions, it is clear that interaction of the glycoproteins with the AECPBA surface is due to a combination of the specific boronate-sugar complexation and non-specific adsorption to the underlying dextran hydrogel matrix. Based on the higher SPR response on the boronic acid surface, the specific complexation reaction of glycoproteins on the boronic acid surface is dominant.

2.3.5 Glycosylated and Non-glycosylated Protein Binding on AECPBA Surfaces

To determine the specificity of the boronic acid ligand for binding glycosylated proteins versus their non- or deglycosylated counterparts, the non-glycosylated protein RNAse A and deglycosylated ExtrAvidin were investigated and compared to RNAse B (glycosylated) and avidin (glycosylated). Parallel comparison of RNAse A (non-glycosylated) and RNAse B (glycosylated) is appropriate given that the two ribonucleases are identical in protein structure and only distinguishable at Asn 34, where a high-mannose-oligosaccharide–containing chain

resides in RNAse B but not in RNAse A.[39,49] In the ideal scenario, any difference between the two in terms of interaction with the boronic acid ligand should be attributable to the presence/absence of the heteroglycan chain at Asn 34. Upon inspection of Table 2.1, it is found that RNAse A has a considerable degree of interaction with the AECPBA surface, although the amount of RNAse B (glycosylated) binding is 21% greater. Interestingly, the level of interaction of the non-glycosylated RNAse A is even greater than some of the other glycosylated proteins studied. This observation can be rationalized by considering the molecular structure of the AECPBA derivative. This structure can be associated with secondary interactions such as hydrophobic, coulombic, coordination, and hydrogen bonding.[11] Therefore, interaction with any material possessing boronic acids is not necessarily limited to the specific boronate/cis-diol ester formation. Conceivably, the properties of the proteins are expected to exert a significant role in the overall interaction process. In the case of the non-glycosylated RNAse A, its interaction with negatively-charged surfaces is well documented in the literature;[40,50] this interaction is facilitated by the presence of a positively-charged protein domain that is known to be situated along the longest axis of the RNAse A molecule, thereby affording a large surface area with positive potential. The p*I* of RNAse A is 9.4,[40] and at the binding pH of 8.00 used here, the protein contains a net positive charge, while the boronic acid surface possesses negative charges from the active boronate ion species. It is then reasonable to say that coulombic interaction accounts very well for the high level of SPR response of RNAse A despite it not being glycosylated. As for RNAse B, it can be deduced that both specific and non-specific interactions contribute to the binding observed on the boronic acid surface. It can then be said that these secondary interactions should be capable of providing additional selectivity if they occur in concert with the

primary specific interaction, but they become detrimental when they favor non-specific adsorption of non-glycosylated analytes, such as is observed with RNAse A.

Another comparative analysis was performed with a glycosylated protein and its deglycosylated variant, namely, avidin and ExtrAvidin, on the AECPBA surface prepared from direct EDC coupling. As shown in the representative sensorgrams in Figure 2.4A, the SPR response for avidin is statistically higher (by ~4-fold) compared to that for ExtrAvidin on the AECPBA surface, with a calculated 9.8 ± 0.5 $ng \cdot cm^{-2}$ avidin bound and 2.6 ± 0.6 $ng \cdot cm^{-2}$ ExtrAvidin bound using tris(hydroxymethyl)aminomethane, Tris, buffer. This difference can be viewed as a consequence of the interaction between the heteroglycan chain in avidin and the boronate groups on the sensor surface. In addition, similar to the observation made with RNAse A (non-glycosylated), ExtrAvidin is found to bind to both boronic acid and hydroxyl-terminated control surfaces with the glycine buffer system used (Figure 2.4B). Importantly, when the buffer was changed to the Tris buffer system, the SPR response for ExtrAvidin was lower than for the glycine buffer case when using the same AECPBA surface (compare Figures 2.4B and 2.4C). Note also with the use of Tris that the SPR response for ExtrAvidin is identical on boronic acid and control surfaces (Figure 2.4C), possibly indicating that non-specific interaction of ExtrAvidin with the carboxymethyl dextran matrix is the sole contributing interaction. It is also possible that the purported single-carbohydrate residue (*N*-acetylglucosamine) of deglycosylated avidin (e.g. ExtrAvidin) per protein subunit causes some of the interaction on the AECPBA surface.[51-54]

Typically, it is discouraged to employ buffer systems (e.g. Tris) that can participate in coordination or esterification reactions with the boronate group,[11] as this can prove detrimental to sugar binding. However, Mattiasson and co-workers demonstrated that Tris can suppress the

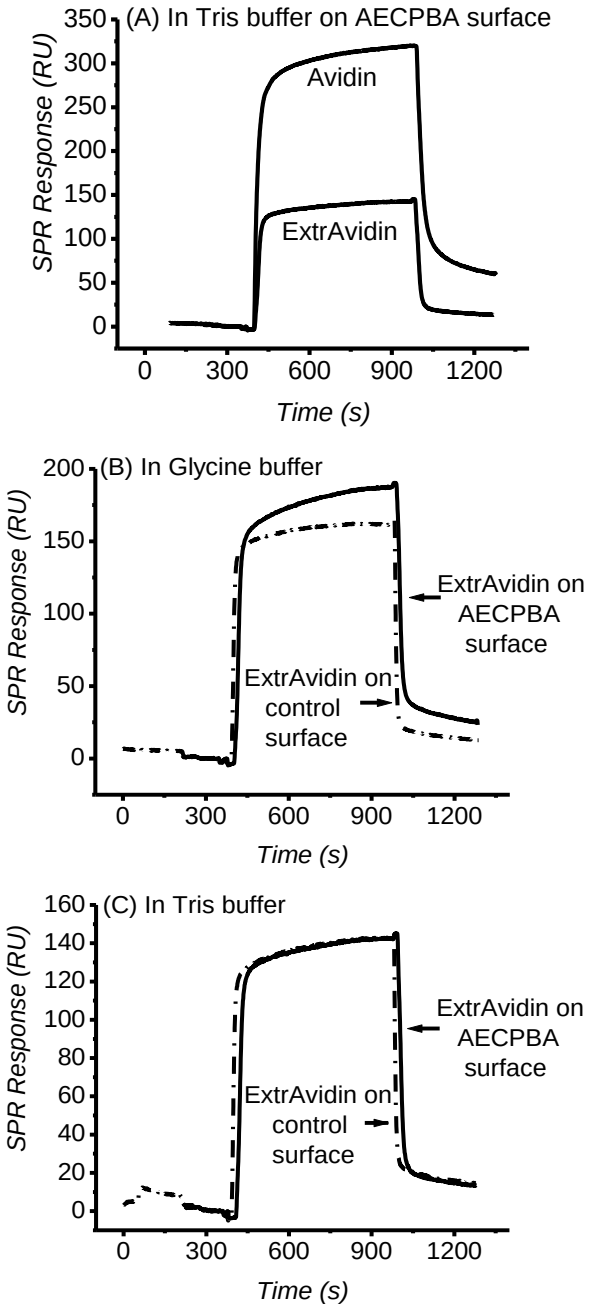

Figure 2.4. Representative SPR sensorgrams during the binding of glycosylated protein avidin and the deglycosylated protein ExtrAvidin. (A) Avidin (5.29×10^{-6} M) versus ExtrAvidin (5.09×10^{-6} M) in pH 9.00 Tris-buffered saline on the AECPBA surface; (B) ExtrAvidin in pH 9.00 glycine-buffered saline and (C) ExtrAvidin in pH 9.00 Tris-buffered saline (right) on AECPBA (solid line) and hydroxyl-terminated control (dash-dot line) surfaces. ExtrAvidin concentrations were 4.94×10^{-6} M and 5.09×10^{-6} M in pH 9.00 glycine-buffered saline and pH 9.00 Tris-buffered saline. Protein binding was performed using 20 μL at 2 μL min^{-1}. The running buffer was kept at a flowrate of 2 μL min^{-1}. The AECPBA surface was prepared through direct EDC coupling.

interaction of the non-glycosylated protein chymotrypsin with boronate ions.[31,55-56] They postulated that Tris has an affinity for the boronate ion that is intermediate to that of sugar diol groups (stronger) and amino acid residues (weaker); thus, Tris acts as a molecular shielder. In other words, Tris, by forming a tridentate complex with the boronate ions, essentially protects the boronates from interacting with amino acid residues of the non-glycosylated proteins but can be competitively displaced by the sugar in the glycoprotein so as to allow glycoprotein binding.

In this work, a similar phenomenon of decreased non-glycosylated protein interaction when glycine buffer was replaced with Tris was observed, even though the structures of ExtrAvidin and chymotrypsin are quite different. It can be surmised that the interaction of ExtrAvidin on the boronic acid surface involves coordination reactions and this interaction is in general likely to occur with any non-glycosylated protein; this should be diminished through use of Tris, as demonstrated here. However, one might suspect that the use of Tris will drastically affect the sensitivity or the responsivity of the surface for glycoprotein binding. As the results suggest, only a mere 30% reduction in the amount of avidin binding is observed. This is likely a consequence of competitive boronic acid binding of Tris versus the sugar chain in avidin. However, as is evident in Figure 2.4A, the larger SPR response of avidin compared to ExtrAvidin indicates that better specificity is achieved by using Tris buffer.

Outcomes from the systematic comparison between RNAse A and B and avidin and ExtrAvidin made here thus strongly suggest that the selectivity of boronic acids can be diminished by non-specific secondary interactions. In general, it is inferred that for boronic acid systems to be entirely discriminatory against non-glycosylated proteins, secondary interactions must be taken into consideration and should facilitate in determining experimental conditions that can increase the selectivity of boronic acid systems for glycoprotein analysis. In the work

herein, a change in buffer system is found to have a profound impact on the selectivity of the boronic acid capture system.

2.4 Conclusions

Interaction analysis between glycoproteins and the boronic acid derivative, AECPBA, was evaluated using AECPBA-derivatized carboxymethyl dextran-coated gold substrates by surface plasmon resonance spectroscopy. Glycoprotein binding to the boronic acid surface was determined to be a function of the terminal saccharide moiety, information that is potentially useful in the design of surface-capture protein concentration devices and for studies on boronic acid interactions with glycoproteins on cell surfaces. Importantly, glycoproteins that are bound to the AECPBA surfaces can be removed readily using borate buffer at moderately elevated pH. The selectivity of immobilized boronic acids can be affected by non-specific secondary interactions, but these secondary interactions can be identified and decreased, thereby allowing for increased glycoprotein separation capability of boronic acid systems on surfaces.

2.5 References

(1) Tian, Y.; Zhang, H. Glycoproteomics and clinical applications. *Proteomics: Clin. Appl.* **2010**, *4*, 124-132.

(2) Orntoft, T. F.; Vestergaard, E. M. Clinical aspects of altered glycosylation of glycoproteins in cancer. *Electrophoresis* **1999**, *20*, 362-371.

(3) Liu, J. T.; Chen, L. Y.; Shih, M. C.; Chang, Y.; Chen, W. Y. The investigation of recognition interaction between phenylboronate monolayer and glycated hemoglobin using surface plasmon resonance. *Anal. Biochem.* **2008**, *375*, 90-96.

(4) Kitano, H.; Anraku, Y.; Shinohara, H. Sensing capabilities of colloidal gold monolayer modified with a phenylboronic acid-carrying polymer brush. *Biomacromolecules* **2006**, *7*, 1065-1071.

(5) Anraku, Y.; Takahashi, Y.; Kitano, H.; Hakari, M. Recognition of sugars on surface-bound cap-shaped gold particles modified with a polymer brush. *Colloids Surf., B* **2007**, *57*, 61-68.

(6) Soh, N.; Sonezaki, M.; Imato, T. Modification of a thin gold film with boronic acid membrane and its application to a saccharide sensor based on surface plasmon resonance. *Electroanalysis* **2003**, *15*, 1281-1290.

(7) Gabai, R.; Sallacan, N.; Chegel, V.; Bourenko, T.; Katz, E.; Willner, I. Characterization of the swelling of acrylamidophenylboronic acid-acrylamide hydrogels upon interaction with glucose by faradaic impedance spectroscopy, chronopotentiometry, quartz-crystal microbalance (QCM), and surface plasmon resonance (SPR) experiments. *J. Phys. Chem. B* **2001**, *105*, 8196-8202.

(8) Chen, H. X.; Lee, M.; Lee, J.; Kim, J. H.; Gal, Y. S.; Hwang, Y. H.; An, W. G.; Koh, K. Formation and characterization of self-assembled phenylboronic acid derivative monolayers toward developing monosaccharide sensing-interface. *Sensors* **2007**, *7*, 1480-1495.

(9) Matsumoto, A.; Ikeda, S.; Harada, A.; Kataoka, K. Glucose-responsive polymer bearing a novel phenylborate derivative as a glucose-sensing moiety operating at physiological pH conditions. *Biomacromolecules* **2003**, *4*, 1410-1416.

(10) Singhal, R. P.; Desilva, S. S. M. Boronate affinity-chromatography. *Adv. Chromatogr.* **1992**, *31*, 293-335.

(11) Liu, X.-C. Boronic acids as ligands for affinity chromatography. *Chin. J. Chromatogr.* **2006**, *24*, 73-80.

(12) Lorand, J. P.; Edwards, J. O. Polyol complexes and structure of the benzeneboronate ion. *J. Org. Chem.* **1959**, *24*, 769-774.

(13) Iwatsuki, S.; Nakajima, S.; Inamo, M.; Takagi, H. D.; Ishihara, K. Which is reactive in alkaline solution, boronate ion or boronic acid? Kinetic evidence for reactive trigonal boronic acid in an alkaline solution. *Inorg. Chem.* **2007**, *46*, 354-356.

(14) Lijuang, Z.; Haojie, L.; Pengyuan, Y. Specific enrichment methods for glycoproteome research. *Anal. Bioanal. Chem.* **2010**, *396*, 199-203.

(15) Lee, M.; Kim, T. I.; Kim, K. H.; Kim, J. H.; Choi, M. S.; Choi, H. J.; Koh, K. Formation of a self-assembled phenylboronic acid monolayer and its application toward developing a surface plasmon resonance-based monosaccharide sensor. *Anal. Biochem.* **2002**, *310*, 163-170.

(16) Takahashi, S.; Anzai, J.-I. Phenylboronic acid monolayer-modified electrodes sensitive to sugars. *Langmuir* **2005**, *21*, 5102-5107.

(17) Pribyl, J.; Skládal, P. Quartz crystal biosensor for detection of sugars and glycated hemoglobin. *Anal. Chim. Acta* **2005**, *530*, 75-84.

(18) Fujii, E.; Shimizu, K.; Kurokawa, Y.; Endo, A.; Sasaki, S.; Kurihara, K.; Citterio, D.; Yamazaki, H.; Suzuki, K. Determination of glycosylated albumin using surface plasmon resonance sensor. *Bunseki Kagaku* **2003**, *52*, 311-317.

(19) Liu, S. Q.; Bakovic, L.; Chen, A. C. Specific binding of glycoproteins with poly(aniline boronic acid) thin film. *J. Electroanal. Chem.* **2006**, *591*, 210-216.

(20) Wilson, W. D. Analyzing biomolecular interactions. *Science* **2002**, *295*, 2103-2105.

(21) Stenberg, E.; Persson, B.; Roos, H.; Urbaniczky, C. Quantitative determination of surface concentration of protein with surface plasmon resonance using radiolabeled proteins. *J. Colloid Interface Sci.* **1991**, *143*, 513-526.

(22) Davis, T. M.; Wilson, W. D. Determination of the refractive index increments of small molecules for correction of surface plasmon resonance data. *Anal. Biochem.* **2000**, *284*, 348-353.

(23) Green, N. M.; Anfinsen, C., Jr.; Edsall, J.; Richards, F. Avidin. In *Advances in protein chemistry*; Academic Press: New York, 1975; Vol. 29, p 85-133.

(24) Delange, R. J. Egg white avidin. 1. Amino acid composition-sequence of amino-terminal and carboxyl-terminal cyanogen bromide peptides. *J. Biol. Chem.* **1970**, *245*, 907-916.

(25) Huang, T. S.; Delange, R. J. Egg white avidin. 2. Isolation, composition, and amino acid sequences of tryptic peptides. *J. Biol. Chem.* **1971**, *246*, 686-697.

(26) Bruch, R. C.; White, H. B. Compositional and structural heterogeneity of avidin glycopeptides. *Biochemistry* **1982**, *21*, 5334-5341.

(27) van der Merwe, P. A.; Barclay, A. N. Analysis of cell-adhesion molecule interactions using surface plasmon resonance. *Curr. Opin. Immunol.* **1996**, *8*, 257-261.

(28) Lahiri, J.; Isaacs, L.; Tien, J.; Whitesides, G. M. A strategy for the generation of surfaces presenting ligands for studies of binding based on an active ester as a common reactive intermediate: A surface plasmon resonance study. *Anal. Chem.* **1999**, *71*, 777-790.

(29) Koyama, T.; Terauchi, K. Synthesis and application of boronic acid-immobilized porous polymer particles: A novel packing for high-performance liquid affinity chromatography. *J. Chromatogr. B* **1996**, *679*, 31-40.

(30) Bouriotis, V.; Galpin, I. J.; Dean, P. D. G. Applications of immobilized phenylboronic acids as supports for group-specific ligands in the affinity-chromatography of enzymes. *J. Chromatogr.* **1981**, *210*, 267-278.

(31) Li, Y.; Larsson, E. L.; Jungvid, H.; Galaev, I. Y.; Mattiasson, B. Shielding of protein-boronate interactions during boronate chromatography of neoglycoproteins. *J. Chromatogr. A* **2001**, *909*, 137-145.

(32) Zhang, X. T.; Wu, Y. F.; Tu, Y. F.; Liu, S. Q. A reusable electrochemical immunosensor for carcinoembryonic antigen via molecular recognition of glycoprotein antibody by phenylboronic acid self-assembly layer on gold. *Analyst* **2008**, *133*, 485-492.

(33) Maestas, R. R.; Prieto, J. R.; Kuehn, G. D.; Hageman, J. H. Polyacrylamide-boronate beads saturated with biomolecules - new general support for affinity-chromatography of enzymes. *J. Chromatogr.* **1980**, *189*, 225-231.

(34) Zou, Y.; Broughton, D. L.; Bicker, K. L.; Thompson, P. R.; Lavigne, J. J. Peptide borono lectins (PBLs): A new tool for glycomics and cancer diagnostics. *ChemBioChem* **2007**, *8*, 2048-2051.

(35) *Biacore sensor surface handbook*; Biacore: Uppsala, 2003.

(36) Spiro, R. G. Studies on fetuin, a glycoprotein of fetal serum. 1. Isolation, chemical composition, and physicochemical properties. *J. Biol. Chem.* **1960**, *235*, 2860-2869.

(37) Seligman, P. A.; Schleicher, R. B.; Allen, R. H. Isolation and characterization of the transferrin receptor from human-placenta. *J. Biol. Chem.* **1979**, *254*, 9943-9946.

(38) Hovanessian, A. G.; Awdeh, Z. L. Gel isoelectric focusing of human-serum transferrin. *Eur. J. Biochem.* **1976**, *68*, 333-338.

(39) Plummer, T. H., Jr.; Hirs, C. H. W. The isolation of ribonuclease B, a glycoprotein, from bovine pancreatic juice. *J. Biol. Chem.* **1963**, *238*, 1396-1401.

(40) Shang, W.; Nuffer, J. H.; Dordick, J. S.; Siegel, R. W. Unfolding of ribonuclease A on silica nanoparticle surfaces. *Nano Lett.* **2007**, *7*, 1991-1995.

(41) Nicholls, M. P.; Paul, P. K. C. Structures of carbohydrate-boronic acid complexes determined by NMR and molecular modelling in aqueous alkaline media. *Org. Biomol. Chem.* **2004**, *2*, 1434-1441.

(42) Otsuka, H.; Uchimura, E.; Koshino, H.; Okano, T.; Kataoka, K. Anomalous binding profile of phenylboronic acid with *N*-acetylneuraminic acid (Neu5Ac) in aqueous solution with varying pH. *J. Am. Chem. Soc.* **2003**, *125*, 3493-3502.

(43) Pezron, E.; Ricard, A.; Lafuma, F.; Audebert, R. Reversible gel formation induced by ion complexation. 1. Borax-galactomannan interactions. *Macromolecules* **1988**, *21*, 1121-1125.

(44) Satomi, Y.; Shimonishi, Y.; Hase, T.; Takao, T. Site-specific carbohydrate profiling of human transferrin by nano-flow liquid chromatography/electrospray ionization mass spectrometry. *Rapid Commun. Mass Spectrom.* **2004**, *18*, 2983-2988.

(45) Nilsson, B.; Norden, N. E.; Svensson, S. Structural studies on the carbohydrate portion of fetuin. *J. Biol. Chem.* **1979**, *254*, 4545-4553.

(46) Irimura, T.; Nicolson, G. L. Carbohydrate-chain analysis by lectin binding to mixtures of glycoproteins, separated by polyacrylamide slab-gel electrophoresis, with *in situ* chemical modifications. *Carbohydr. Res.* **1983**, *115*, 209-220.

(47) Bolivar, J. G.; Soper, S. A.; McCarley, R. L. Nitroavidin as a ligand for the surface capture and release of biotinylated proteins. *Anal. Chem.* **2008**, *80*, 9336-9342.

(48) Martwiset, S.; Koh, A. E.; Chen, W. Nonfouling characteristics of dextran-containing surfaces. *Langmuir* **2006**, *22*, 8192-8196.

(49) Plummer, T. H., Jr. Glycoproteins of bovine pancreatic juice. Isolation of ribonucleases C and D. *J. Biol. Chem.* **1968**, *243*, 5961-5966.

(50) Lee, C. S.; Belfort, G. Changing activity of ribonuclease A during adsorption: A molecular explanation. *Proc. Nat. Acad. Sci. U.S.A.* **1989**, *86*, 8392-8396.

(51) Livnah, O.; Bayer, E. A.; Wilchek, M.; Sussman, J. L. 3-dimensional structures of avidin and the avidin-biotin complex. *Proc. Nat. Acad. Sci. U.S.A.* **1993**, *90*, 5076-5080.

(52) Bayer, E. A.; Livnah, O.; Sussman, J. L.; Wilchek, M. The cryptic sugar residue of deglycosylated avidin. *Glycoconjugate J.* **1993**, *10*, 276-277.

(53) Bayer, E. A.; Demeester, F.; Kulik, T.; Wilchek, M. Preparation of deglycosylated egg-white avidin. *Appl. Biochem. Biotechnol.* **1995**, *53*, 1-9.

(54) Hiller, Y.; Gershoni, J. M.; Bayer, E. A.; Wilchek, M. Biotin binding to avidin. Oligosaccharide side chain not required for ligand association. *Biochem. J.* **1987**, *248*, 167-171.

(55) Li, Y.; Larsson, E.; Jungvid, H.; Galaev, I.; Mattiasson, B. Separation of neoglycoproteins with different degrees of glycosylation by boronate chromatography. *Chromatographia* **2001**, *54*, 213-217.

(56) Li, Y.; Larsson, E. L.; Jungvid, H.; Galaev, I. Y.; Mattiasson, B. Affinity chromatography of neoglycoproteins. *Bioseparation* **2000**, *9*, 315-323.

CHAPTER 3

PREPARATION, CHARACTERIZATION, AND EVALUATION OF 4-[(2-AMINOETHYL)CARBAMOYL]PHENYLBORONIC ACID–POLY(METHYL METHACRYLATE) SURFACES FOR GLYCOPROTEIN CAPTURE AND RELEASE

3.1 Introduction

Glycosylation of proteins has been identified as perhaps the most ubiquitous post-translational modification process that is involved in the human physiology and pathology known to date. In fact, roughly 50% of naturally-occuring proteins—albeit in minute quantities—have been identified as being glycosylated.[1-2] This fraction is likely an underestimate because a growing number of cancer and disease biomarkers are being found to be glycosylated.[2-4] In view of this, much effort is currently dedicated toward developing strategies and methodologies whose aim is the identification, isolation, and structural determination—in terms of sugar composition and glycosylation site—of glycoproteins,[1,5] especially in the context of establishing differences between normal and abnormally-expressed proteins.

Any advancement in glycoprotein analysis would aid in clinical diagnostics and therapeutics where applications can be realized toward point-of-care testing, an area that is becoming increasingly important for the early and cost-effective detection of cancer and other diseases. Advancing this burgeoning area of analysis is the implementation of biomicroelectromechanical sytems (bioMEMS)—or micrototal analysis systems (μTAS), lab-on-a-chip, or microfluidic devices—that were initially reported over a decade ago.[6-8] These systems hold the promise of improved analytical performance, minimal sample and reagent consumption, fast analysis time, portable format, component integration and automation, multiplexing, and economically-sound devices. These are precisely the advantages that are required if glycoprotein analysis is to advance to a level where physiological fluids can be easily processed.

Perhaps one of the biggest challenges being faced by glycoprotein analyses is the need for sensitive methods of analysis with low limits of target detection because glycoproteins exist in minute quantities in most clinical samples; for example, Yang and Hancock found that 10% (w/w) of human serum proteins were glycosylated,[9] while Whelan *et al.*[10] cited that disease-related proteins in serum amounts to 1% (i.e. 99% make up the highly abundant normal serum proteins). To this end, microfluidic-based glycoprotein analysis has begun to be investigated.[5,11-14] For example, a lectin affinity chromatograph in microfluidic format was able to achieve the separation of different glycoforms of egg white glycoproteins, which required pg amounts of glycoprotein samples.[12] Further improvement in sensitivity should be easily addressed by the coupling of microfluidics with mass spectrometry.[5]

Another major challenge in glycoprotein analysis is the inherent microheterogeneity of glycoproteins in a protein pool. Glycoproteins exist in glycoforms, different glycosylated variants of a particular glycoprotein. For example, chicken ovalbumin contains in its modification (glycosylation) site at Asn 293, 13 different glycans (sugar chains) that comprise the glycoforms of chicken ovalbumin.

Because of the aforementioned challenges in glycoprotein analyses, such analyses require proper protein isolation, separation, and preconcentration modalities prior to downstream protein processing/identification, such as by MS analysis. To achieve the first step of proper protein isolation, capture of all glycosylated proteins in a sample is necessary. Attempts to do so commonly include affinity-based isolation (concentration) techniques.[2,15] Lectins are often times used in these affinity capture methods, because they are proteins of non-immune origin that have a specificity toward a particular sugar residue in the glycoprotein. However, small structural

differences, such as in the case of glycoforms, may preclude isolation of other glycoproteins that may be of interest.

Therefore, the first step to any glycoprotein analysis should be the isolation of *all* glycoprotein components so to obtain more "global" information about the protein sample. Such an isolation strategy will require use of a capture agent/receptor that recognizes the general sugar motif of the various glycoproteins possible; a class of receptors that can perhaps fulfill this requirement is that based on boronic acids. As illustrated in various literature reports[16] and the previous chapter (Chapter 2), boronic acid derivatives exhibit general specificity toward glycoproteins, as they only discriminate between diol (1,2- or 1,3-)–containing versus non-diol–containing materials.

A variety of boronic acid-containing materials that may be appropriate for glycoprotein capture/isolation exist, both in the literature or as obtained from commercial sources. Several suppliers provide them as 3-aminophenylboronic acid covalently immobilized on polyacrylamide spherical gel beads (Affi-gel from Biorad and immobilized boronic acid gel from Pierce), on agarose beads (from Sigma or the Aminophenyl Boronate A6XL from ProMetic Biosciences), on acrylic beads (from Sigma), on polymethacrylate beads (TSKgel Boronate-5PW from Tosoh Bioscience), or as poly(methyl methacrylate)-bound boronic acid (the boric acid gel from Aldrich). Non-commercial preparations with 3-aminophenylboronic acid as the recognition element have been made on silica beads,[17-18] silica capillaries,[19] magnetic particles,[20-21] polymer beads,[22-23] glassy carbon electrodes,[24] gold electrodes,[25] and gold[26-29] and glass surfaces.[30] Magnetic glyco-capturing beads with immobilized boronic acid (Bruker Daltonic GMBH, Germany) afforded the largest number of glycoproteins captured from human serum compared to the beads with immobilized lectins (of broad sugar specificity);[20] this indicates that boronic acid

is a more global capture element than most commonly used lectins. Xu *et al.*[18] was able to demonstrate that glycopeptides from tryptic digest of a mixture of four glycoproteins were all isolated with the use of boronic acid-functionalized mesoporous silica; no glycopeptides were observed in the flow-through fraction (i.e. unbound fraction). This suggests 100% efficiency of glycopeptide binding to boronic acid materials.

While miniaturized lectin affinity chromatography has been explored in the literature,[12] a miniaturized system containing a boronic acid as the sensing element has not. Plastics or polymers—such as poly(methyl methacrylate) (PMMA), poly(dimethyl siloxane) (PDMS), polystyrene (PS), and polycarbonate (PC)—are established substrates for the fabrication of microanalytical devices and offer several advantages over their glass, SiO_2, or quartz counterparts, perhaps leading to their gain in popularity.[31-36] A few of the notable advantages that can be translated into superior qualities and capabilities for low-glass-transition temperature (T_g)[7,36-37] polymer-based microanalytical devices include capabilities to produce high-aspect-ratio microstructures (HARMS) using relatively inexpensive materials and a variety of micromachining methods that are easy to implement.

Perhaps one of the initial major disadvantages of using polymeric substrates for fabrication of microfluidic devices—that made them somewhat inferior to glass—was their inert nature towards surface chemical modification. Unlike glass for which silane-based derivatization methods are well-established, many polymeric substrates lack the functional handle to accommodate various ligands on its surface that are suitable for a variety of applications. However, polymeric substrates have seen a boost in the area of chemical modification over the years. For PMMA in particular, carboxylic acids were introduced by UV irradiation[33] and oxygen plasma treatment.[32] Amine-terminated surfaces were prepared by

aminolysis reactions.[34,38] PMMA sheets with integrated and exposed glycidyl methacrylate groups (PGMAMMA) were prepared by thermally-induced, free-radical polymerization, and further elaboration of the reactive glycidyl groups was performed via amination.[39]

To date, no boronic acid derivatives have been immobilized on the surface of polymeric microfluidic devices and subsequently used as possible capture elements. Because of the surface modification chemistries available and the widespread use of PMMA in the construction of microfluidic devices, I have investigated the immobilization of an amino-boronic acid derivative on PMMA surfaces. This chapter presents the preparation of4-[(2-aminoethyl)carbamoyl]phenyl-boronic acid-functionalized PMMA, AECPBA–PMMA, surfaces through simple carbodiimide coupling on carboxylic acid-terminated PMMA, and its subsequent surface characterization by X-ray photoelectron spectroscopy (XPS), carminic acid method, and contact angle titration. Initial modification of the surface to yield carboxylic acid groups was accomplished using UV irradiation; a protocol that is reliable, convenient and easy to perform. Preparation of this boronic acid-modified PMMA surface was the first step toward developing microfluidic enrichment and sepration channels for glycoproteins. Protein (glycosylated and non-glycosylated) adsorption on and desorption from the AECPBA–PMMA surface was examined. Non-specific adsorption of proteins—by hydrophobic interactions—on the surface was addressed during the binding and elution process.

3.2 Experimental Section

3.2.1 Materials

AECPBA was prepared as previously reported.[40] Poly(methyl methacrylate), PMMA, sheets (0.50-mm thickness, impact-modified) were obtained from Goodfellow (Huntington, England). Avidin, BSA, fetuin, asialofetuin, human transferrin, and cytochrome C were obtained

from Sigma. 1-Ethyl-3-[3-dimethylaminopropyl]carbodiimide hydrochloride (EDC, Sigma), 2-(*N*-morpholino)ethanesulfonic acid (MES, Sigma, 99%), 4-(2-hydroxyethyl)-1-piperazineethanesulfonic acid (HEPES, Sigma), 4-carboxyphenylboronic acid (CPBA, Aldrich), carmine dye (Acros, high purity), tris(hydroxymethyl)aminomethane (Tris, Sigma), glycine (Sigma, 99%), Tween 20 (Fluka), boric acid (EM Sciences), isopropanol (EMD, HPLC grade), and sulfuric acid (Fisher, ACS grade) were used as received. All solutions were prepared in Nanopure water (Barnstead, >18 MΩ·cm).

3.2.2 Preparation of AECPBA–PMMA Surface

Poly(methyl methacrylate), PMMA, pieces (3 × 1 × 0.05 cm) were cleaned by sonication in 25% isopropanol (IPA), rinsed with nanopure water, and dried with house N_2. Both faces of the PMMA were exposed to UV light for 30 minutes each, cooled to room temperature, and placed in small capped vials. The home-built UV light source is made of a low-pressure mercury lamp with an emission spectrum from 240 to 425 nm where the strongest intensity band is centered at 254 nm. To each vial was added 2.00×10^{-3} g of 4-[(2-aminoethyl)carbamoyl]phenylboronic acid, AECPBA, and immediately followed by 2.00 mL of 5.0×10^{-4} M EDC in pH 5.00, 0.0250 M MES buffer. The final mixture contained the PMMA piece, 5.00×10^{-3} M AECPBA, and 5.0×10^{-4} M EDC. The samples were shaken at room temperature for 20 h. The solution was removed, and the PMMA pieces were shaken with 1.00 mL of pH 8.50, 0.050 M ethanolamine solution for 30 min to cap any remaining activated carboxylic acid groups. The PMMA pieces were removed, rinsed with MES buffer and nanopure water, and dried with house N_2. In cases where small sample sizes were needed, the AECPBA–PMMA pieces were cut to the desired size with scissors.

3.2.3 Surface Concentration of AECPBA Using the Carminic Acid Method

The carmine solution was prepared by dissolving 0.09200 g of carmine dye in concentrated sulfuric acid to make 100.00 mL dye solution. *Note: Dissolution of carmine dye in concentrated sulfuric acid is exothermic. Small volume increments of concentrated sulfuric acid were added to the dye with swirling.* The boric acid standard solutions were prepared in nanopure water and the 4-carboxyphenylboronic acid (CPBA) standard solutions were prepared in DMSO. The AECPBA–PMMA pieces were placed in soda lime test tubes and exposed to 2.00 mL of concentrated sulfuric acid for 1 min to dissolve the surface of the AECPBA–PMMA. The AECPBA–PMMA pieces were taken out, and to the resulting solutions a drop of concentrated hydrochloric acid were added while on ice bath to remove any nitrates present. 5.00 mL of concentrated sulfuric acid was added in small volume increments with occasional shaking. After the solution cooled to room temperature, 5.00 mL of the carmine dye solution was added and the tubes were capped and inverted several times to become homogeneous. The solutions were allowed to stand for 1 h in the dark for color development. The same procedure was performed for the standard solutions. The absorbances of the solutions were determined at 606 nm in a quartz cuvette using a Cary 50 UV-vis spectrophotometer.

3.2.4 Contact Angle Titration of AECPBA–PMMA Surfaces

Sessile-drop contact angle measurements were performed with a VCA goniometer. ~2 μL drops of buffered solutions were placed on the AECPBA–PMMA surface using the automated syringe and the contact angle was determined using the software provided. A few seconds was allowed to let the droplet equilibrate on the surface. The contact angle for each surface and pH were measured at several locations on the surface. A new surface was used each time the pH of the solution was changed.

3.2.5 Binding of Glycosylated and Non-glycosylated Proteins on the AECPBA–PMMA Surface and Their Subsequent Elution

To 1 × 1 cm pieces of AECPBA–PMMA in a small vial was added 1.00 mL of solutions of proteins (glycosylated and non-glycosylated) prepared in pH 8.00, 0.050 M glycine buffer with 0.150 M NaCl and 0.05% (v/v) Tween 20 (GBST). The mixture was shaken at room temperature for 1 h. The AECPBA–PMMA pieces were removed and rinsed with the same glycine buffer and then nanopure water, dried with house N_2, and left overnight under high vacuum. For experiments where elution was performed, after the AECPBA–PMMA piece was removed, it was shaken at room temperature in 2.00 mL of pH 10.00, 0.10 M borate with 0.30 M NaCl and 0.005% (v/v) Tween 20 for 2 to 4 times for 10 min each time. The AECPBA–PMMA was rinsed with nanopure water, dried with house N_2, and left overnight under high vacuum.

3.2.6 Analysis by X-ray Photoelectron Spectroscopy (XPS)

The surfaces prepared were investigated using a Kratos AXIS 165 X-ray Photoelectron spectrometer. The samples were positioned on the sample holder using a double-sided adhesive Cu tape. X-ray sources used were either the monochromatic Al K_α (1486.6 eV) or the non-monochromatic Mg K_α (1253.6 eV). Each resulting survey (0–1200 eV) and high-resolution scans (eV range is element-dependent) were averages of at least two scans of each at defined pass energies. Spectra were collected at a photoelectron take-off angle of 90°. In all cases, the charge neutralizer was turned on to eliminate any charge effects on the non-conducting samples. The pressure of the anaysis chamber was maintained at 10^{-9} torr. Determination of atomic concentrations or elemental compositions was accomplished using the software provided by the manufacturer.

3.3 Background Information

3.3.1 Preparation of the AECPBA–PMMA Surface

The boronic acid derivative, 4-[(2-aminoethyl)carbamoyl]phenylboronic acid (AECPBA), used here was prepared according to the literature[40] and as decribed in Chapter 2. This boronic acid derivative is attractive as it offers a terminal amine functionality that can be utilized for surface attachment. In addition, the pK_a of the boronic acid is low (pK_a = 8.0), and this allows for the binding of diol groups at or near physiological pH. This low pK_a is advantageous, as the commonly used 3-aminophenylboronic acid has a pKa of 8.88. Surface modification of the PMMA is essential in order to provide a functional handle to which subsequent surface modifications may be performed. For PMMA, carboxylic acid groups can be formed by direct UV exposure in an oxygen-rich environment. The PMMA surface was exposed to UV radiation with a maximum exposure time of 30 min. The formation of surface carboxylic acid was verified by contact angle measurements and the values found are consistent with the literature.[33] Following the creation of carboxylic acid-terminated PMMA (CT–PMMA), AECPBA was introduced on the surface via aqueous carbodiimide coupling.

3.3.2 X-ray Photoelectron Spectroscopy (XPS)

Most of the results presented here are obtained from XPS analysis and therefore this section is devoted to some background information about XPS. Since the development by Kai Siegbahn (Uppsala, Sweden) of what was then called Electron Spectroscopy for Chemical Analysis (ESCA),[41] currently formally known as X-ray Photoelectron Spectroscopy (XPS), the technique has become an essential tool for surface analyses. XPS operates by the photoelectric effect whereby X-ray light, upon interacting with a surface, transfers energy to the core level electrons thereby causing photoemission. The ejected photoelectron has an associated energy

(binding energy, E_B) that is characteristic of the element and its atomic orbital. The binding energy is defined as $E_B = h\nu - E_K - W$, where $h\nu$ is the X-ray energy, E_K is the kinetic energy of the photoelectron, and W is the spectrometer work function. The atom relaxes by having a lower energy electron occupy the hole created in the higher energy orbital with subsequent ejection of a low energy electron (Auger electron) or X-ray fluorescence. The surface sensitivity of XPS arises from the short distance that the photoelectrons can traverse the solid before suffering from energy loss through inelastic scattering (inelastic mean free pathlength or IMFP, λ) even though the X-ray penetration depth is 10^2–10^3 nm. This sampling depth is therefore defined as $d = 3\lambda$.

XPS can provide both qualitative and quantitative information. Because binding energy is an intrinsic property of the atom, XPS can yield elemental composition of the surface. In addition, the binding energy of a given element is influenced by its chemical environment; therefore, chemical shifts arise which depends on the chemical state of the atom. Atomic concentration can be determined from peak area or intensity calculations. The intensity of the photoelectron peak is given by $I = J\rho\sigma K\lambda$ where J is the photon flux, ρ is the concentration of atom or ion in the solid surface, σ is the cross-section for photoelectron emission, K is the instrumental factors, and λ is the IMFP. The atomic concentration of a particular element (A) is then calculated by $A\% = [(I_A/F_A)/\Sigma\,(I/F)]\times 100$ where F is the sensitivity factor that is a function of σ, K, and λ.

A typical spectrometer contains an X-ray source, a monochromator, an electron energy analyzer, and a detector. The system is operated under ultra-high vacuum (UHV) because of surface sensitivity. The X-ray source consists of an Al or Mg anode that is capable of producing 1486.6 eV (Al K_α) and 1253.6 eV (Mg K_α) photon energy upon bombardment of the anode by high energy electrons from a thermal source. A monochomator is often used for Al K_α sources

and is made of crystalline quartz; a narrow X-ray line is selected via interference effects. The resulting X-ray photoelectron spectrum from a monochromatized source has a lower background, free of X-ray satellite peaks and bremsstrahlung continuum, and has narrower XPS peaks. The electron energy analyser often used is a hemispherical sector analyser (HSA), an analyser that consists of an outer and inner hemisphere which separates photoelectrons according to energy (i.e. a larger radius is traversed by high energy photoelectrons and a smaller radius is traversed by low energy photoelectrons). At the end of the analyser, several channel detectors (electron multiplier) collect the photoelectrons.

3.4 Results and Discussion

3.4.1 Characterization of the AECPBA–PMMA Surface

The accumulation of boronic acid species on the surface of the PMMA was followed by XPS. In Figure 3.1 are shown B 1s and N 1s spectra for carboxyl-terminated PMMA (CT–PMMA) surfaces that were exposed to EDC and/or AECPBA. The peak observed at 190 eV and the large signal at 399 eV for the CT–PMMA exposed to EDC and AECPBA are characteristic of boron and nitrogen, respectively, and indicates the presence of AECPBA on the surface. When the B 1s and the N 1s regions were examined for the CT–PMMA exposed to EDC or AECPBA alone (controls), there was no observable peak at 190 eV but there is an exceedingly low amount of nitrogen signal at 399 eV. In addition, CT–PMMA exposed to EDC and 4-carboxyphenylboronic acid did not lead to observation of a peak at 190 eV (data not shown); 4-carboxyphenylboronic acid is carboxylic acid-terminated, therefore it will not attach to the CT–PMMA surface by the carbodiimide coupling reaction. Taken together, these results indicate that the observed B 1s and N 1s signals for the CT–PMMA exposed to EDC and AECPBA is a result of covalent attachment of AECPBA to the PMMA surface via an amide

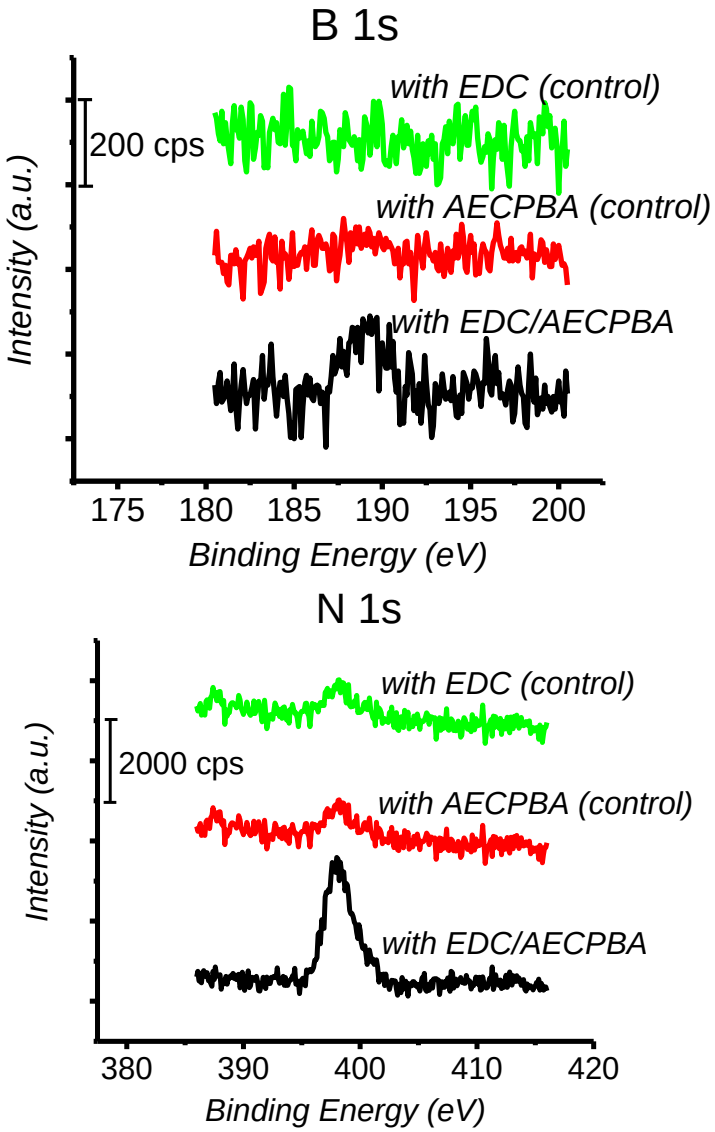

Figure 3.1. Representative X-ray photoelectron spectra in the B 1s and N 1s regions for CT–PMMA surfaces that were exposed to the carboxylic acid-activating agent EDC and/or the boronic acid derivative AECPBA.

bond. However, it should be noted that the characteristic B 1s peak observed here may not be due to the trigonal boronic acid or tetrahedral boronate ion. Several reports on SAMS of boronic acid on Au pointed to the formation of boronic anhydrides under UHV conditions (during XPS data acquisition).[42-43] Therefore, the observed chemical shift of boron obtained here may be due to the anhydride form. Regardless of what occurs in UHV, the boronic acids on the PMMA

surface should have the trigonal/tetrahedral form under ambient conditions that is necessary for diol binding, as boronic anhydrides are unstable under these conditions.[42-43]

In order to increase the surface boronic acid density, the number of carboxylic acid sites on the CT–PMMA can be increased. It can be hypothesized that the greater the number of ligand attachment sites available, the higher would be the number of ligands that can be attached to the surface, under the assumption that the efficiency of reaction is constant regardless of surface functional group density. It was found that the carboxylic acid concentration on the PMMA surface increases with UV irradiation time.[33] Therefore, the PMMA was exposed to UV radiation at various times and then covalent coupling of AECPBA via EDC coupling was carried out. The experimental conditions were kept constant throughout; the only difference is the length of UV irradiation time. As shown in Figure 3.2, the B 1s and N 1s peaks characteristic of the AECPBA on the PMMA surface increases with UV irradiation time. Atomic concentrations in Table 3.1 demonstrate that the boron and nitrogen content increases with the length of exposure of the PMMA surface to UV radiation, an indication that the number of AECPBA molecules on the surface increased as the number of surface carboxylic acid groups increased. Due to the inherently low signals obtained for B 1s —the intensity of XPS transitions decreases with atomic number—all elemental scans were performed at 160 eV pass energy from which the atomic concentrations were calculated. The UV irradiation time was limited to a maximum of 30 min as the surface concentration of carboxylic acid does not increase significantly beyond a 30-min exposure;[33] therefore, the amount of AECPBA on the surface is not expected to increase significantly beyond the 30-minute UV exposure, unless a different modification protocol were to be employed.

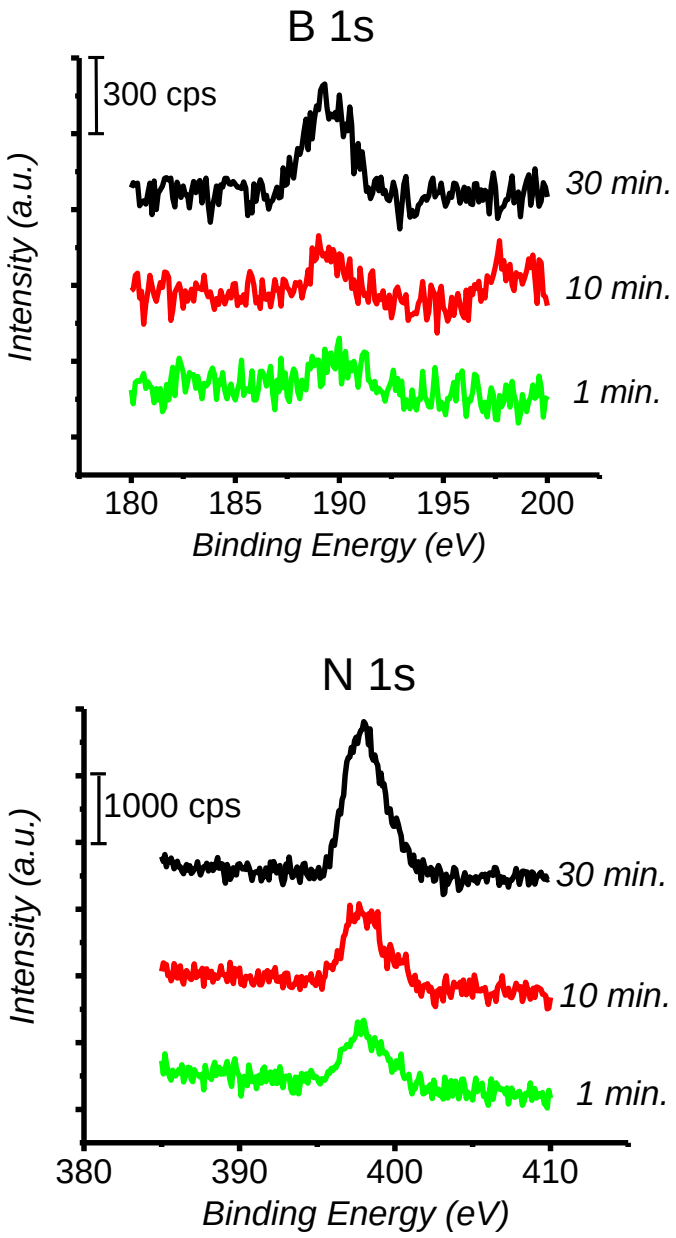

Figure 3.2. Representative X-ray photoelectron spectra in the B 1s and N 1s regions for AECPBA–modified PMMA surfaces as a function of the initial UV exposure time.

The surface concentration of AECPBA was determined with a colorimetric method that used the carmine method.[44-45] The presence of boron is verified by a color change from bright red to blue and can be followed spectrophotometrically. Using this method, the AECPBA

surface concentration was calculated to be 1.52 ± 0.39 nmol cm^{-2} from an initial 30-min UV exposure time. In contrast, a close-packed monolayer of thioaliphatic acid–3-aminophenylboronic acid conjugate SAM on Au gave rise to a 0.33 nmol cm^{-2} surface coverage.[26-27] Currently, the rationale for this greater-than-monolayer coverage is not known. However, it should be noted that the value determined here is calculated without correction for surface roughness of the AECPBA–PMMA surface. In the absence of a topographical image of the AECPBA–PMMA surface, a corrected surface coverage cannot be accurately determined. However, if the same rough surface of a CT–PMMA[33] is adopted following AECPBA attachment, the surface coverage is expected to be lower than 1.52 nmol cm^{-2}. Using the roughness correction factor (*R*) value previously determined for PMMA exposed to UV light for 30 min,[33] the surface coverage after correction for surface roughness is 1.42 ± 0.37. This value is still greater-than-monolayer coverage in comparison with the 0.33 nmol cm^{-2} surface coverage obtained for thioaliphatic acid–3-aminophenylboronic acid conjugate SAM on Au. However, with the type of AECPBA used here (boron is *para* to the organic "tail" compared to *meta* for the 3-aminophenylboronic acid in the SAM above), the molecular cross-sections on the surface of AECPBA and the thioaliphatic acid–3-aminophenylboronic acid conjugate SAM is not likely to be identical.[46] Hence, the 0.33 nmol cm^{-2} coverage for the latter may not be the same for a close-packed monolayer of AECPBA, and comparing the two values may be inappropriate. Regardless, this surface coverage should be the maximum attainable given that the CT–PMMA initially used has a surface coverage that was maximum with the UV modification protocol adapted. However, this does not indicate the degree of organization of the boronic acid derivatives on the surface. It is likely though that the molecules are arranged in a disordered fashion such that some patches of PMMA are exposed (*vide infra*).

Table 3.1. XPS quantification of the elemental composition of AECPBA–PMMA surfaces as a function of time of exposure of pristine PMMA to UV light that created the carboxylic acid groups that were used for the covalent attachment of AECPBA. The reported values are the average of 3 replicates with ± one standard deviation.

UV modification time (min)	Atomic Concentration (%)			
	C 1s	O 1s	N 1s	B 1s
1	79.01 ± 1.47	20.43 ± 1.58	0.47 ± 0.06	0.08 ± 0.09
10	76.16 ± 0.27	23.18 ± 0.39	0.56 ± 0.12	0.10 ± 0.02
30	71.28 ± 4.90	26.74 ± 4.51	1.68 ± 0.36	0.29 ± 0.04

In order to assess the surface properties of modified solids, contact angle goniometry is a convenient and versatile tool that provides information about the wettability of the surface (i.e. hydrophilicity or hydrophobicity of the surface). Upon contact of a surface with a contacting liquid, the contact angle at the gas-liquid-solid interface provides a measure of the interaction of the surface with the liquid, namely a polar or an apolar interaction. In general, hydrophilic and hydrophobic surfaces are characterized by a water contact angle of 0–30° and 70–90°, respectively. A surface with intermediate polarity would exhibit a contact angle between 30° and 70°.

Another important aspect of contact angle measurements is the capability to determine the acid-base behavior of surfaces that possess ionizable groups.[47-51] This technique, often referred to as contact angle titration, relies on the changes in hydrophilicity of the surface as a consequence of the ionization of the functional groups, and it forms the basis for determining thermodynamic properties such as surface pK_a.

The experiment was conducted by measuring the contact angle on freshly-prepared surfaces using buffered solutions of varying pH as the contact liquid. The contact angle was calculated using the software provided by the manufacturer. In addition, multiple measurements of contact angle were performed at different locations on freshly-prepared surfaces at each pH. The AECPBA–PMMA, that was prepared following a 30-min UV exposure, results in a contact angle titration curve that shows consistently high contact angle at pH values ≤ 6, and then a rapid decrease in contact angle followed by contact angle values that progressively decreased with pH. This break in the curve is assumed to represent the region where the pK_a of the surface lies, as the buffering capacity of the contact liquid should be adequate (0.050 M) so as to prevent any buffering effects by the surface ionizable groups. Thus, the dramatic change in the contact angle as pH is changed (Figure 3.3) suggests a change in the hydrophilicity of the surface due to ionization of groups on the surface. The pK_a of AECPBA in solution was experimentally determined in this work to be 8.0; therefore, the break in the curve and the subsequent decrease in contact angle can be regarded as a result of the transformation of the boronic acid derivative from a neutral trigonal boronic acid species to a charged tetrahedral boronate ion as a result of hydroxyl group introduction.[52] However, it should be noted that CT–PMMA (from a 30-min UV exposure) that was exposed to EDC only gave an almost identical titration curve except that it exhibited a more hydrophilic surface (lower contact angle) compared to the AECPBA–PMMA at almost all pH values examined. Both AECPBA–PMMA and EDC-exposed CT–PMMA are found to be less hydrophilic than the initial CT–PMMA. It is likely that the increase in contact angle of the EDC-exposed CT–PMMA at low pH values is a consequence of increased surface roughness due to the removal of low molecular weight polymers from the surface[33] after it is subjected to the e xperimental protocol (e.g. shaking, washing etc.). It is also evident that this

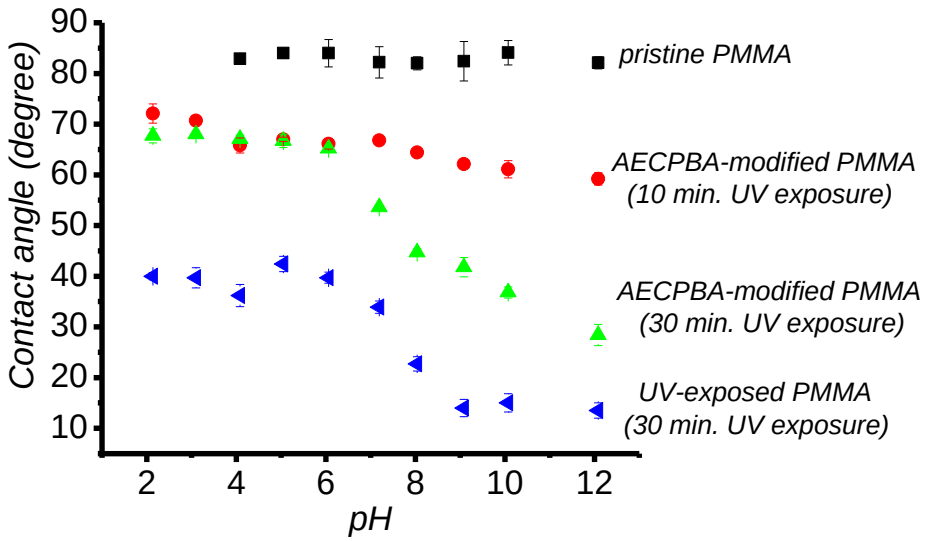

Figure 3.3. Sessile water drop contact angle titration of variously-treated PMMA surfaces: black squares–untreated PMMA; blue triangles–exposure to UV light for 30 min; green triangles–modified by exposure to UV radiation for 30 min (CT–PMMA) and subsequently reacted with the boronic acid derivative AECPBA via carbodiimide coupling; and red circles–modified by exposure to UV radiation for 10 min (CT–PMMA) and subsequently reacted with the boronic acid derivative AECPBA. Contact angles were determined using 2 μL of aqueous buffer solutions. Each point in the measurement is the average of 4–6 drops of contact liquid on fresh surfaces with ± one standard deviation being reported as the error.

EDC-exposed CT–PMMA surface has exposed carboxylic acid groups even after exposure to EDC, a possible outcome because the EDC-activated carboxylic acid groups are susceptible to hydrolysis in the absence of a nucleophile (i.e. the EDC-exposed CT–PMMA was not exposed to ethanolamine.[53] On the other hand, this surface can be distinguished from the AECPBA–PMMA surface because the latter exhibits a more hydrophobic surface (higher contact angle), consistent with the presence of aromatic rings on the AECPBA–PMMA surface. In general, the decrease in the contact angle for the AECPBA–PMMA surface can be attributed to the transformation of the AECPBA from boronic acid to boronate species and the ionization of any unreacted carboxylic acid groups. The surfaces probed for the contact angle titration experiment were not passivated with any capping reagent such as ethanolamine, therefore, any unreacted carboxylic acid would

be exposed to the contact liquid. Nevertheless, the AECPBA–PMMA surface is shown to exhibit acid-base behavior that is consistent with a surface possessing exposed ionizable groups that have the characteristics of a boronic acid with a pK_a similar to that of the AECPBA. An AECPBA–PMMA surface prepared from PMMA exposed to UV light for 10 min also exhibits a difference in hydrophilicity with pH, although it is not as significant as the AECPBA–PMMA from PMMA exposed to UV light for 30 min; this observation is consistent with a surface having a lower surface density of ionizable groups. In contrast, a pristine PMMA surface (i.e. the surface did not undergo modification by UV) had contact angles that were virtually constant (~ 83°) throughout the pH range studied. If there are any carboxylic acid groups that exist due to the manufacturing process or during storage,[33] the lack of a break in the contact angle-pH curve indicates that the carboxylic acid concentration is not sufficient to cause a sufficient enough change in the hydrophilicity of the surface resulting from the ionization process.

3.4.2 XPS Evaluation of Protein Binding to and Elution from AECPBA–PMMA Surfaces

Initial investigation of the capability of the AECPBA–PMMA surface to recognize and bind glycoproteins from solution, as well as demonstrate selectivity against non-glycosylated proteins, was conducted using avidin (glycosylated) and BSA (non-glycosylated), respectively. Avidin is a 68 kDa glycosylated protein containing four *N*-linked glycosylation sites that primarily consist of high mannose and hybrid-type oligosaccharide chains.[54-57] BSA is a 66 kDa protein that occurs naturally as non-glycosylated. This protein is also documented in the literature for its non-specific adsorption to surfaces.[32,58-60] Tris was used as the sample binding buffer according to its reported shielding effect that minimizes non-specific adsorption (via amino acid–boronic acid/boronate interaction) of non-glycosylated proteins (see Chapter 2). Figure 3.4 illustrates the adsorption of proteins on the AECPBA–PMMA surface as examined by

XPS. Because the N 1s core level signal is predominant in proteins but only occurs to a small extent on the AECPBA–PMMA surface—due to the amide nitrogen from attached AECPBA—it was chosen as the element to indicate the presence/absence of surface-adsorbed proteins. In comparison to an AECPBA–PMMA surface that was exposed to the binding buffer Tris (control), the significantly higher N 1s signal of the surface following its exposure to avidin

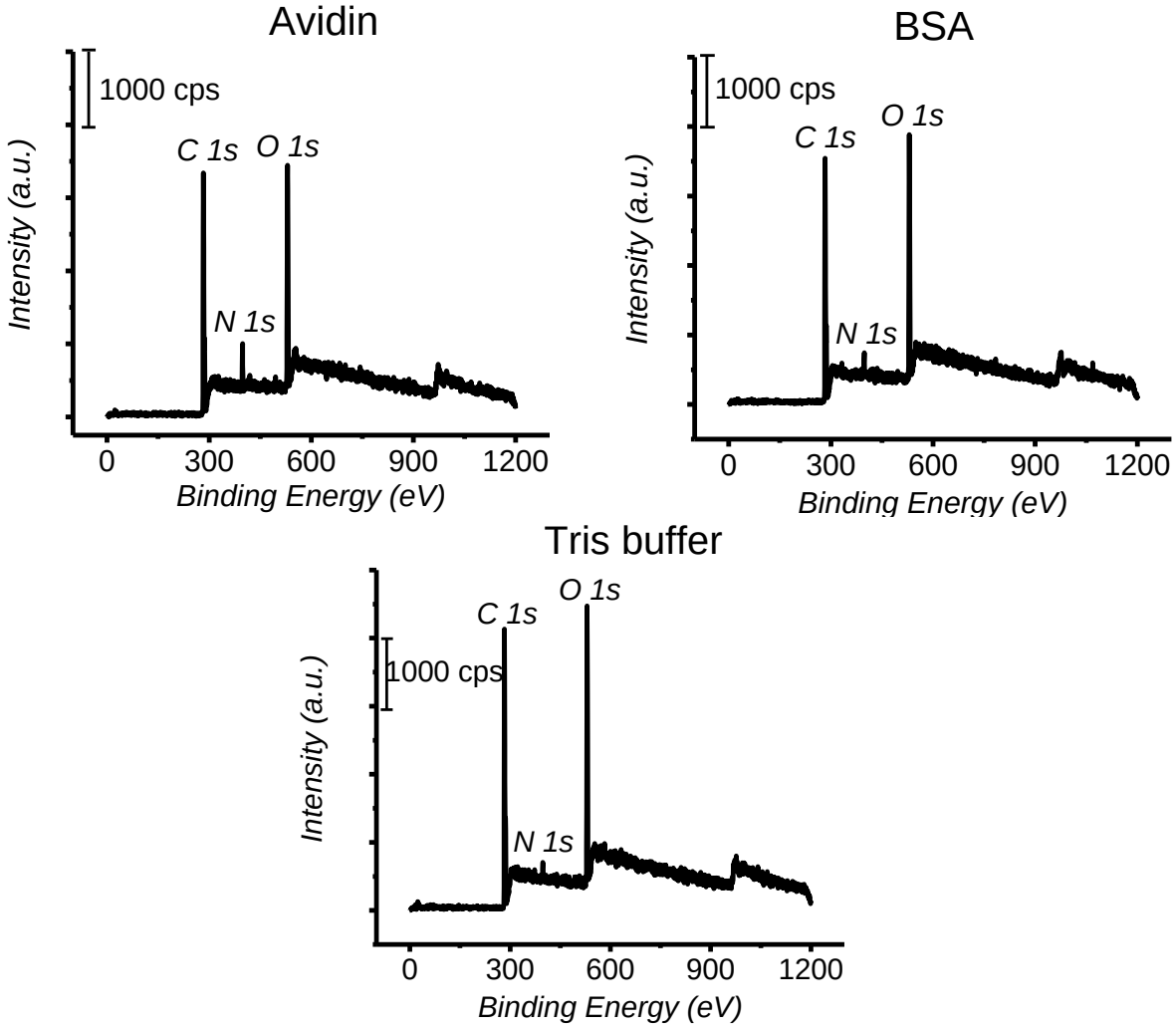

Figure 3.4. Representative X-ray photoelectron survey spectra for the AECPBA-modified PMMA surfaces after exposure to the glycoprotein avidin, non-glycosylated protein BSA, and pH 8.00 Tris-buffered saline. Protein solutions were prepared in pH 8.00, 0.050 M Tris with 0.50 M NaCl. Survey scans were obtained at 40 eV pass energy.

suggests that the protein was bound to it. On the other hand, a similar surface exposed to only BSA shows a smaller N 1s signal, although significant when compared to the control. Based on the difference in the N 1s signal, it is clear that there is preferential adsorption of the glycosylated avidin on the AECPBA–PMMA surface compared to the non-glycosylated BSA, an indication that the boronic acid–sugar interaction is dominant. Comparing the N 1s signal is valid here, as the proteins used have almost identical molecular weight indicating that they have more or less similar nitrogen content. Regarding the nature of the non-specific adsorption of BSA to the AECPBA-PMMA surface, it is likely attributed to hydrophobic interactions with any exposed underivatized PMMA region—BSA is known to adsorb on hydrophobic surfaces such as PMMA[58-59]—or with the phenyl ring of the boronic acid derivative.[61]

Attempts to remove (i.e. elute) the bound avidin from the surface started with the use of the most common eluting agent employed in boronic acid chromatography; a low pH buffer with a pH below the pK_a of the boronic acid derivative. This takes advantage of the boronic acid/boronate equilibria where conversion to the neutral trigonal boronic acid species—any diol-boronic acid interaction with the neutral species is unstable due to fast hydrolysis—is accomplished at a pH below the pK_a of the boronic acid. As shown in Figure 3.5, X-ray photoelectron survey spectra of AECPBA–PMMA surfaces that were exposed to avidin and subsequently exposed to a pH 5 eluting buffer did not result in a change in the N 1s signal (see the inset in Figure 3.5), suggesting that removal of bound avidin did not occur. This observation is consistent with that found on the AECPBA–CM5 sensor surface in Chapter 2. It would, therefore, be argued that electrostatic interaction is operative in this scenario, an interaction that is documented as one of the secondary interactions that is established (prevalent) in boronic acid systems,[61] which is why elution did not take place. It is of no question that this electrostatic

interaction is concomitantly occurring during the binding of avidin on the AECPBA–PMMA surface, as discussed previously for observations with the AECPBA–CM5 surface (Chapter 2). However, under the mechanism of elution that is offered by a low pH buffer (pH 5 in this case), there should not be a significant amount of ionized boronic acid present. Hence, electrostatic interactions would not occur during the eluting step with avidin, because its p*I* of 10–10.5 would render it net positively charged at pH 5. Therefore, a different mechanism of adsorption that resists the elution of bound avidin from the boronic acid surface must be operational (vide infra). A second attempt at elution was performed using pH 10 borate-buffered saline. From observations with the AECPBA–CM5 surface in Chapter 2, this eluting agent was successful in removing bound glycoproteins from that surface. However, Figure 3.6 illustrates that only 20% of bound avidin was removed from the surface.

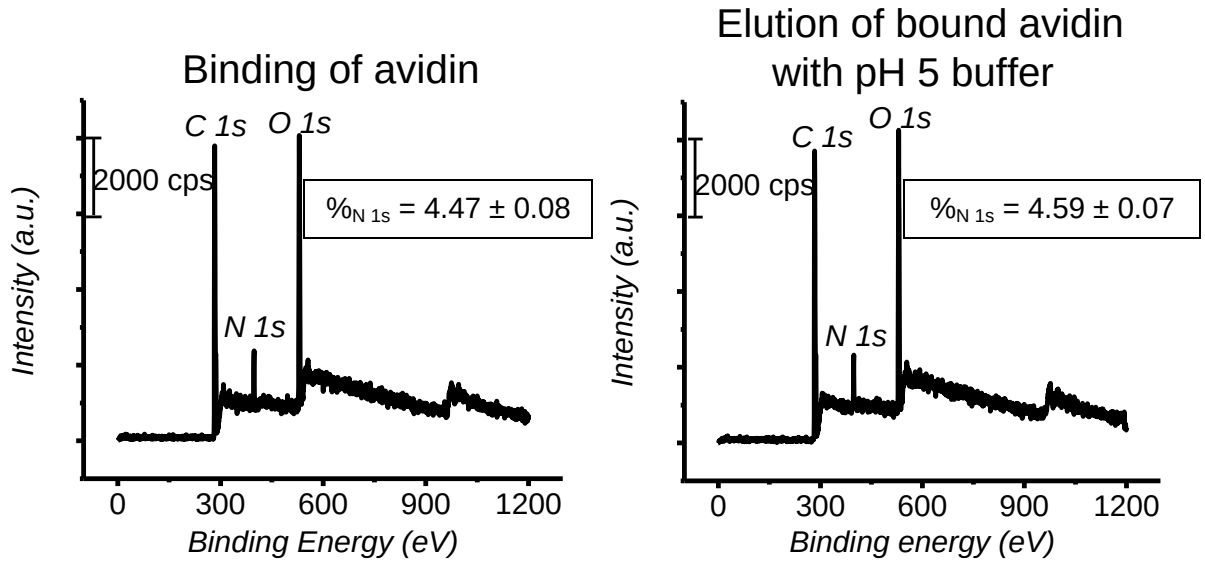

Figure 3.5. Representative X-ray photoelectron survey spectra showing the binding of the glycosylated protein avidin and its subsequent elution attempt using pH 5.00, 0.050 M acetate buffer. Binding of avidin was performed in pH 8.00, 0.050 M Tris with 0.50 M NaCl. Survey scans were obtained at 40 eV pass energy. Inset shows the XPS quantification value obtained for N 1s.

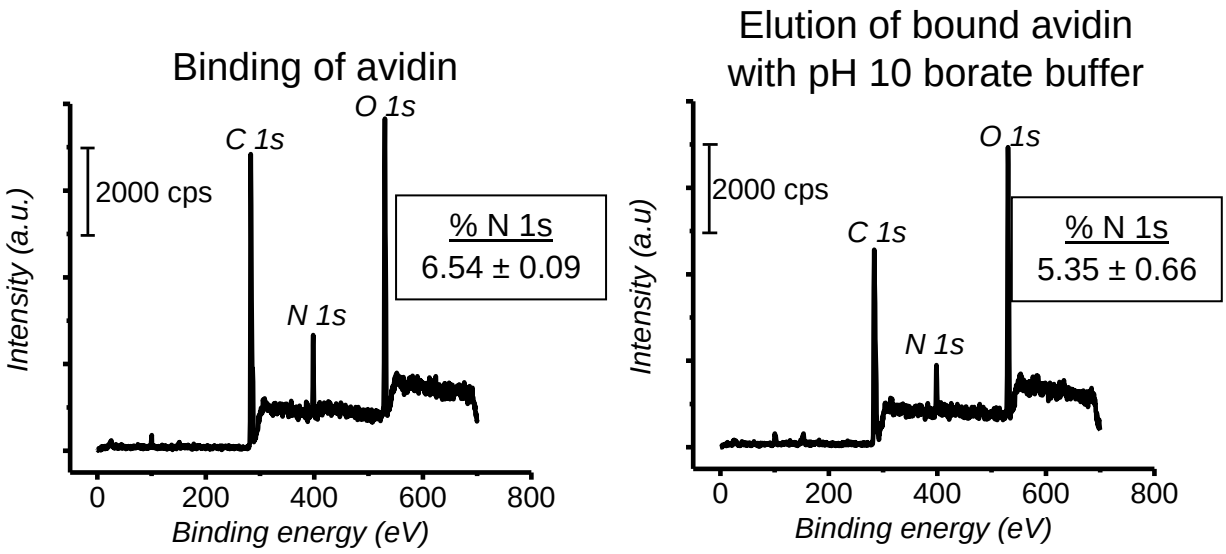

Figure 3.6. Representative X-ray photoelectron survey spectra showing the binding of the glycosylated protein avidin and its subsequent elution attempt using pH 10.00, 0.050 M borate with 0.30 M NaCl. Binding of avidin was performed in pH 9.00, 0.050 M Tris with 0.150 M NaCl. Survey scans were obtained at 40 eV pass energy. Inset shows the XPS quantification value obtained for N 1s.

These observations merited further investigation regarding the nature of adsorption of avidin on the AECPBA–PMMA surface even after exposure to eluting agents. It was later found, through a control experiment, that avidin exhibits non-specific adsorption to both CT–PMMA and even to hydroxyl-terminated PMMA (i.e. carboxylic acid groups on the PMMA was capped with ethanolamine by carbodiimide coupling) (Figure 3.7). Based on this outcome, the inability to elute the majority of bound avidin on the AECPBA–PMMA surface can be attributed to its adsorption to the underlying PMMA substrate. Although electrostatic attraction may account for the adsorption of avidin to CT–PMMA, this does not explain the observed adsorption to the hydroxyl-terminated PMMA, unless a substantial amount of the activated carboxylic acid groups are not accessible during the ethanolamine capping step, which would result in formation of carboxylic acid sites.

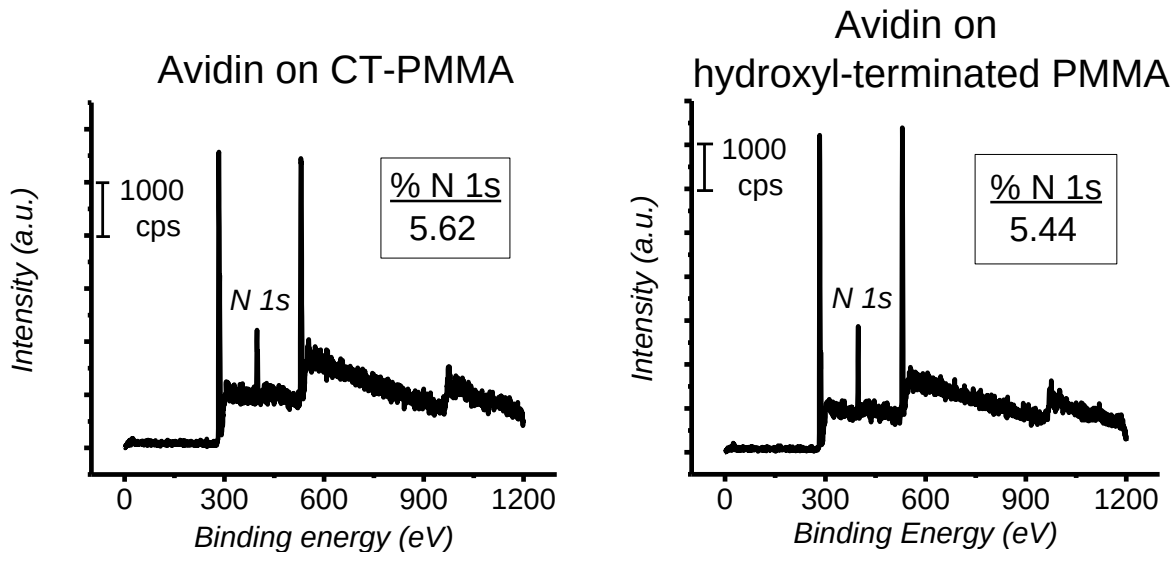

Figure 3.7 Representative X-ray photoelectron survey spectra showing the binding of the glycosylated protein avidin on carboxylic acid-terminated PMMA (CT–PMMA) and hydroxyl-terminated PMMA. Binding of avidin was performed in pH 8.00, 0.050 M Tris with 0.150 M NaCl. Survey scans were obtained at 40 eV pass energy. Inset shows the quantification value obtained for N 1s.

One possible scenario to explain the resistance of avidin elution from the AECPBA–PMMA surface is a hydrophobic interaction between the avidin and the AECPBA–PMMA surface. To test this hypothesis on the AECPBA–PMMA surface, the non-ionic surfactant Tween 20 was added to the pH 10 borate-buffered saline eluting agent. PMMA surfaces are known to be notorious with respect to hydrophobic interactions with proteins due to the somewhat hydrophobic nature of the surface.[32,60,62] In fact, significant efforts have been dedicated to address this issue of non-specific adsorption. Both dynamic coating[62-65] and surface grafting[32,60] methods have been used, and they have provided significant improvement in suppressing non-specific adsorption by passivating the PMMA surface with neutral hydrophilic residues. Dynamic coating is perhaps the most widely employed method because of its simplicity and the ease by which it is performed. Dynamic coating additives that have been successfully used to reduce/eliminate non-specific adsorption to the PMMA surface include

cellulose derivatives (e.g. methyl cellulose, hydroxypropylmethyl cellulose, and hydroxyethyl cellulose),[62-63,65] neutral polymers (e.g. poly(ethylene oxide) and poly(vinyl pyrrolidone)),[64] and non-ionic detergents (e.g. Tween 20).[65] Tween 20 was chosen herein to be investigated first because of its availability.

Without Tween 20, the quantity of eluted avidin amounted to 20%, while with Tween 20, it amounted to 26%. Although only a small difference is afforded by the addition of Tween 20, there is no doubt that Tween 20 facilitates in the suppression of non-specific adsorption to the AECPBA–PMMA surface, as will be shown later using other proteins. The observation made with Tween 20 thus indicates that there are non-derivatized hydrophobic PMMA regions even after capping of the AECPBA–PMMA surface with ethanolamine, such that even if borate was effective in breaking the diol–boronate interaction, hydrophobic interaction between the protein and the PMMA surface keeps the protein from being removed from the surface. This result arguably contradicts that surface coverage found, which is greater-than-a-monolayer coverage, for the AECPBA–PMMA surface. However, this may support the hypothesis that the AECPBA exists on the surface in a disordered fashion which allows patches or regions of PMMA to be exposed to the proteins.

In Figure 3.8 are shown the results for studies of protein binding to AECPBA–PMMA surfaces and their attempted elution as a function of protein category with respect to glycosylation (glycosylated and non-glycosylated) for several proteins. Assessment of protein binding on the AECPBA–PMMA surfaces was made using the N 1s XPS signal near 400 eV; to more readily track differences resulting from elution treatments, the recorded signals were normalized to an AECPBA–PMMA surface exposed to buffer solution not containing any protein. It should be noted that Tween 20 was added to the binding buffer so as to provide a

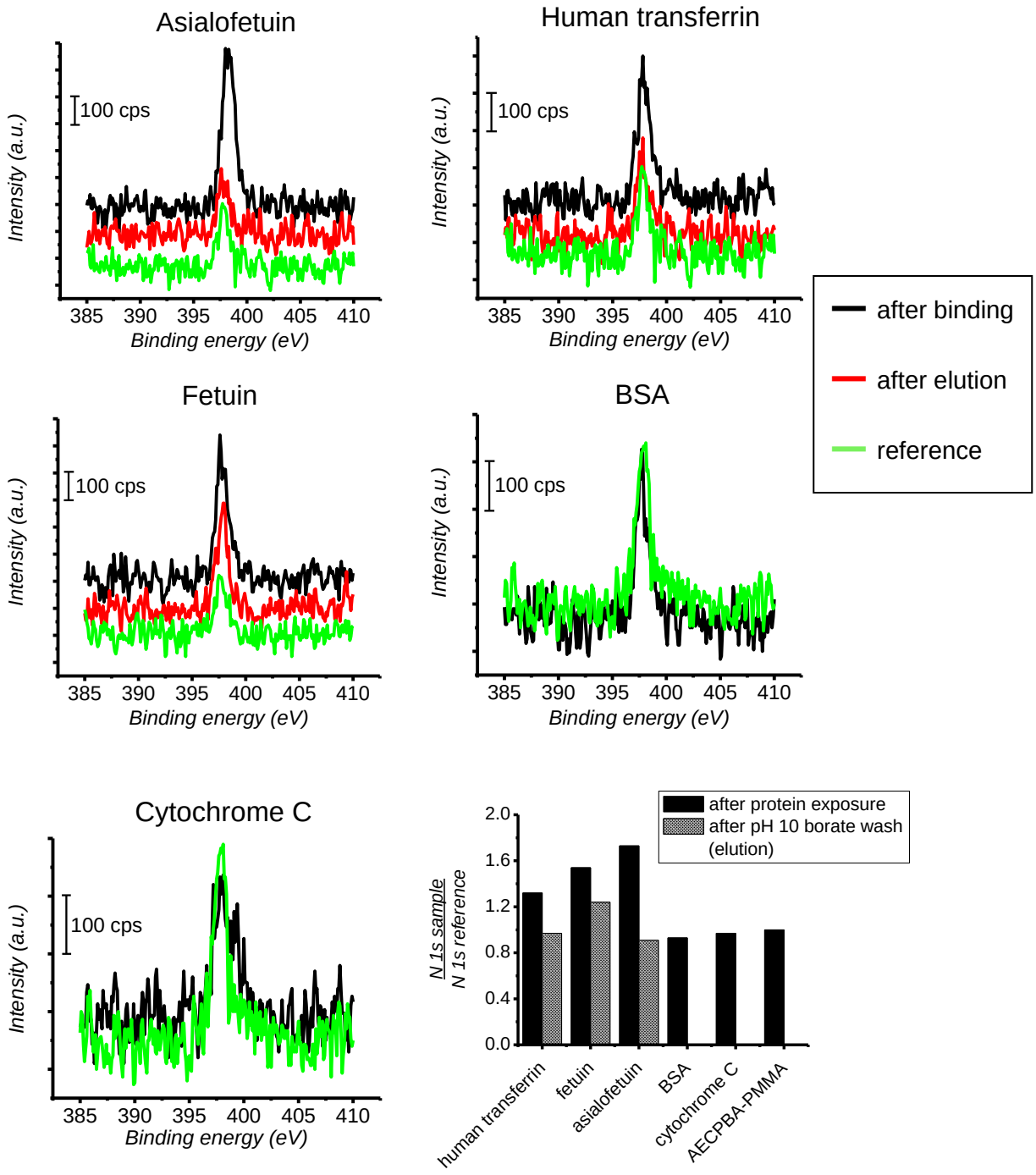

Figure 3.8. Representative high-resolution XPS N 1s scans of AECPBA–PMMA surfaces after exposure to glycosylated (asialofetuin, human transferrin, and fetuin) and non-glycosylated proteins (BSA and cytochrome C) and subsequent attempted elution of bound proteins by washing of the surfaces using a pH 10 borate-buffered saline solution containing Tween 20. Spectra were collected using a pass energy of 20 eV. Inset is the reference-normalized N 1s signal for the various proteins, before and after attempted elution with borate buffer.

dynamic coating that should prevent non-specific binding events. For all proteins examined here, whether glycosylated or non-glycosylated, there was no evidence of non-specific adsorption on CT–PMMA surfaces based on the lack of any measureable N 1s signal from these surfaces after exposure to the proteins in the presence of Tween 20; X-ray photoelectron spectra are given in Figure 3.9 for representative glycosylated and non-glycosylated proteins. Therefore, any binding to the AECPBA–PMMA surface by the glycoproteins can be attributed to the specific diol–boronate interaction, as well as any secondary interactions with the boronic/boronate ligand, as discussed in Chapter 2 (e.g. electrostatic, hydrogen bonding, hydrophobic, and coordination reactions).

Based on the significantly higher N 1s signal observed in Figure 3.8 for AECPBA–PMMA surfaces exposed to solutions of asialofetuin (a desialylated analogue of fetuin) versus the N 1s signal for AECPBA–PMMA surfaces not exposed to the protein, the asialofetuin is present. Subsequent regeneration of the surface (protein elution) was effected with the pH 10 borate-buffered saline containing Tween 20. It is quite important to note the near identical values for the N 1s signal of the eluted/regenerated asialofetuin-AECPBA–PMMA and reference AECPBA–PMMA surface, as this outcome strongly indicates that the initially bound asialofetuin was removed from the surface. A similar outcome is observed for AECPBA–PMMA surfaces exposed to the glycoprotein human transferrin. However, fetuin is not totally removed from the surface (~50%) upon attempted elution with the borate buffer. It is currently unclear why fetuin is not removed during this process, because asialofetuin—which is fetuin that has been desialylated by an enzymatic process and differs from fetuin by only the terminal sialic acid sugar residue—is removed from the AECPBA–PMMA surface following the same elution protocol.

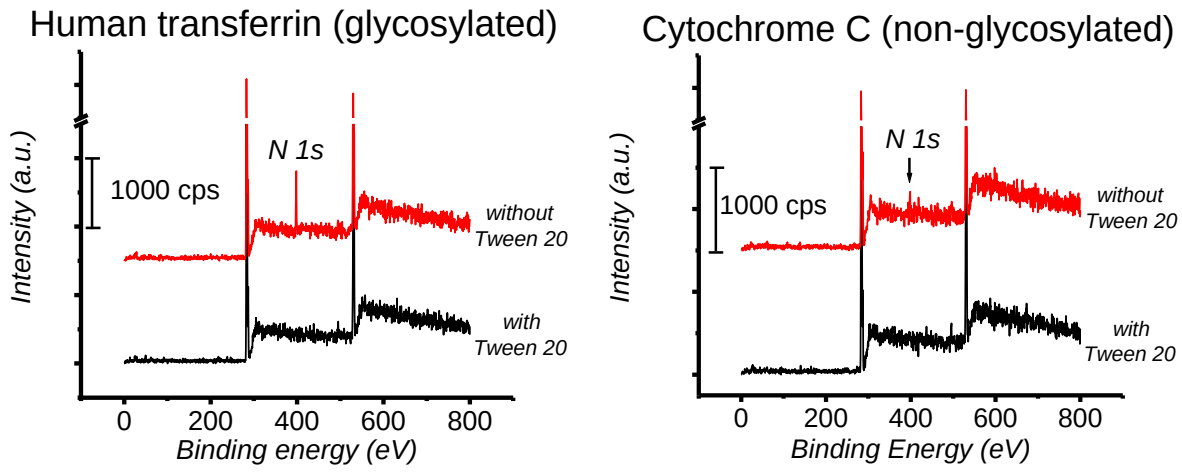

Figure 3.9 Representative X-ray photoelectron survey spectra showing the adsorption of human transferrin (glycosylated) and cytochrome C (non-glycosylated) on CT–PMMA surfaces in the presence/absence of Tween 20.

It is noteworthy that there is a similarity in the degree of binding of asialofetuin, fetuin, and human transferrin on the AECPBA–PMMA surface and on the AECPBA–CM5 surface described in Chapter 2. Asialofetuin, a glycoprotein whose glycan chains are terminated with galactose units, binds to a greater extent compared to fetuin and human transferrin, both of which have glycan chains terminated with *N*-acetylneuraminic acid (a.k.a. sialic acid). The results here firmly supports the conclusions made from SPR investigations that the interaction of boronic acids with glycoproteins is largely based on the type of sugar terminus (see Chapter 2). When non-glycosylated proteins were exposed to the AECPBA–PMMA surface, both the BSA and cytochrome C did not exhibit any adsorption to the surface, judging from the virtually identical N 1s signal of these surfaces compared to a reference surface, see Figure 3.8 inset. This can be taken as further evidence that Tween 20 was effective in suppressing non-specific protein adsorption on underivatized PMMA surfaces. In general, addition of Tween 20, acting as a dynamic coating, on the AECPBA-PMMA surface improves the selectivity of the surface with

respect to hydrophobic interactions of non-glycosylated proteins with hydrophobic regions on the PMMA surface.

3.5 Conclusions

The preparation of a boronic acid-derivatized PMMA microfluidic surface, AECPBA–PMMA, was investigated for the first time. Characterization by XPS, UV-vis absorption measurements, and contact angle titration has demonstrated the covalent attachment of AECPBA on UV-modified PMMA surfaces through simple carbodiimide coupling. The binding—using glycine- and tris-buffered saline—and elution, using borate-buffered saline, of glycoproteins were accomplished with the aid of Tween 20, as a dynamic coating, which suppressed the hydrophobic interactions between the proteins and exposed underivatized regions of PMMA. Non-specific adsorption of non-glycosylated proteins was not apparent under the binding buffer system employed. The results presented here demonstrates the capacity of the AECPBA–PMMA surface to capture glycoproteins from solution, and the ability of said capture surfaces to have their surface contents efficiently eluted at a later time; these outcomes bode well for use of these and similar surfaces in microfluidic devices for protein capture, release and identification.

3.6 References

(1) Brooks, S. A. Strategies for analysis of the glycosylation of proteins: Current status and future perspectives. *Mol. Biotechnol.* **2009**, *43*, 76-88.

(2) Tian, Y.; Zhang, H. Glycoproteomics and clinical applications. *Proteomics: Clin. Appl.* **2010**, *4*, 124-132.

(3) Manservigi, R.; Cassai, E. The glycoproteins of the human herpes viruses. *Comparative Immunology, Microbiology and Infectious Diseases* **1991**, *14*, 81-95.

(4) Hwang, H.; Zhang, J.; Chung, K. A.; Leverenz, J. B.; Zabetian, C. P.; Peskind, E. R.; Jankovic, J.; Su, Z.; Hancock, A. M.; Pan, C.; Montine, T. J.; Pan, S.; Nutt, J.; Albin, R.; Gearing, M.; Beyer, R. P.; Shi, M.; Zhang, J. Glycoproteomics in neurodegenerative diseases. *Mass Spectrom. Rev.* **2010**, *29*, 79-125.

(5) Bindila, L.; Peter-Katalinić, J. Chip-mass spectrometry for glycomic studies. *Mass Spectrom. Rev.* **2009**, *28*, 223-253.

(6) Manz, A.; Harrison, D. J.; Verpoorte, E. M. J.; Fettinger, J. C.; Paulus, A.; Lüdi, H.; Widmer, H. M. Planar chips technology for miniaturization and integration of separation techniques into monitoring systems: Capillary electrophoresis on a chip. *J. Chromatogr. A* **1992**, *593*, 253-258.

(7) Arora, A.; Simone, G.; Salieb-Beugelaar, G. B.; Kim, J. T.; Manz, A. Latest developments in micro total analysis systems. *Anal. Chem.* **2010**, *82*, 4830-4847.

(8) Harrison, D. J.; Fluri, K.; Seiler, K.; Fan, Z.; Effenhauser, C. S.; Manz, A. Micromachining a miniaturized capillary electrophoresis-based chemical analysis system on a chip. *Science* **1993**, *261*, 895-897.

(9) Yang, Z. P.; Hancock, W. S. Approach to the comprehensive analysis of glycoproteins isolated from human serum using a multi-lectin affinity column. *J. Chromatogr. A* **2004**, *1053*, 79-88.

(10) Whelan, S. A.; Lu, M.; He, J.; Yan, W.; Saxton, R. E.; Faull, K. F.; Whitelegge, J. P.; Chang, H. R. Mass spectrometry (LC/MS-MS) site-mapping of *N*-glycosylated membrane proteins for breast cancer biomarkers. *J. Proteome Res.* **2009**, *8*, 4151-4160.

(11) Mao, X.; Wang, K.; Du, Y.; Lin, B. Analysis of chicken and turkey ovalbumins by microchip electrophoresis combined with exoglycosidase digestion. *Electrophoresis* **2003**, *24*, 3273-3278.

(12) Mao, X.; Luo, Y.; Dai, Z.; Wang, K.; Du, Y.; Lin, B. Integrated lectin affinity microfluidic chip for glycoform separation. *Anal. Chem.* **2004**, *76*, 6941-6947.

(13) Mao, X.; Chu, I. K.; Lin, B. A sheath-flow nanoelectrospray interface of microchip electrophoresis MS for glycoprotein and glycopeptide analysis. *Electrophoresis* **2006**, *27*, 5059-5067.

(14) Bynum, M.; Baginski, T.; Killeen, K.; Keck, R. Integrated microfluidic LC-MS. *Pharm. Technol.* **2010**, *34*, s32-s39.

(15) Mechref, Y.; Madera, M.; Novotny, M. V. Glycoprotein enrichment through lectin affinity techniques. *Methods Mol. Biol.* **2008**, *424*, 373-396.

(16) refer to Chapter 2 for references

(17) Hagemeier, E.; Boos, K. S.; Schlimme, E.; Lechtenborger, K.; Kettrup, A. Synthesis and application of a boronic acid substituted silica for high-performance liquid affinity-chromatography. *J. Chromatogr.* **1983**, *268*, 291-295.

(18) Xu, Y.; Wu, Z.; Zhang, L.; Lu, H.; Yang, P.; Webley, P. A.; Zhao, D. Highly specific enrichment of glycopeptides using boronic acid-functionalized mesoporous silica. *Anal. Chem.* **2009**, *81*, 503-508.

(19) Bossi, A.; Castelletti, L.; Piletsky, S. A.; Turner, A. P. F.; Righetti, P. G. Properties of poly(aminophenyl boronate) coatings in capillary electrophoresis for the selective separation of diastereoisomers and glycoproteins. *J. Chromatogr. A* **2004**, *1023*, 297-303.

(20) Sparbier, K.; Asperger, A.; Kessler, I.; Koch, S.; Shi, G.; Wenzel, T.; Kostrzewa, M. Identification and characterization of glycoproteins in human serum by means of glyco-specific magnetic bead separation and LC-MALDI analysis. *Mol. Cell Proteomics* **2006**, *5*, S134-S134.

(21) Zhou, W.; Yao, N.; Yao, G. P.; Deng, C. H.; Zhang, X. M.; Yang, P. Y. Facile synthesis of aminophenylboronic acid-functionalized magnetic nanoparticles for selective separation of glycopeptides and glycoproteins. *Chem. Commun.* **2008**, 5577-5579.

(22) Khavkin, J. A.; Roytman, M. J.; Khavkine, M. J. Accumulative solid-phase sorption of pollutants as a method for hygienic and environmental inspection. III. Detection of biowaste using boronylated carrier. *Anal. Lett.* **2004**, *37*, 781-788.

(23) Koyama, T.; Terauchi, K. Synthesis and application of boronic acid-immobilized porous polymer particles: A novel packing for high-performance liquid affinity chromatography. *J. Chromatogr. B* **1996**, *679*, 31-40.

(24) Liu, S. Q.; Miller, B.; Chen, A. C. Phenylboronic acid self-assembled layer on glassy carbon electrode for recognition of glycoprotein peroxidase. *Electrochem. Commun.* **2005**, *7*, 1232-1236.

(25) Zayats, M.; Katz, E.; Willner, I. Electrical contacting of glucose oxidase by surface-reconstitution of the apo-protein on a relay-boronic acid-FAD cofactor monolayer. *J. Am. Chem. Soc.* **2002**, *124*, 2120-2121.

(26) Kanayama, N.; Kitano, H. Interfacial recognition of sugars by boronic acid-carrying self-assembled monolayer. *Langmuir* **1999**, *16*, 577-583.

(27) Chen, H. X.; Lee, M.; Lee, J.; Kim, J. H.; Gal, Y. S.; Hwang, Y. H.; An, W. G.; Koh, K. Formation and characterization of self-assembled phenylboronic acid derivative monolayers toward developing monosaccharide sensing-interface. *Sensors* **2007**, *7*, 1480-1495.

(28) Anraku, Y.; Takahashi, Y.; Kitano, H.; Hakari, M. Recognition of sugars on surface-bound cap-shaped gold particles modified with a polymer brush. *Colloids Surf., B* **2007**, *57*, 61-68.

(29) Kitano, H.; Anraku, Y.; Shinohara, H. Sensing capabilities of colloidal gold monolayer modified with a phenylboronic acid-carrying polymer brush. *Biomacromolecules* **2006**, *7*, 1065-1071.

(30) Ivanov, A. E.; Eccles, J.; Panahi, H. A.; Kumar, A.; Kuzimenkova, M. V.; Nilsson, L.; Bergenstahl, B.; Long, N.; Phillips, G. J.; Mikhalovsky, S. V.; Galaev, I. Y.; Mattiasson, B. Boronate-containing polymer brushes: Characterization, interaction with saccharides and mammalian cancer cells. *J. Biomed. Mater. Res., Part A* **2009**, *88A*, 213-225.

(31) McDonald, J. C.; Whitesides, G. M. Poly(dimethyl siloxane) as a material for fabricating microfluidic devices. *Acc. Chem. Res.* **2002**, *35*, 491-499.

(32) Liu, J.; Pan, T.; Woolley, A. T.; Lee, M. L. Surface-modified poly(methyl methacrylate) capillary electrophoresis microchips for protein and peptide analysis. *Anal. Chem.* **2004**, *76*, 6948-6955.

(33) Wei, S.; Vaidya, B.; Patel, A. B.; Soper, S. A.; McCarley, R. L. Photochemically patterned poly(methyl methacrylate) surfaces used in the fabrication of microanalytical devices. *J. Phys. Chem. B* **2005**, *109*, 16988-16996.

(34) Soper, S. A.; Henry, A. C.; Vaidya, B.; Galloway, M.; Wabuyele, M.; McCarley, R. L. Surface modification of polymer-based microfluidic devices. *Anal. Chim. Acta* **2002**, *470*, 87-99.

(35) Becker, H.; Locascio, L. E. Polymer microfluidic devices. *Talanta* **2002**, *56*, 267-287.

(36) Soper, S. A.; Ford, S. M.; Qi, S.; McCarley, R. L.; Kelly, K.; Murphy, M. C. Peer reviewed: Polymeric microelectromechanical systems. *Anal. Chem.* **2000**, *72*, 642A-651A.

(37) Kelly, R. T.; Woolley, A. T. Thermal bonding of polymeric capillary electrophoresis microdevices in water. *Anal. Chem.* **2003**, *75*, 1941-1945.

(38) Henry, A. C.; Tutt, T. J.; Galloway, M.; Davidson, Y. Y.; McWhorter, C. S.; Soper, S. A.; McCarley, R. L. Surface modification of poly(methyl methacrylate) used in the fabrication of microanalytical devices. *Anal. Chem.* **2000**, *72*, 5331-5337.

(39) Liu, J.; Sun, X.; Lee, M. L. Surface-reactive acrylic copolymer for fabrication of microfluidic devices. *Anal. Chem.* **2005**, *77*, 6280-6287.

(40) Matsumoto, A.; Ikeda, S.; Harada, A.; Kataoka, K. Glucose-responsive polymer bearing a novel phenylborate derivative as a glucose-sensing moiety operating at physiological pH conditions. *Biomacromolecules* **2003**, *4*, 1410-1416.

(41) Siegbahn, K. Electron spectroscopy for chemical analysis (E.S.C.A.). *Philos. Trans. R. Soc. London, Ser. A* **1970**, *268*, 33-57.

(42) Carey, R. I.; Folkers, J. P.; Whitesides, G. M. Self-assembled monolayers containing ω-mercaptoalkyl boronic acids adsorbed onto gold form a highly cross-linked, thermally stable borate glass surface. *Langmuir* **1994**, *10*, 2228-2234.

(43) Barriet, D.; Yam, C. M.; Shmakova, O. E.; Jamison, A. C.; Lee, T. R. 4-mercaptophenylboronic acid SAMs on gold: Comparison with SAMs derived from thiophenol, 4-mercaptophenol, and 4-mercaptobenzoic acid. *Langmuir* **2007**, *23*, 8866-8875.

(44) Elmas, B.; Onur, M. A.; Şenel, S.; Tuncel, A. Temperature controlled RNA isolation by *N*-isopropylacrylamide–vinylphenyl boronic acid copolymer latex. *Colloid. Polym. Sci.* **2002**, *280*, 1137-1146.

(45) Hatcher, J. T.; Wilcox, L. V. Colorimetric determination of boron using carmine. *Anal. Chem.* **1950**, *22*, 567-569.

(46) Buscher, C. T.; McBranch, D.; Li, D. Understanding the relationship between surface coverage and molecular orientation in polar self-assembled monolayers. *J. Am. Chem. Soc.* **1996**, *118*, 2950-2953.

(47) Holmes-Farley, S. R.; Reamey, R. H.; McCarthy, T. J.; Deutch, J.; Whitesides, G. M. Acid-base behavior of carboxylic acid groups covalently attached at the surface of polyethylene: The usefulness of contact angle in following the ionization of surface functionality. *Langmuir* **1985**, *1*, 725-740.

(48) Bain, C. D.; Whitesides, G. M. A study by contact angle of the acid-base behavior of monolayers containing ω-mercaptocarboxylic acids adsorbed on gold: An example of reactive spreading. *Langmuir* **1989**, *5*, 1370-1378.

(49) Holmes-Farley, S. R.; Bain, C. D.; Whitesides, G. M. Wetting of functionalized polyethylene film having ionizable organic acids and bases at the polymer-water interface: Relations between functional group polarity, extent of ionization, and contact angle with water. *Langmuir* **1988**, *4*, 921-937.

(50) Lee, T. R.; Carey, R. I.; Biebuyck, H. A.; Whitesides, G. M. The wetting of monolayer films exposing ionizable acids and bases. *Langmuir* **1994**, *10*, 741-749.

(51) Wamser, C. C.; Gilbert, M. I. Detection of surface functional group asymmetry in interfacially-polymerized films by contact angle titrations. *Langmuir* **1992**, *8*, 1608-1614.

(52) Lorand, J. P.; Edwards, J. O. Polyol complexes and structure of the benzeneboronate ion. *J. Org. Chem.* **1959**, *24*, 769-774.

(53) Nakajima, N.; Ikada, Y. Mechanism of amide formation by carbodiimide for bioconjugation in aqueous media. *Bioconjugate Chem.* **1995**, *6*, 123-130.

(54) Delange, R. J. Egg white avidin. 1. Amino acid composition-sequence of amino-terminal and carboxyl-terminal cyanogen bromide peptides. *J. Biol. Chem.* **1970**, *245*, 907-916.

(55) Huang, T. S.; Delange, R. J. Egg white avidin. 2. Isolation, composition, and amino acid sequences of tryptic peptides. *J. Biol. Chem.* **1971**, *246*, 686-697.

(56) Green, N. M.; Anfinsen, C., Jr.; Edsall, J.; Richards, F. Avidin. In *Advances in protein chemistry*; Academic Press: New York, 1975; Vol. 29, p 85-133.

(57) Bruch, R. C.; White, H. B. Compositional and structural heterogeneity of avidin glycopeptides. *Biochemistry* **1982**, *21*, 5334-5341.

(58) Cheng, Y. L.; Darst, S. A.; Robertson, C. R. Bovine serum albumin adsorption and desorption rates on solid surfaces with varying surface properties. *J. Colloid Interface Sci.* **1987**, *118*, 212-223.

(59) Suzawa, T.; Murakami, T. Adsorption of bovine serum albumin on synthetic polymer latices. *J. Colloid Interface Sci.* **1980**, *78*, 266-268.

(60) Iguerb, O.; Bertrand, P. Graft photopolymerization of polyethylene glycol monoacrylate (PEGA) on poly(methyl methacrylate) (PMMA) films to prevent BSA adsorption. *Surf. Interface Anal.* **2008**, *40*, 386-390.

(61) Liu, X.-C. Boronic acids as ligands for affinity chromatography. *Chin. J. Chromatogr.* **2006**, *24*, 73-80.

(62) Dang, F.; Kakehi, K.; Cheng, J.; Tabata, O.; Kurokawa, M.; Nakajima, K.; Ishikawa, M.; Baba, Y. Hybrid dynamic coating with *N*-dodecyl-D-maltoside and methyl cellulose for high-performance carbohydrate analysis on poly(methyl methacrylate) chips. *Anal. Chem.* **2006**, *78*, 1452-1458.

(63) Dang, F.; Zhang, L.; Hagiwara, H.; Mishina, Y.; Baba, Y. Ultrafast analysis of oligosaccharides on microchip with light-emitting diode confocal fluorescence detection. *Electrophoresis* **2003**, *24*, 714-721.

(64) Lin, Y.-W.; Chang, H.-T. Modification of poly(methyl methacrylate) microchannels for highly efficient and reproducible electrophoretic separations of double-stranded DNA. *J. Chromatogr. A* **2005**, *1073*, 191-199.

(65) Mohamadi, M. R.; Mahmoudian, L.; Kaji, N.; Tokeshi, M.; Baba, Y. Dynamic coating using methylcellulose and polysorbate 20 for nondenaturing electrophoresis of proteins on plastic microchips. *Electrophoresis* **2007**, *28*, 830-836.

CHAPTER 4

ATRP-DERIVED THERMORESPONSIVE TERPOLYMERS ORTHOGONALLY DERIVATIZED WITH A LECTIN AND ITS COMPLEMENTARY BINDING SUGAR

4.1 Introduction

Engineering macromolecules to give well-defined composition, a high degree of functionality, and complex architectures to suit specific applications requires the development of powerful and diverse strategies for polymer synthesis. It is not surprising that polymer synthesis techniques based on living/controlled free radical polymerization (LFRP) in tandem with click chemistry have received particular attention, owing to the benefits associated with high fidelity, simple, and efficient reactions.[1-11] Although it is attractive to directly copolymerize groups to increase synthetic throughput, even the advances made by LFRP in terms of enabling monomer functionality tolerance has, in general, not allowed for a broad range of moieties to be directly introduced via copolymerization. Hence, post-polymerization modification[5] is still an attractive strategy to create complex functional materials. The success of post-polymerization strategies still relies heavily on the availability of synthetic polymers that possess functionalizable side groups that can be efficiently converted so as to endow the polymer with new functionalities that are key to formation of complex functional materials with desired characteristics. It would seem that this is counterproductive due to the number of reaction steps that must be carried out to obtain the final material, but several researchers have capitalized on either simultaneous or cascade reactions to limit the synthetic route for the creation of multiply-functionalized materials.[2-3] In fact, it can also be argued that having a precursor polymer is economical and practical because a library of materials[3,12] can be prepared without the need to optimize the reaction conditions to create each resulting material, such as would be in the case with direct copolymerization.

Much of polymer synthesis is directed at biological applications (e.g. medicine and biotechnology).[12] For polymers to be extremely viable for such, they must behave as both a sensor and an actuator (i.e. one that identifies and acts on a particular stimulus). Thus, synthetic polymers usually possess stimuli-responsive functionalities that are sensitive to changes in pH, light, temperature, reducing agents, or a combination thereof.[2,13-15] Poly(*N*-isopropyl-acrylamide), in particular, has been at the forefront of synthetic investigations, owing to its temperature-responsive nature that is characterized by a phase transition that occurs at near physiological temperature (i.e. lower critical solution temperature, LCST = 32 °C) in aqueous medium.[16] At this temperature, microscopically, poly(*N*-isopropylacrylamide) exhibits a coil-to-globule transition that manifests itself as a phase change at the macroscopic scale.[17] This phenomenon has been exploited for potential applications in separations,[14,18] drug delivery,[19] and diagnostics.[20]

The fusion of thermoresponsive character and the capability for modification of multiple functionalities in a single polymer is very attractive in the preparation of diverse, multi-functional "smart" materials. A synthetic strategy/route for the modification of a thermoresponsive terpolymer is presented. It is also demonstrated that glycidyl methacrylate and *tert*-butyl acrylate can be efficiently copolymerized with *N*-isopropylacrylamide by atom transfer radical polymerization (ATRP) and each functionality can be subsequently modified with biologically relevant molecules, namely a lectin protein and its complementary eluting sugar, in a stepwise fashion. The synthetic route presented here is amenable for adaptation in the fabrication of microfluidic surfaces/devices that operates by capturing and releasing a unique set of glycoprotein without the need for externally-added eluting agents.

4.2 Experimental Section

4.2.1 Materials

N-isopropylacrylamide (NIPAAM, 97%, Aldrich) was purified by recrystallization from *n*-hexane twice. *N*-acryloxysuccinimide (NAS, 99%, Acros) was recrystallized twice using 2:1 (v/v) hexane/ethyl acetate. *Tert*-butyl acrylate (tBA, 99%, Acros) was passed through an inhibitor remover column (Aldrich), followed by reduced pressure distillation, to remove the monomethyl ether hydroquinone (MEHQ) inhibitor. Glycidyl methacrylate (GMA, 97%, Fluka) was passed through the inhibitor remover column twice to remove MEHQ. All monomers were stored at 4 °C immediately after their purification. 1,4,8,11-tetramethyl-1,4,8,11-tetraazacyclotetradecane (Me_4cyclam, 98%, Aldrich), CuBr (99.998%, Alfa-Aesar), ethyl 2-bromopropionate (EBP, 99%, Acros), 1,3,5-trimethylbenzene (TMB, 98%, Aldrich), propargylamine (98%, Aldrich), 1-azido-1-deoxy-β-D-lactopyranoside (97%, Aldrich), *N*,*N*-diisopropylethylamine (DIPEA, 99.5+%, Acros), trifluoroacetic acid (TFA, 98%, Alfa Aesar), *N*-(3-dimethylaminopropyl)-*N*′-ethylcarbodiimide hydrochloride (EDC, Sigma), *N*-hydroxysuccinimide (NHS, Sigma), *Ricinus communis* agglutinin (RCA_{120}, Sigma), D-lactose monohydrate (Sigma), anhydrous dimethylformamide (DMF, Acros), dichloromethane (DCM, stabilized, Mallinckrodt Chemicals), anhydrous diethyl ether (stabilized, ACS grade, Mallinckrodt Chemicals), anhydrous ethanol (Pharmco-Aaper), neutral alumina (80–200 mesh, Fisher), Dowex Marathon MSC hydrogen form ion exchange resin (20–50 mesh, Sigma-Aldrich), Spectra/Por Float-A-Lyzer G2 (100-500 Da MWCO, Spectrum Laboratories Inc.), and Whatman Anotop disposable syringe filters (0.2 μm, Fisher Scientific) were used as received. Buffer solutions were prepared in Nanopure water (> 18 MΩ·cm, Barnstead). $CuBr(PPh_3)_3$ was prepared according to the literature.[21]

4.2.2 ATRP Synthesis of Poly(*N*-isopropylacrylamide–*co*–*N*-acryloxysuccinimide–*co*–*tert*-butyl acrylate)—Poly(NIPAAM–NAS–tBA)

All liquid reagents were degassed by bubbling ultra-high-purity (UHP) Ar through them immediately prior to use. Degassed syringes were used when introducing liquid reagents and removing aliquots. *N*-isopropylacrylamide (NIPAAM), *N*-acryloxysuccinimide (NAS), and *tert*-butyl acrylate (tBA) were varied in terms of their composition in the polymerization mixture while maintaining a total monomer composition of 0.01 mol. The monomer feed ratio is given in Table 4.1. Typically, a dry 3-neck round bottom flask connected to a vacuum and Ar source (Schlenk line) was charged with NIPAAM, NAS, and Me_4cyclam (27.40 mg, 1.100×10^{-4} mol). The flask was deoxygenated with three vacuum-Ar cycles. CuBr (15.80 mg, 1.100×10^{-4} mol) was introduced under Ar protection, followed by two vacuum-Ar cycles. DMF (4.50 mL) was added and the reaction mixture was stirred to allow complex formation of the catalyst. To the flask was added tBA, followed by TMB (0.50 mL, internal standard). The reaction was initiated by the addition of ethyl 2-bromopropionate, EBP, (130.00 μL, 1.0000×10^{-3} mol; or 13.00 μL, 1.000×10^{-4} mol), and the reaction mixture was stirred at room temperature under slight positive Ar pressure. For monomer conversion measurements made by ^{1}H NMR, an initial sample was obtained before addition of EBP, and subsequent samples were obtained at predetermined times. After 24 h, the reaction mixture was opened to the atmosphere to quench the reaction. The cloudy blue mixture originally in DMF was precipitated in anhydrous diethyl ether, redissolved in DCM, and precipitated again in anhydrous diethyl ether. The resulting blue solid was redissolved in DCM and passed through a short neutral alumina column three times to remove the catalyst, then the solution was concentrated, and the polymer was precipitated by addition of the concentrated solution to anhydrous diethyl ether. ^{1}H NMR (400 MHz, DMSO-d_6): δ (ppm) =

1.04 (s, 6H, 2×$CH_{3(NIPAAM)}$); 1.37 (s, 9H, 3×$CH_{3(tert\text{-}butyl)}$); 1.25-2.20 (m, $CH_2CH_{backbone}$); 2.83 (s, 4H, 2×$CH_{2(NAS)}$); 3.83 (s, 1H, CH_{NIPAAM}); 6.90-7.70 (b, 1H, NH_{NIPAAM}).

4.2.3 ATRP Synthesis of Poly(*N*-isopropylacrylamide–*co*–glycidyl methacrylate–*co*–*tert*-butyl acrylate)—Poly(NIPAAM–GMA–tBA)

The synthesis and isolation of poly(NIPAAM–GMA–tBA) follows the synthetic procedure above, with GMA introduced into the reaction mixture following the addition of TMB. This is to ensure that the catalyst complex has already formed to avoid the reaction between the free amine and the oxirane ring. ^{1}H NMR (400 MHz, $CDCl_3$): δ (ppm) = 0.90 (s, 3H, $CH_{3(GMA\ backbone)}$); 1.14 (s, 6H, 2×$CH_{3(NIPAAM)}$); 1.42 (s, 9H, 3×$CH_{3,\ tert\text{-}butyl}$); 1.50-2.30 (m, $CH_2CH_{(backbone)}$); 2.73 and 2.88 (2H, $CH_{2(oxirane\ ring)}$); 3.33 (1H, $CH_{(oxirane\ ring)}$); 3.84 (s, 1H of $CH_{2(GMA)}$); 4.00 (b, 1H, $CH_{(NIPAAM)}$); 4.25 (s, 1H of $CH_{2(GMA)}$); 5.70-7.10 (b, 1H, $NH_{(NIPAAM)}$).

4.2.4 Functionalization of Epoxy Groups of Poly(NIPAAM-GMA-tBA) with Propargylamine—Poly(NIPAAM–ppg–tBA)

Poly(NIPAAM–GMA–tBA), 500.00 mg, was added to a dry 2-neck round bottom flask. Following purging with Ar gas, degassed anhydrous ethanol (5.00 mL) and propargylamine (96.00 μL, 1.500×10^{-3} mol) were added. The solution was stirred at 30 °C for 47 h under slight positive Ar pressure. Ethanol was removed by rotary evaporation. The resulting off white polymer was isolated following repeated redissolution (in DCM)-precipitation (in anhydrous diethyl ether) cycles, and finally solvent removal under high vacuum. ^{1}H NMR (400 MHz, $CDCl_3$): δ (ppm) = 0.90 (s, 3H, $CH_{3,GMA\ backbone}$); 1.14 (s, 6H, 2×$CH_{3,NIPAAM}$); 1.42 (s, 9H, 3×$CH_{3,\ tert\text{-}butyl}$); 1.50-2.20 (m, $CH_2CH_{backbone}$); 2.27 (s, 1H, $CH_{terminal\ alkyne}$); 2.82 (s, 2H, OH-CH-CH_2-NH); 3.47 (s, 2H, NH-CH_2-C); 4.00 (b, 4H, CH_{NIPAAM}, O-CH_2-CH-OH); 4.80-5.40 (b, 1H, OH); 5.75-7.25 (b, 1H, NH_{NIPAAM}).

4.2.5 Click Reaction Between Poly(NIPAAM–ppg–tBA) and 1-Azido-1-deoxy-*β*-D-lactopyranoside—Poly(NIPAAM–lac–tBA)

The procedure for the click reaction was adapted from the literature[3] with slight modifications. A solution containing poly(NIPAAM–ppg–tBA) (100.00 mg), 1-azido-1-deoxy-*β*-D-lactopyranoside (56.00 mg, 1.500×10^{-4} mol), degassed anhydrous DMF (5.00 mL), and degassed DIPEA (13.00 μL, 7.500×10^{-5} mol) in a round bottom flask was purged with Ar. $CuBr(PPh_3)_3$ (29.00 mg, 3.000×10^{-5} mol) was added and the reaction was carried out at 50 °C for 40 h under Ar protection. Dowex Marathon hydrogen ion exchange resin was then added, and the solution was stirred overnight at room temperature. The resin was removed, the resulting solution was concentrated, and then the polymer precipitated in diethyl ether. The solid obtained was washed with THF and recovered following centrifugation and high vacuum removal of solvent.

4.2.6 Deprotection of Poly(NIPAAM–lac–tBA)—Poly(NIPAAM–lac–Aac)

To 100.00 mg of poly(NIPAAM–lac–tBA), trifluoroacetic acid (2.50 mL) was added at 0 °C. The reaction mixture was stirred for 2 h at 0 °C and then 4 h at room temperature under positive Ar pressure. The resulting orange-pink solution was concentrated and the polymer then precipitated by addition of the solution to anhydrous diethyl ether. The polymer was isolated by centrifugation and the polymer was washed with anhydrous diethyl ether two times. Following a high-vacuum drying step, the resulting orange-pink powder was dissolved in 0.10 M $NaHCO_3$, filtered with a 0.2-μm Whatman Anotop syringe filter, and then dialyzed (Spectra/Por Float-A-Lyzer G2 with CE membrane, MWCO = 100-500 Da) extensively against Nanopure water. The dialyzed solution was freeze-dried to give a white powder, thereafter named poly(NIPAAM–lac–Aac).

4.2.7 Conjugation of RCA_{120} to Poly(NIPAAM–lac–Aac)—Poly(NIPAAM–lac–RCA_{120})

Using an ice bath to control the temperature, a solution of poly(NIPAAM–lac–Aac) (11.00 mg) in pH 7.26, 0.10 M phosphate buffer was added quickly to a solution containing RCA_{120} (1.00 mg, 8.30×10^{-9} mol) and D-lactose (6.10 mg, 1.70×10^{-8} mol) in the same buffer. EDC (19.10 mg, 10.00×10^{-5} mol) and NHS (1.70 mg, 1.50×10^{-5} mol) were immediately added, and the solution was allowed to stir for 4 h (using the ice bath) and then at room temperature for another 22 h. The resulting solution was dialyzed using Nanopure water with a Microcon YM-50 (Nominal molecular weight limit = 50,000 Da) centrifugal filter device (Millipore).

4.2.8 Measurements

Monomer conversion data (1,3,5-trimethylbenzene as internal standard) and polymer characterization were obtained from ^{1}H NMR spectra. A Bruker AV-400 (400 MHz) spectrometer was used, and samples were dissolved in either DMSO-d_6 or $CDCl_3$. Molecular weights and distribution data were collected from an Agilent 1200 Series System (Agilent 1200 Series degasser, Isocratic Pump, Autosampler, and Column Heater) equipped with three Phenogel 5 μm, 300 × 7.8 mm columns (100 Å, 1000 Å and Linear(2)) connected in series. A Wyatt EOS Multi-Angle Light Scattering (MALS) with a GaAs 25 mW laser at λ = 690 nm and a Wyatt rEX Differential Refractive Index detector with a 690 nm light source were the detectors used. Sample preparation and GPC separation were performed using DMF with added 0.10 M LiBr. Column and detector temperatures were kept constant at 50 °C and 25 °C, respectively. Molecular weight and polydispersity data were obtained using monodisperse polystyrene standards (590–1472000 g mol^{-1} MW). Polymer cloud point (CP), the temperature where transmittance is reduced by 50%, was determined from turbidimetry measurements using the

following protocol. The change in optical transmittance of a 1% aqueous solution of the polymer in a cuvette positioned in a thermostated holder was monitored as a function of increasing temperature. Data was acquired using a HP 8453 UV-vis Chemstation at 500 nm wavelength. For analysis of the product from the conjugation reaction, SDS–PAGE gel electrophoresis was performed. The samples were dissolved in Laemmli buffer (Biorad) under non-reducing conditions and loaded onto 4–15% precast polyacrylamide gels (Biorad). Electrophoresis was run in 1× Tris/glycine/SDS buffer using a Biorad PowerPac Basic power supply. Staining and destaining procedures were based on the protocol for SimplyBlue SafeStain (Invitrogen).

4.3 Results and Discussion

4.3.1 ATRP Synthesis of Poly(NIPAAM–NAS–tBA)

The polymerization by ATRP of *N*-isopropylacrylamide (NIPAAM), *N*-acryloxysuccinimide (NAS), and *tert*-butyl acrylate (tBA) in an attempt to yield a thermoresponsive polymer was initially investigated in DMF solvent using the CuBr/Me_4cyclam catalytic system shown in Scheme 4.1. Because NIPAAM is envisioned in this work to be the monomer of highest proportion in the terpolymer so as to yield a polymer with significant thermoresponsive behavior in aqueous systems, the choice for the catalyst and solvent systems was largely dependent on the success of the ATRP of NIPAAM. Independent investigations by Matyjaszewski[22] and Brittain[23] on the ATRP of acrylamides and methacrylamides revealed high monomer conversion in relatively short times with Me_4cyclam-based systems in polar solvents, albeit with uncontrolled polymerization of monomer. The loss of control over the ATRP reaction was attributed largely to slow deactivation of radical chain ends. Although both authors offered several reasons to support the claim, they agreed that complexation of the Cu salts to the amide of the propagating chains contributes to the uncontrolled polymerization they observed.

Several other literature reports also describe the synthesis of poly(NIPAAM) by ATRP, with good control over the polymerization using CuCl/Me_6TREN catalytic system, but required the synthesis and use of Me_6TREN ligand.[4,24-25] Previous work by Balamurugan *et al.*[26] on surface-initiated ATRP of NIPAAM made use of the Me_4cyclam-based catalytic system, and they obtained polymer brush surfaces that exhibited thermoresponsive behavior. This successful formation of surface-immobilized *responsive* polymers bodes well for future work in the development of responsive polymer surfaces possessing poly(NIPAAM) and other polymeric functionalities. On the basis of that study[26] and those of Matyjaszewski and Brittain,[22-23] CuBr/Me_4cyclam was selected as the catalyst of choice for the work herein.

In order to generate a multifunctional thermoresponsive polymer that is based on NIPAAM and is capable of being subsequently modified, direct polymerization of NIPAAM with orthogonally functionalizable monomers is required. A review of functional monomers that are amenable to direct polymerization led us to choose initially *N*-acryloxysuccinimide (NAS) and *tert*-butyl acrylate (tBA).[5] In particular, NAS and tBA were chosen as comonomers because of their potential reactivity toward amines, with the latter requiring a deprotection step. If successful, such a choice would result in a polymer with sufficient orthogonality in its post-polymerization modification chemistries so that independent attachment of various functionalities can be readily achieved. In addition, both monomers have been successfully homo- or copolymerized under various ATRP conditions.[2,7,27-33] This strategy of having dual functionality should allow for predefined composition of the terpolymer such that each group can be modified independently of each other, thereby resulting in a polymer of controlled composition. Also, by creating a precursor polymer having individually addressable functional group types (orthogonality), the potential is great for generating a library of complex polymers

that exhibits structure-property relationships that otherwise cannot be prepared by extant methods.

Scheme 4.1. Synthesis of thermoresponsive terpolymers and their subsequent post-polymerization functionalization.[a]

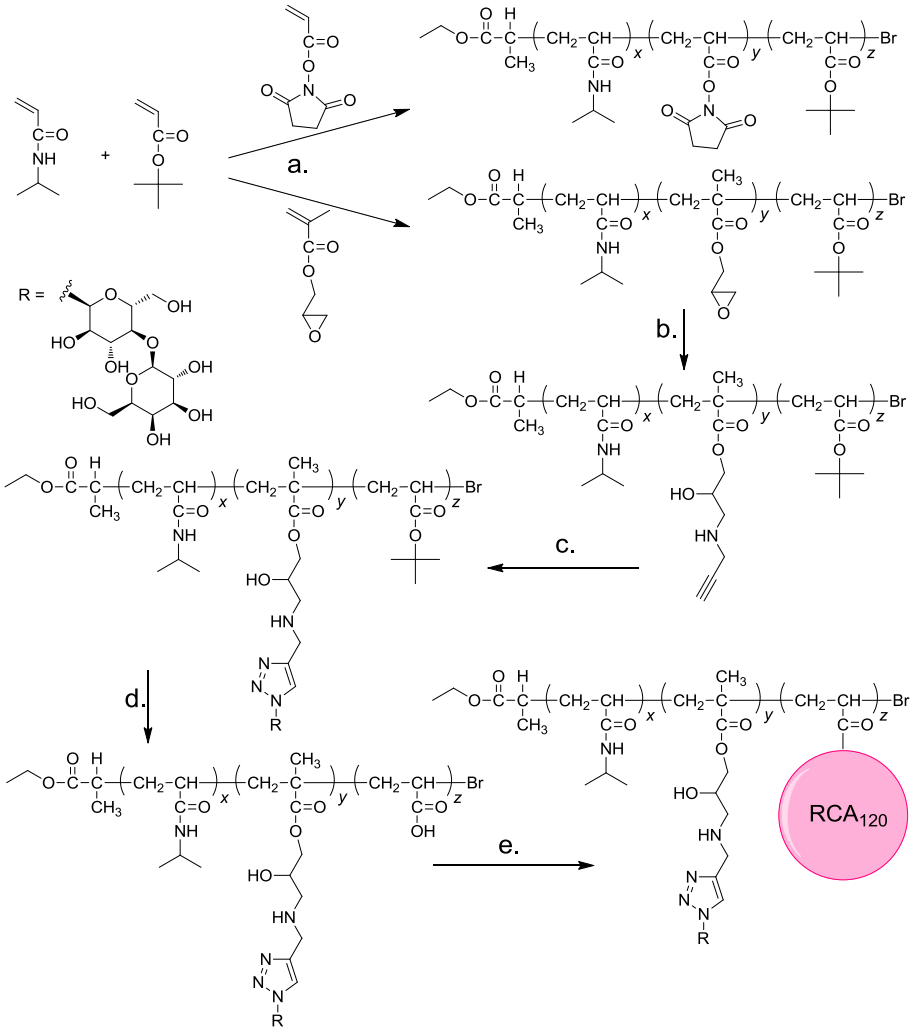

[a]Reagents and conditions: a. CuBr/1,4,8,11-tetramethyl-1,4,8,11-tetraazacyclotetradecane, ethyl-2-bromopropionate, DMF, 1,3,5-trimethylbenzene (internal standard), room temp.; b. propargylamine, ethanol, 30 °C; c. 1-azido-1-deoxy-β-D-lactopyranoside, $Cu(PPh_3)_3Br$, DIPEA, DMF, 50 °C; d. TFA, 0 °C to room temp.; e. *Ricinus communis* agglutinin (RCA_{120}), EDC/NHS, H_2O, room temp.

Successful formation of the terpolymer from *N*-acryloxysuccinimide (NAS), *tert*-butyl acrylate (tBA), and *N*-isopropylacrylamide (NIPAAM) using ATRP was indicated upon inspection of ^{1}H NMR spectra obtained in DMSO-d_6, Figure 4.1. Proton resonances for the isopropyl group of NIPAAM occur at 1.04 and 3.83 ppm, while presence of the amide proton is evidenced as a broad peak in the vicinity of 6.90–7.70 ppm. The transition associated with the three methyl groups of the *tert*-butyl moiety of the tBA is found at 1.37 ppm, and that for the methylenes of the succinimide ring of NAS is centered at 2.83 ppm. Furthermore, NAS and tBA groups are successfully incorporated into the polymer in higher amounts with increases in the monomer feed fraction of NAS and tBA, as evidenced by increases in the relative area of the corresponding proton peaks *d* and *e*, respectively (Figure 4.1 and Table 4.1). Inspection of the gel-permeation chromatography, GPC, traces of the terpolymers obtained with DMF solvent with added 0.10 M LiBr (Figure 4.2) leads to observation of an asymmetric elution profile with significant distribution of low molecular weight polymer eluting at a later time, suggesting premature chain termination during the polymerization. This fact, in conjunction with the high polydispersity values observed (Table 4.1), strongly indicates lack of control in the polymerization; controlled polymerization should result in a characteristically low polydispersity values ($M_w/M_n < 1.1$) and symmetric elution profiles in the GPC chromatogram, among other things.[34]

It was found that the amount of monomer conversion during the polymerization was highly sensitive to increasing amounts of NAS and tBA. The homopolymerization of NIPAAM proceeded at a relatively fast rate at room temperature, as noted by the observed 85% consumption of monomer within 15 min. However, polymerizations that employed equimolar amounts of NAS and tBA in increasing proportion versus NIPAAM resulted in a significant

decrease in NIPAAM conversion. At a valueof 90:5:5 (NIPAAM:NAS:tBA), the conversion of NIPAAM monomer was found to be only 8% (Table 4.1). A reduction of this magnitude for monomer conversion caused by addition of a small amount of functional monomers is unfavorable from the standpoint of practicality and efficiency. Furthermore, this route will not allow for the creation of materials with a desired terpolymer composition and molecular weight, nor can be created elaborate and orthogonally functionalized polymer architectures.

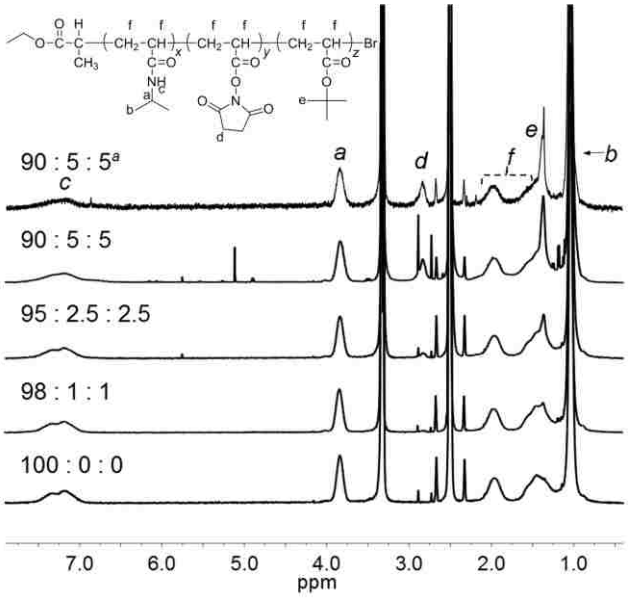

Figure 4.1. ^{1}H NMR (DMSO-d_6) of poly(NIPAAM–NAS–tBA) prepared using different monomer feed ratios. [a]Monomer:Initiator = 100:1; all others prepared using a Monomer:Initiator = 100:10.

Because tBA has been successfully polymerized under Me_4cyclam-initiated ATRP,[35] the attention is drawn to NAS as the comonomer that is responsible for the low conversion obtained in the polymerizations. In fact, Savariar and Thayumanavan[27] reported that copolymerization of NIPAAM and the *N*-hydroxysuccinimide ester of methacrylic acid with CuCl/Me_6TREN or CuBr/PMDETA catalysts resulted in poor yields (10–24%). Although they offered no

Table 4.1. Properties of terpolymers resulting from polymerization of NIPAAM and tBA with NAS or GMA (*Y*).

% monomer feed ratio[a]	comonomer *Y*	% composition[b]	time (h)	% conv[c]	$M_{n,theo}$[d]	$M_{n,GPC}$[e]	M_w/M_n	CP (°C)[f]
100:0:0	-	100:0:0	0.25	85	1140	88700	1.74	29.5
98:1:1	NAS	94:1:5	24	77	1065	57300	1.37	27.4
95:2.5:2.5	NAS	88:4:8	24	18	450	56900	1.42	24.3
90:5:5	NAS	79:10:11	24	8	410	64200	1.41	16.5
90:5:5[g]	NAS	70:18:12	24	12	2890	43500	1.25	n.d.[h]
91:8:1[g]	GMA	80:16:4	24	81	9790	61000	1.57	17.9
90:5:5[g]	GMA	81:10:9	24	93	11000	94700	1.61	19.6

[a]NIPAAM:*Y*:tBA. $[M_t]_0/[Cu]_0/[L]_0/[I]_0 = 100/1/1/10$. [b]Percentage of each monomer in the terpolymer was calculated from ^{1}H NMR integration; for example, % NIPAAM = $(H_{NIPAAM,1.04ppm}/6) / [(H_{NIPAAM,1.04ppm}/6) + (H_{NAS,2.83\ ppm}/4) + (H_{tBA,1.36\ ppm}/9)]$, where $H_{NIPAAM,1.04ppm}$ is the integrated signal intensity of the NIPAAM transition at 1.04 ppm. [c] % conv = $\{1 - [(H_{NIPAAM}/H_{TMB})_t / (H_{NIPAAM}/H_{TMB})_{t=0}]\} \times 100$, where H_{NIPAAM} is the integrated signal intensity of the 1 vinyl proton of NIPAAM at 5.45 ppm and H_{TMB} is the integrated signal intensity of the aromatic proton resonance of the internal standard at 6.66 ppm. % conv was measured using NIPAAM only, because it is the monomer that has significant intensity in the NMR spectra. [d]$M_{n,theo} = \{\Sigma([M]_o \times MW \times conv)_i / [EBP]\} + MW_{EBP}$. The $M_{n,theo}$ was calculated based on the % conv values and the assumption that both NAS and tBA give 100% conversion. [e]$M_{n,GPC}$ was obtained using monodisperse polystyrene standards in DMF with 0.1 M LiBr. [f]Cloud point (CP) is defined as the temperature at which T_{norm} decreased by 50% with $T_{norm} = [(T - T_{min})/(T_{max} - T_{min})]$. CPs from independent scans for each polymer sample varied by at most 0.3 °C. [g]$[M_t]_0/[Cu]_0/[L]_0/[I]_0 = 100/1/1/1$. [h]Not determined due to insufficient amount of material.

explanation for their observations, it is evident that the commonality between the work herein and theirs is the presence of an *N*-hydroxysuccinimide ester of an acrylic acid. At this point, it is not clear the role that NAS plays in termination of the polymerization reaction. However, it was observed that as the amount of NAS and tBA was increased, the faster was the rate at which the color of the polymerization reaction mixture changed from light green to dark blue after addition of initiator. Based on this qualitative observation, it is clear that $CuBr_2$ (blue) is formed more readily in the presence of NAS, and in turn its presence would be expected to yield a high concentration of radicals capable of causing efficient termination of the polymerization reaction at an early stage. This lack of control in the polymerization is also reflected by the pronounced asymmetric elution profile observed in the gel-permeation chromatograms of the terpolymers, Figure 4.2. An alternative explanation is the Cu catalyst became inactivated by NAS coordination to the Cu salts,[30] in a manner similar to catalyst inactivation during acrylamide polymerization, as described by Matyjaszewski and Brittain.[22-23] However, such a proposed complexation/deactivation path is not in accord with the successful polymerization of the *N*-hydroxysuccinimide ester of methacrylic acid or NAS using a bipyridine-based catalytic system[29-31,36] and not in Me_4cyclam-based ATRP. No matter the precise nature of the events, NAS is suspected as the main cause for the low monomer conversion that is caused by termination of the polymerization process. Though successful polymerization of the *N*-hydroxysuccinimide ester of methacrylic acid and NAS was accomplished with substituted and unsubstituted bipyridine-based catalyst systems, the use of this class of ligand results in inefficient polymerization of acrylamides;[22,24] therefore no attempt was made to perform the ATRP procedure using bipyridine-based catalysts.

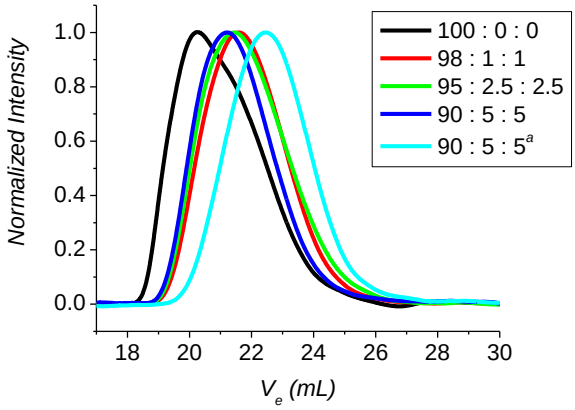

Figure 4.2. GPC traces of poly(NIPAAM–NAS–tBA) (DMF with added 0.1 M LiBr) prepared using different monomer feed ratios. [a]Monomer:Initiator = 100:1; all others prepared using a Monomer:Initiator = 100:10.

4.3.2 ATRP Synthesis of Poly(NIPAAM–GMA–tBA)

With the issue regarding the low monomer conversion that was encountered in the ATRP polymerization of NIPAAM, NAS, and tBA, I sought to replace NAS with another monomer that can be integrated into the polymer and more importantly, one possessing a chemical functionality that can be readily modified. Among the various commercially-available functional monomers, glycidyl methacrylate (GMA) is very attractive due to its pendant oxirane ring that can undergo ring opening reactions with a range of nucleophiles, such as amines, thiols, azides, and acids.[10,37] The fact that it reacts with a wide variety of functional groups adds versatility to any subsequent post-polymerization modification routes. Successful homopolymerization and copolymerization of GMA by ATRP is well-documented in the literature,[10,38-39] with controlled polymerization being achieved with a variety of ligand systems, including bipyridine derivatives and multidentate amines. Although it was unknown if polymerization of GMA with the Me_4cyclam-based system would be successful given the lack of literature precedent, it was still the initial catalyst of choice owing to reasons described above. The polymerization of NIPAAM and tBA

with GMA was carried out according to the same ATRP conditions described for poly(NIPAAM–NAS–tBA), with a slight modification. GMA was introduced after the catalyst complex had formed, so as to avoid the reaction between the free amine (uncomplexed ligand) and the oxirane ring that may result in a branched or cross-linked terpolymer.

In Figure 4.3 is shown the ^{1}H NMR data for the resulting terpolymer of NIPAAM–GMA–tBA. Aside from the characteristic NIPAAM and tBA peaks, the oxirane ring gives rise to proton resonances at 3.33 ppm and at 2.88 and 2.73 ppm. The latter two signals come about because the associated protons have different chemical environments. The resonances from the protons of the methylene side chain have distinct chemical environments and are observed at 4.41 ppm and 3.84 ppm, with the latter being slightly convoluted with the methynyl proton of NIPAAM.

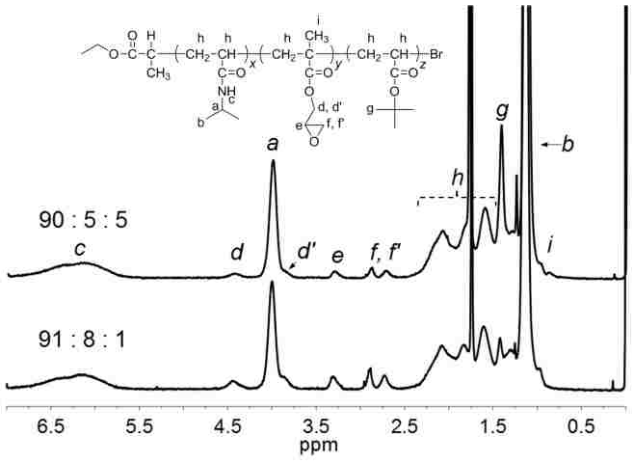

Figure 4.3. ^{1}H NMR ($CDCl_3$) of poly(NIPAAM–GMA–tBA) prepared using two different monomer feed ratios.

Perhaps the most striking result revealed by replacing NAS with GMA in the polymerization is *monomer conversion is significantly improved with GMA under the same monomer feed composition and ATRP conditions*, i.e. 93% conversion with GMA versus 12% conversion with NAS (Table 4.1). This result clearly strengthens the hypothesis that NAS is

responsible for the low monomer conversion discussed above. Although a slight decrease in monomer conversion was found upon increasing the GMA feed from 5% to 8%, the resulting 81% monomer conversion achieved is impossible with NAS under the ATRP conditions employed. Clearly, the use of GMA, under the ATRP conditions employed herein, results in a more efficient polymerization with NIPAAM and tBA, which in turn allows for the possibility of tailoring the composition of the terpolymer. The GMA and tBA contents of the terpolymers are found to be at least twice of that expected based on the monomer feed ratios, an outcome that is likely caused by some differences in the reactivities of the NIPAAM, GMA, and tBA monomers under the conditions used here.

The gel-permeation chromatograms for poly(NIPAAM–GMA–tBA) exhibit an asymmetric elution profile (Figure 4.4), similar to those obtained for the terpolymer containing NAS, once again suggesting uncontrolled polymerization. This is also supported by the large polydispersity of the resulting terpolymers (Table 4.1). However, the reasons for the lack of control of the polymerization observed here are most likely different from those of the NAS terpolymer, where the polymerization with NAS resulted in low monomer conversion. It should be noted that high monomer conversions are still achievable even with uncontrolled polymerization.[22-23] Perhaps the lack of polymerization control is associated with slow deactivation of propagating radicals, similar to that observed with ATRP of acrylamides under the CuBr/Me_4cyclam catalytic system.[22-23] As shown in Table 4.1, the GPC-determined molecular weights, $M_{n,GPC}$, for poly(NIPAAM–GMA–tBA) are higher than those for poly(NIPAAM–NAS–tBA) and are even comparable to that of NIPAAM homopolymer. Such a similarity in M_n values points to the possibility that the high monomer conversion values obtained during the formation of poly(NIPAAM–GMA–tBA) translates to longer polymer

chains; the length is longer for the GMA-containing terpolymers compared to the NAS-containing terpolymers under the same ATRP conditions. However, this speculation is predicated on GPC-determined molecular weights with polystyrene standards; the relationship between hydrodynamic volume and molecular weight may be quite different for the terpolymers versus the polystyrene standards.

4.3.3 Functionalization of Epoxy Groups of Poly(NIPAAM–GMA–tBA) with Propargylamine—Poly(NIPAAM–ppg–tBA)

To demonstrate the versatility of the terpolymer with regard to orthogonal post-polymerization modifications, the chemical transformation of the oxirane ring of the GMA units was investigated. Although the oxirane ring can be utilized in a one-step reaction to add a desired final moiety, another route was targeted that would allow for further elaboration of the resulting chemical modification at the oxirane sites. Thus, the oxirane units was chosen to be modified with "clickable" groups so as to generate a terpolymer with reactive sites that are highly specific with respect to chemical reactivity and allow for further increases in creation of more complex polymer architectures. Click chemistry, a term popularized by Sharpless,[11,40] refers to chemical transformations that offer simple reaction conditions and method of product isolation, broad scope, stoichiometric yields, high selectivity, and generate benign by-products. The Cu(I)-catalyzed variant[11,40-42] of the Huisgen[43] 1,3-dipolar cycloaddition reaction between azides and alkynes has met this stringent criteria, gaining increasing interest with practitioners of various fields since its inception.

The choice for the alkyne necessary for click chemical modification of the terpolymer is the propargyl moiety. NIPAAM polymers with pendant propargyl groups have been synthesized both by conventional free radical polymerization[44] and ATRP.[45] However, the route proposed here in Scheme 4.1 is a more practical way of synthesizing alkyne-containing polymers because

direct ATRP of propargyl-containing monomers requires an organosilyl-protected monomer that has to be synthesized, and there is a subsequent deprotection step to yield a polymer with accessible alkyne groups.[3,45-46] This protection of the monomer is necessary so as to prevent complexation of the propargyl group with the Cu catalyst during ATRP[47] as well as any possible cross-linking that results from addition reactions of propargyl radicals that form.[3] Another approach is the preparation of azide-containing polymers.[10,48] However, the direct ATRP of azido-monomers is complicated by the synthesis and purification of the monomer.[48] The ring-opening reaction of GMA-containing polymer with sodium azide results in an efficient incorporation of azide moieties.[10] However, propargyl-derivatized sugars is not as well-documented as azido-functionalized sugars;[49] an important consideration for the next task at hand.

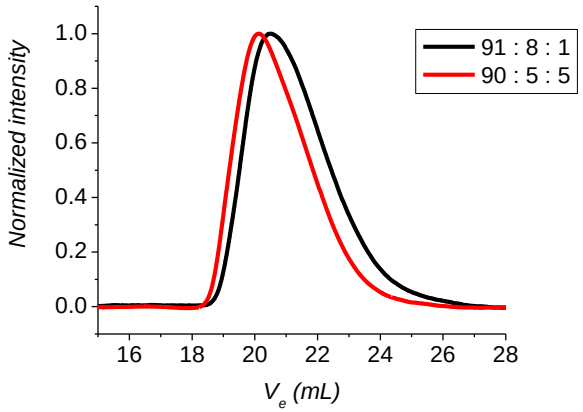

Figure 4.4. GPC traces of poly(NIPAAM-GMA-tBA) (DMF with added 0.1 M LiBr) prepared using two different monomer feed ratios.

For addition of the propargyl group to the terpolymer, poly($NIPAAM_{80}$–GMA_{16}–tBA_4) was selected as a testbed case; the subscripts denote the ^1H NMR-determined % monomer content of the terpolymer. In Figure 4.5 (upper trace) is shown the ^1H NMR (in $CDCl_3$) spectrum after derivatization of the pendant GMA groups with propargylamine via a mild ring-

opening reaction to yield poly(NIPAAM–ppg–tBA). Completion of the oxirane ring-opening reaction is supported by the absence of the ^{1}H resonances associated with the intact oxirane ring and the presence of new ^{1}H signals assigned to the proton resonances of the terminal alkyne hydrogen at 2.27 ppm, the methylene protons adjacent to the amine at 2.85 ppm, the methylene protons of the nearby alkyne at 3.48 ppm, and protons from the methylene group at the neighboring ester and the methyne adjacent to the hydroxyl group that collectively overlap with the methyne peak of NIPAAM at 4.00 ppm; see Figure 4.6 for the detailed assignments. A broad, almost indistinguishable peak, centered at 5.00 ppm, is thought to be due to the secondary alcohol generated from ring opening. The propargyl units of the poly(NIPAAM–ppg–tBA) can then be further elaborated with biologically important materials.

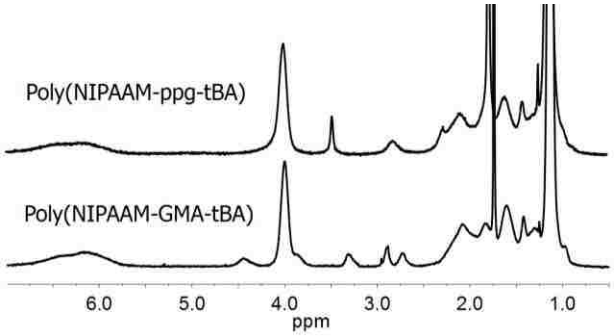

Figure 4.5. Comparison of the ^{1}H NMR spectra ($CDCl_3$) for the propargylamine-modified terpolymer, poly(NIPAAM–ppg–tBA), synthesized from poly(NIPAAM–GMA–tBA) as per Scheme 4.1.

4.3.4 Click Reaction Between poly(NIPAAM–ppg–tBA) and 1-Azido-1-deoxy-*β*-D-lactopyranoside—Poly(NIPAAM–lac–tBA)

To demonstrate the utility of poly(NIPAAM–ppg–tBA) toward modifications and create biologically-relevant materials, the terpolymer was modified with a lectin protein and its complementary binding sugar for potential application in temperature-facilitated affinity chromatography, a system that was introduced by Yamanaka, Okano and coworkers.[18] *Ricinus communis* agglutinin (RCA_{120}) and its binding sugar lactose were chosen as model partners

because of their commercial availability and the lectin's well-known specificity to galactose-containing materials.[50-51] This system, upon integration into microfluidic devices, can then serve to capture and isolate glycoproteins bearing a specific sugar moiety (galactose in this case). Strategically, the structure of the poly(NIPAAM–ppg–tBA) is such that the two pendant functional groups (propargyl and *tert*-butyl groups) can be modified sequentially and independent of each other without side reactions/cross reactions. In addition, having multiple pendant functionalities of predefined composition should also provide better control over the composition of the individual components in the resulting polymer after the modifications are performed, a task that is difficult to achieve when only one functionality is available for use to append two or more substituents.

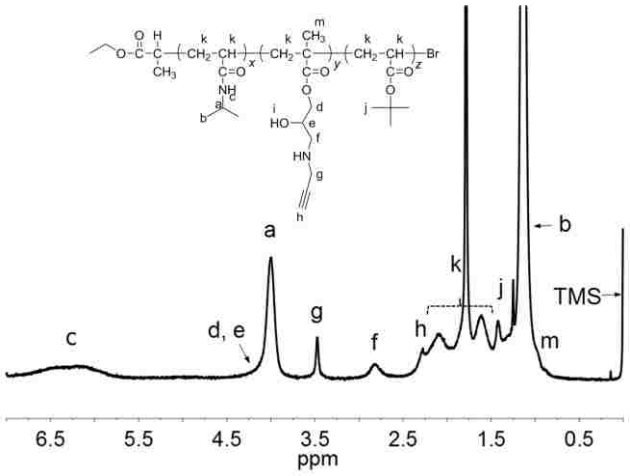

Figure 4.6. ^{1}H NMR ($CDCl_3$) of poly(NIPAAM–ppg–tBA).

Synthetically, for modifications of the poly(NIPAAM–ppg–tBA), the propargyl groups were modified first via click chemistry to avoid any side reactions that might occur with the unmodified propargyl moiety if acid deprotection of the *tert*-butyl ester groups were to be performed first. This route was selected because the *tert*-butyl ester groups of the poly(NIPAAM–ppg–tBA) should be inert under conditions that are often used for click

chemistry. Hence, the first step towards modification of the terpolymer with the biologically-relevant molecules selected is to utilize the propargyl groups to accommodate multiple copies of the binding sugar along the thermoresponsive terpolymer backbone. Although the lectin protein could have been attached through the propargyl groups in the first step, the sugar was chosen due to the commercial availability of azide-modifed sugars and because sugars are not likely to be extremely affected by the reaction conditions of the acid deprotection that is to follow. In addition, if lectins will be utilized for click chemistry, another step would be required to afford the protein with azide functionalities.

Neoglycopolymers have been successfully prepared by click chemistry in both aqueous and organic environments using propargyl-functionalized polymers.[3,9,46,49] The click method employed here is based on the approach of Hawker and coworkers,[3] with slight modifications. In their development of an orthogonal functionalization method of vinyl polymers, $CuBr(PPh_3)_3$ and DIPEA were used as the catalyst and the base, respectively, in THF solvent. However, the azide-functionalized lactopyranoside used herein was not sufficiently soluble in THF; after screening various solvents, DMF was chosen. As shown in Figure 4.7, ^{1}H NMR analysis led to observation of the unique resonance of the triazole hydrogen signal at 8.15 ppm (designated as *h* in Figure 4.7). The modification is also verified by the increase in the cloud point, CP, *vide infra*. Importantly, the *tert*-butyl groups were unaffected by the click chemistry conditions, as evidenced by inspection of the ^{1}H NMR spectrum.

4.3.5 Deprotection of poly(NIPAAM–lac–tBA) by TFA—Poly(NIPAAM–lac–Aac)

In order to generate the carboxylic acid functionality necessary for further modification, hydrolysis of the *tert*-butyl ester groups of the poly(NIPAAM–lac–tBA) was performed with neat TFA at room temperature. This reaction is widely known to convert a variety of *tert*-butyl

ester groups to their corresponding carboxylic acid counterparts. However, with the excess TFA used, trifluoroacetylation of the hydroxyl groups in the terpolymer[52-53] (e.g. from the ring opening reaction and from pendant lactose) is a potential side reaction. But, such esters are unstable and are rapidly cleaved in the presence of water to reveal the hydroxyl groups.[53-54] Therefore, extensive dialysis in $NaHCO_3$ solution was performed as part of the purification procedure. After 6 h reaction with TFA and subsequent workup, the ^{1}H NMR spectrum of the poly(NIPAAM–lac–Aac) revealed the lack of the proton signal for the *tert*-butyl resonance at 1.37 ppm (Figure 4.8), an observation that is consistent with that reported by Matyjaszewski for ATRP-prepared poly(*tert*-butyl acrylates).[32]

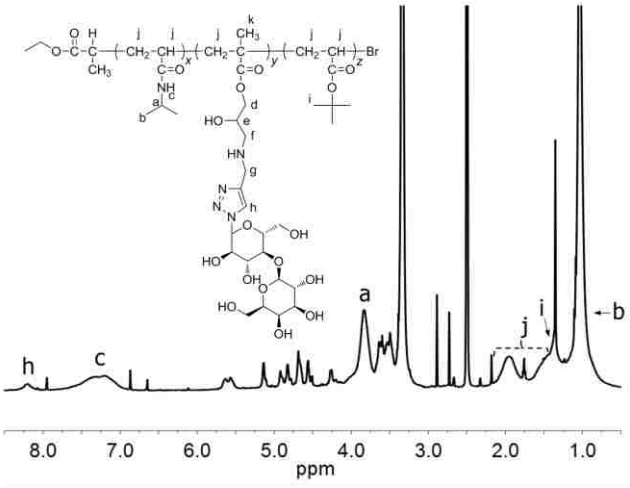

Figure 4.7. ^{1}H NMR (DMSO-d_6) of poly(NIPAAM–lac–tBA).

4.3.6 Conjugation of RCA_{120} with Poly(NIPAAM–lac–Aac)—Poly(NIPAAM–lac–RCA_{120})

Covalent linking of *Ricinus communis* agglutinin, RCA_{120}, to the free carboxylic acid groups of the poly(NIPAAM–lac–Aac) was achieved by aqueous carbodiimide coupling that employed EDC and NHS. As is typically the case for such coupling reactions of proteins,[55] the presumed actor in the reaction is the lysine group of the protein (lectin). Because the long-term application of the poly(NIPAAM–lac–RCA_{120}) materials is for affinity chromatography

purifications of glycosylated proteins, it is necessary to keep the lectin binding site accessible. Therefore, free lactose was added to the reaction mixture to prevent polymer attachment to the RCA_{120} at locations on the RCA_{120} lectin that are near or at its sugar binding site.

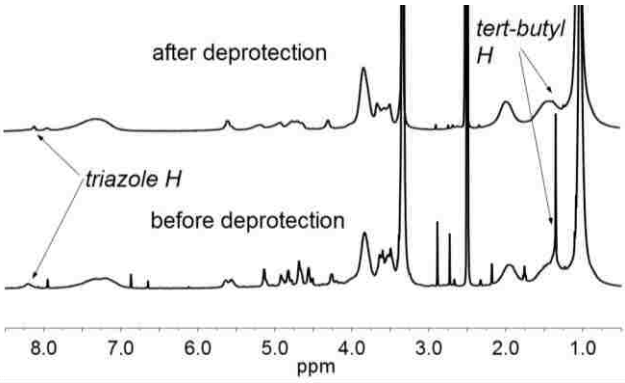

Figure 4.8. ^{1}H NMR (DMSO-d_6) of poly(NIPAAM–lac–tBA) before and after removal of the *tert*-butyl protecting groups.

Following desalting procedures, the poly(NIPAAM–lac–RCA_{120}) was subjected to SDS–PAGE analysis, Figure 4.9. SDS–PAGE results obtained under non-reducing conditions reveal that the RCA_{120} was conjugated to the activated terpolymer based on the following observations: (1) quite evident is an intense band near the gel loading well (see arrow) in lane 3 and a diffuse band emanating away from the intense band. These two observations support the presence of high-molecular-weight materials that are assigned to the conjugated product; (2) there is no free RCA_{120} apparent in lane 3 (terpolymer-RCA_{120} conjugate), as judged by comparison to lane 2 for RCA_{120} loaded on the gel at roughly half the concentration of that loaded in lane 3. This lack of free RCA_{120} indicates its complete reaction with the EDC/NHS-activated poly(NIPAAM–lac–Aac); (3) upon inspection of the control experiment in lane 4, for a mixture of RCA_{120} and *unactivated* poly(NIPAAM–lac–Aac), the RCA_{120} band is clearly observable. The presence of free RCA_{120} in this control experiment indicates that there is no significant binding of free RCA_{120} to the *unactivated* poly(NIPAAM–lac–Aac); this strongly suggests that RCA_{120} is

covalently attached to the terpolymer chains after the conjugation reaction, thereby verifying the results in lane 3. Thus, it can be concluded that the RCA_{120} was successfully conjugated to the activated poly(NIPAAM–lac–Aac) via amide functionalities to yield the desired poly(NIPAAM–lac–RCA_{120}). It should be noted that although RCA_{120} has a nominal molecular weight of 120 kDa, its protein band here appears at significantly higher molecular weight which is due to the fact that the SDS–PAGE was run in non-reducing conditions (i.e. no β-mercaptoethanol) resulting in a different migration rate compared to a totally linear protein. It can be ascertained, however, that the bands observed are indeed from RCA_{120} because under reducing conditions (i.e. with β-mercaptoethanol), the 4 subunits of the same RCA_{120} solution appeared between 32 and 38 kDa of the molecular weight standards (data not shown), in good agreement with published results.

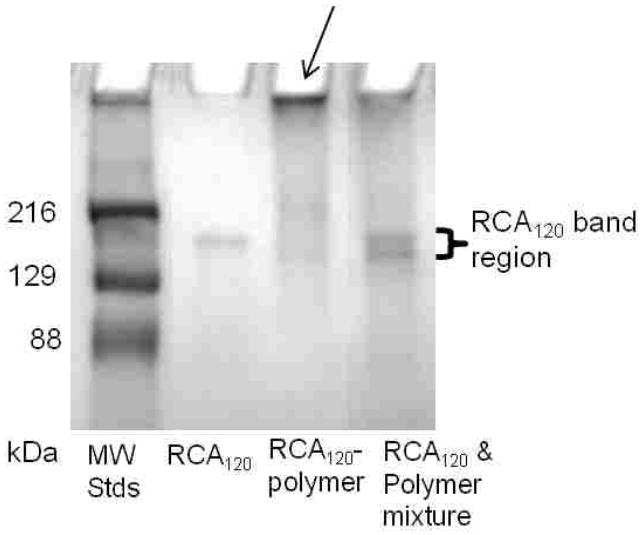

Figure 4.9. SDS–PAGE of poly(NIPAAM–lac–RCA_{120}). Lane 1: protein molecular weight standards. Lane 2: RCA_{120} (0.5 μg). Lane 3: crude conjugate mixture (1 μg total RCA_{120} and 10 μg poly(NIPAAM–lac–Aac); free or conjugated). Lane 4: control — mixture of terpolymer and RCA_{120} (1 μg RCA_{120} and 10 μg poly(NIPAAM–lac–Aac).

At this time, the data in hand will not allow for assignment of the stoichiometry of the RCA_{120} and terpolymer in the conjugate. The rationale for this is two-fold in nature. First,

RCA_{120} possesses several lysine groups that possibly can be attached to the poly(NIPAAM–lac–Aac).[56] Second, the molecular weight of the poly(NIPAAM–lac–Aac) is not accurately known. Regardless, the goal of developing and implementing a synthetic strategy for creating a terpolymer bearing propargyl and *tert*-butyl groups that can be independently modified was achieved. This is demonstrated for the specific case of lactose and RCA_{120} being appended to the polymer, and it is clear that the rich chemistries available with the propargyl and *tert*-butyl groups hold much potential for the creation of other complex dual functionality polymers. The pertinent question at hand and that which I now turn my attention is that regarding retention of thermoresponsivity in the terpolymer as a function of derivatization step.

4.3.7 Thermal Response of Poly(NIPAAM) and Poly(NIPAAM–NAS–tBA)

A unique property of thermoresponsive polymers that is quite important in polymer physics and solution dynamics, and has been exploited in numerous applications, is the coil-to-globule transition that occurs at the lower critical solution temperature (LCST), where a reversible phase separation is observed.[17,57-58] This critical temperature is characteristic of the particular polymer and provides additional information such as chain length[25,59] and composition;[60-61] that is, the chain length and composition of the polymer impact the LCST. For poly(*N*-isopropylacrylamide), the LCST is near 32 °C in aqueous media.[16] The solubility of poly(NIPAAM) below its LCST is attributed to hydrogen bonding between amide groups and the surrounding water molecules. As the solution temperature approaches the polymer LCST, hydrogen bonding weakens and hydrophobic interactions between isopropyl groups become dominant due to the release of structured water around the isopropyl groups.[60]

In general, the polymers prepared from NIPAAM, NAS, and tBA elicited thermoresponsive behavior. The homopolymer of NIPAAM afforded a cloud point (CP)

temperature that was consistently around 29.5 °C. As the NAS, tBA, and GMA content of the terpolymer was increased, the cloud point temperature decreased accordingly (Table 4.1). This is a likely outcome because incorporation of relatively hydrophobic comonomers tends to decrease the phase transition temperature due to perturbation of the overall hydrophilic/hydrophobic balance of the polymer.[60-61]

It is interesting to note that the cloud point temperature recorded for the NIPAAM homopolymer prepared here is at least two degrees lower than that of poly(NIPAAM) in the literature.[16] To ensure that the manner of solution preparation for cloud point temperature studies and any fluctuations of the temperature-sensing device are not responsible for this observation, a solution of commercial poly(NIPAAM) was prepared and investigated side by side with the ATRP-prepared poly(NIPAAM). The cloud point temperature obtained for commercial poly(NIPAAM) is 32.8 °C (data not shown), a value that lies in the typical range and is three degrees higher than obtained for the poly(NIPAAM) by ATRP.

Based on the experimental outcomes and those from others in the literature, it is proposed that the lower-than-expected cloud point temperature of the ATRP-derived PNIPAAM obtained herein is likely influenced by the chain length and the mildly hydrophobic nature of the ethyl propionate and bromine end groups. Recently, Stöver and co-workers[25,59] elucidated the relationship between cloud point temperature and molecular weight of poly(NIPAAM) prepared by ATRP, taking into consideration any effects posed by the end groups (i.e. from the initiator used during the polymerization). In their studies, it was found that for polymers with low dispersities of molecular weight, the phase transition temperature dramatically decreased with increasing molecular weight, with the sensitivity of the decrease being largely dependent on the identity (type) of end groups. To the best of my knowledge, Stöver's study is the only report in

the literature that discusses the dependence of cloud point temperature with molecular weight of ATRP-prepared poly(NIPAAM). However, this literature is not applicable to aid in understanding the lower-than-expected cloud point temperature observed in this work, for several reasons. First, it is evident from the GPC data (Figure 4.2 and Table 4.1) that the poly(NIPAAM) prepared herein is polydisperse. A basic premise of the study conducted by Stöver and co-workers was elimination of ambiguity concerning the molecular weight effects from conventionally-prepared poly(NIPAAM) samples because of their polydispersity. Secondly, Stöver and co-workers employed chloro initiators while a bromo initator (as ethyl 2-bromopropionate) was utilized in the work herein. It has been previously reported that end groups have a profound effect on the cloud points of poly(NIPAAM)[25,61] because the high mobility of the end group is apparently responsible for the initiation of the phase separation.[61] However, as investigations from Stöver and co-workers were focused on polymer end groups that were obtained from chloro-based initiators, the magnitude of the effect of bromine as an end group cannot be deduced. Thirdly, the molecular weight of the PNIPAAM prepared herein is not accurately known. The M_n values obtained from GPC experiments and displayed in Table 4.1 should only be used to reveal trends because the hydrodynamic volume of poly(NIPAAM) homopolymer and terpolymers may not be identical to that of the polystyrene standards used or the polymer chains could have aggregated during the GPC experiment, like those observed in THF-based GPC.[62-63] If the argument of Stöver and co-workers would be assumed valid herein, the low cloud point temperature obtained in the work herein for poly(NIPAAM) would be characteristic of high molecular weight samples with ethylpropionate and bromine as end groups. There is compelling evidence that the molecular weight is higher than the predicted (theoretical M_n) because NMR analysis led to observation of a substantial amount of unreacted initiator after

the polymerization reaction was stopped (data not shown), indicating that initiation was not 100% efficient. Thus, a lesser number of initiation sites would result in longer polymer chains. However, in the absence of an absolutely known MW, any claim cannot be made with regard to the basis of the unexpected low cloud point temperature of ATRP-prepared poly(NIPAAM) observed in this work. For now, it is sufficient to say that the cloud point temperature of the poly(NIPAAM) obtained herein is likely influenced by the chain length and the mildly hydrophobic nature of the ethyl propionate and bromine end groups.

4.3.8 Thermal Response of Terpolymers—Orthogonally Derivatized Poly(NIPAAM–GMA–tBA) Materials

A comparison of the transmittance versus temperature curves for the poly(NIPAAM–GMA–tBA) as a function of state of chemical modification is shown in Figure 4.10. Upon examination of the response for each macromolecule in detail, it is found that poly(NIPAAM–GMA–tBA) has the lowest phase transition temperature due to the presence of relatively hydrophobic glycidyl and *tert*-butyl groups. Conversion of the glycidyl group to yield a terpolymer containing propargyl groups, poly(NIPAAM–ppg–tBA), results in the presence of hydroxyl groups that are hydrophilic, and as expected, a shift toward higher phase transition temperature is noted. After click reaction of the propargyl groups in poly(NIPAAM–ppg–tBA) with lactose to give poly(NIPAAM–lac–tBA), an aqueous solution of this polymer exhibited a very slow decrease in transmittance at the temperature range studied, with no distinct transition noted; a 50% decrease in transmittance was not reached even at ~70 °C, although slight cloudiness was visible by eye. This observation is understandable, as the presence of the highly hydrophilic lactose groups is expected to perturb dramatically the hydrophilic/hydrophobic balance of the terpolymer. A significantly high phase transition temperature is thus expected for

the poly(NIPAAM–lac–tBA), similar to those previously observed with thermoresponsive glycopolymers.[64-65]

Interestingly, the presence of acrylic acid side chains in poly(NIPAAM–lac–Aac) that result from removal of the *tert*-butyl groups in poly(NIPAAM–lac–tBA) leads to a large change in the thermal response. From the curve generated from a solution of poly(NIPAAM–lac–Aac), the decrease in transmittance is observed earlier and is more pronounced than for the poly(NIPAAM–lac–tBA), i.e. cloud point temperature is lower. The lower transition temperature of the poly(NIPAAM–lac–Aac) points to a scenario wherein the terpolymer is now less hydrophilic than its predecessor terpolymer, poly(NIPAAM–lac–tBA). This seems counterintuitive as conversion from *tert*-butyl groups to acrylic acid groups should result in increased hydrophilicity of the terpolymer, thereby raising its phase transition temperature, similar to what is generally observed for random copolymers of NIPAAM with acrylic acid or hydrophilic monomers.[60,64-67] It is posited that the more hydrophobic nature of the terpolymer poly(NIPAAM–lac–Aac), as noted by the lower CP value, can be rationalized as a result of decreased hydrogen bonding interaction between polar groups (–CONH– from NIPAAM, –OH from lactose, and –COOH/–COO^- from acrylic acid) and water because of favorable inter- and intramolecular hydrogen bonding of the polar groups. This is a very likely scenario because polysaccharides and poly(carboxylic acids) are known to form interpolymer complexes through hydrogen bonding.[68] It is possible that the close proximity of the lactose –OH groups and the carboxylic acid groups along the terpolymer chain makes it favorable to form hydrogen bonds. This would decrease the overall hydrophilicity of the terpolymer as a result of decreased interaction between the terpolymer and water leading to a decreased CP value. When the pH of the solution was made acidic (pH 2.77), the change in transmittance of the solution was observed

at a lower temperature (data not shown) compared to the terpolymer at pH 7.38. This reinforces the hypothesis, because interpolymer complex formation should become more favorable as the number of –COOH groups increases. An alternative explanation for the lower cloud point temperature of the poly(NIPAAM–lac–Aac) is the creation of a hydrophobic environment after possible ester formation between the –OH groups of lactose and the $–COO^-$ of acrylic acid, similar to esterification reactions of polyhydroxy compounds with trifluoroacetates[52-54] or dextran with bioactive carboxylic acid.[69] However, in the absence of a catalyst, the ester formation is very unlikely to occur.

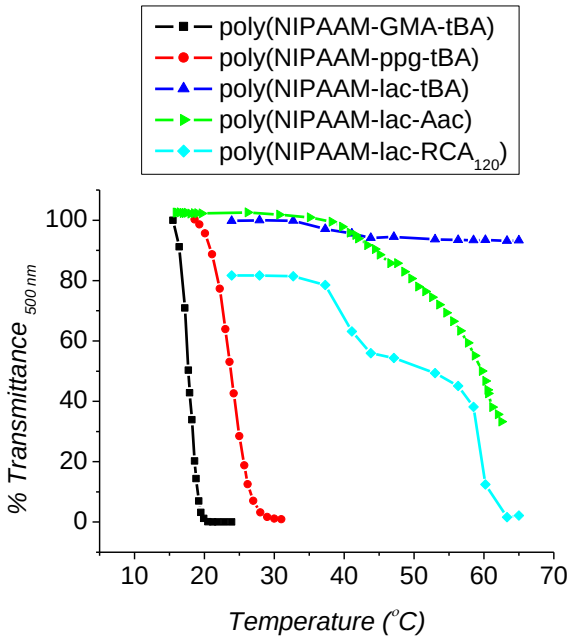

Figure 4.10. Thermoresponsive behavior of the terpolymers in aqueous solution (1% w/v) as judged by transmittance measurements at 500 nm.

Upon conjugation of poly(NIPAAM–lac–Aac) to RCA_{120}, the conjugation product, poly(NIPAAM–lac–RCA_{120}), possesses a temperature response curve that indicates a lower cloud point temperature, but one that is much more complex in nature than that of poly(NIPAAM–lac–Aac). Many research studies on protein–poly(NIPAAM) conjugates

prepared either by single-point terminal grafting[70-71] or multi-point random grafting[55,72] have reported phase transition temperatures that are about the same as the homopolymer poly(NIPAAM). However, it should be noted that the conjugates have been composed primarily of poly(NIPAAM) and protein. The conjugate that is prepared herein involves a more complicated system in that the two terpolymer groups, namely RCA_{120} and lactose, are binding partners. Therefore, the lower CP observed here for poly(NIPAAM–lac–RCA_{120}) is likely a consequence of the interaction of lactose and RCA_{120}, both of which are attached to the terpolymer. A highly reproducible two-step decrease in transmittance is observed, pointing to two different processes. At present it is not clear what is the origin of these transitions. Nevertheless, the poly(NIPAAM–lac–RCA_{120}) exhibits thermoresponsive behavior that is key in the long-term use of this dual-functionalized material as a capture agent for glycosylated (galactose-modified) proteins.

4.4 Conclusions

A terpolymer consisting of *N*-isopropylacrylamide, glycidyl methacrylate, and *tert*-butyl acrylate was synthesized with high monomer yields by atom transfer radical polymerization employing a CuBr/Me_4cyclam catalytic system, namely, poly(NIPAAM–GMA–tBA). In contrast, low monomer conversion was observed when *N*-acryloxysuccinimide was used as comonomer instead of glycidyl methacrylate. Importantly, the poly(NIPAAM–GMA–tBA) exhibits thermoresponsive behavior, and its possession of two functional groups with the unique ability to be further elaborated in an orthogonal manner allows for versatile post-polymerization modifications. This terpolymer was easily transformed into a propargyl-containing terpolymer that is capable of participating in click reactions. To demonstrate its high capacity to contain multiple groups along the backbone, this terpolymer was modified in a multi-step fashion to

yield a terpolymer possessing two distinct biologically-important materials, namely a lectin (RCA_{120}) and a sugar (lactose). The resulting polymer conjugate, poly(NIPAAM–lac–RCA_{120}), exhibits thermoresponsive behavior. The synthetic strategy proposed here is general in nature and is relevant for the preparation of multi-functional "smart" microfluidic surfaces and devices that would allow capture and release of unique set of glycoproteins.

4.5 References

(1) Tsarevsky, N. V.; Matyjaszewski, K. "Green" atom transfer radical polymerization: From process design to preparation of well-defined environmentally friendly polymeric materials. *Chem. Rev.* **2007**, *107*, 2270-2299.

(2) Ghosh, S.; Basu, S.; Thayumanavan, S. Simultaneous and reversible functionalization of copolymers for biological applications. *Macromolecules* **2006**, *39*, 5595-5597.

(3) Malkoch, M.; Thibault, R. J.; Drockenmuller, E.; Messerschmidt, M.; Voit, B.; Russell, T. P.; Hawker, C. J. Orthogonal approaches to the simultaneous and cascade functionalization of macromolecules using click chemistry. *J. Am. Chem. Soc.* **2005**, *127*, 14942-14949.

(4) Xu, J.; Ye, J.; Liu, S. Synthesis of well-defined cyclic poly(*N*-isopropylacrylamide) via click chemistry and its unique thermal phase transition behavior. *Macromolecules* **2007**, *40*, 9103-9110.

(5) Gauthier, M. A.; Gibson, M. I.; Klok, H. A. Synthesis of functional polymers by post-polymerization modification. *Angew. Chem. Int. Ed.* **2009**, *48*, 48-58.

(6) Braunecker, W. A.; Matyjaszewski, K. Controlled/living radical polymerization: Features, developments, and perspectives. *Prog. Polym. Sci.* **2007**, *32*, 93-146.

(7) Johnson, J. A.; Lewis, D. R.; Diaz, D. D.; Finn, M. G.; Koberstein, J. T.; Turro, N. J. Synthesis of degradable model networks via ATRP and click chemistry. *J. Am. Chem. Soc.* **2006**, *128*, 6564-6565.

(8) Sumerlin, B. S.; Vogt, A. P. Macromolecular engineering through click chemistry and other efficient transformations. *Macromolecules* **2010**, *43*, 1-13.

(9) Geng, J.; Lindqvist, J.; Mantovani, G.; Haddleton, D. M. Simultaneous copper(I)-catalyzed azide-alkyne cycloaddition (CuAAC) and living radical polymerization. *Angew. Chem. Int. Ed.* **2008**, *47*, 4180-4183.

(10) Tsarevsky, N. V.; Bencherif, S. A.; Matyjaszewski, K. Graft copolymers by a combination of ATRP and two different consecutive click reactions. *Macromolecules* **2007**, *40*, 4439-4445.

(11) Kolb, H. C.; Finn, M. G.; Sharpless, K. B. Click chemistry: Diverse chemical function from a few good reactions. *Angew. Chem. Int. Ed.* **2001**, *40*, 2004-2021.

(12) Langer, R.; Tirrell, D. A. Designing materials for biology and medicine. *Nature* **2004**, *428*, 487-492.

(13) Spafford, M.; Polozova, A.; Winnik, F. M. Synthesis and characterization of a hydrophobically modified copolymer of *N*-isopropylacrylamide and glycinyl acrylamide. *Macromolecules* **1998**, *31*, 7099-7102.

(14) Sun, X. L.; Haller, C. A.; Wu, X. Y.; Conticello, V. P.; Chaikof, E. L. One-pot glyco-affinity precipitation purification for enhanced proteomics: The flexible alignment of solution-phase capture/release and solid-phase separation. *J. Proteome Res.* **2005**, *4*, 2355-2359.

(15) Gong, C. B.; Wong, K. L.; Lam, M. H. W. Photoresponsive molecularly imprinted hydrogels for the photoregulated release and uptake of pharmaceuticals in the aqueous media. *Chem. Mater.* **2008**, *20*, 1353-1358.

(16) Schild, H. G. Poly (*N*-isopropylacrylamide) - experiment, theory and application. *Prog. Polym. Sci.* **1992**, *17*, 163-249.

(17) Tiktopulo, E. I.; Uversky, V. N.; Lushchik, V. B.; Klenin, S. I.; Bychkova, V. E.; Ptitsyn, O. B. Domain coil-globule transition in homopolymers. *Macromolecules* **1995**, *28*, 7519-7524.

(18) Yamanaka, H.; Yoshizako, K.; Akiyama, Y.; Sota, H.; Hasegawa, Y.; Shinohara, Y.; Kikuchi, A.; Okano, T. Affinity chromatography with collapsibly tethered ligands. *Anal. Chem.* **2003**, *75*, 1658-1663.

(19) Li, Z.; Wang, F.; Roy, S.; Sen, C. K.; Guan, J. J. Injectable, highly flexible, and thermosensitive hydrogels capable of delivering superoxide dismutase. *Biomacromolecules* **2009**, *10*, 3306-3316.

(20) Kulkarni, S.; Schilli, C.; Muller, A. H. E.; Hoffman, A. S.; Stayton, P. S. Reversible meso-scale smart polymer-protein particles of controlled sizes. *Bioconjugate Chem.* **2004**, *15*, 747-753.

(21) Gujadhur, R.; Venkataraman, D.; Kintigh, J. T. Formation of aryl---nitrogen bonds using a soluble copper(I) catalyst. *Tetrahedron Lett.* **2001**, *42*, 4791-4793.

(22) Teodorescu, M.; Matyjaszewski, K. Atom transfer radical polymerization of (meth)acrylamides. *Macromolecules* **1999**, *32*, 4826-4831.

(23) Rademacher, J. T.; Baum, M.; Pallack, M. E.; Brittain, W. J.; Simonsick, W. J. Atom transfer radical polymerization of *N*,*N*-dimethylacrylamide. *Macromolecules* **2000**, *33*, 284-288.

(24) Masci, G.; Giacomelli, L.; Crescenzi, V. Atom transfer radical polymerization of *N*-isopropylacrylamide. *Macromol. Rapid Commun.* **2004**, *25*, 559-564.

(25) Xia, Y.; Burke, N. A. D.; Stover, H. D. H. End group effect on the thermal response of narrow-disperse poly(*N*-isopropylacrylamide) prepared by atom transfer radical polymerization. *Macromolecules* **2006**, *39*, 2275-2283.

(26) Balamurugan, S.; Mendez, S.; Balamurugan, S. S.; O'Brie, M. J.; Lopez, G. P. Thermal response of poly(*N*-isopropylacrylamide) brushes probed by surface plasmon resonance. *Langmuir* **2003**, *19*, 2545-2549.

(27) Savariar, E. N.; Thayumanavan, S. Controlled polymerization of *N*-isopropylacrylamide with an activated methacrylic ester. *J. Polym. Sci., Part A: Polym. Chem.* **2004**, *42*, 6340-6345.

(28) Monge, S.; Giani, O.; Ruiz, E.; Cavalier, M.; Robin, J. J. A new route for the modification of halogen end groups to amino end-functionalized poly(*tert*-butyl acrylate)s. *Macromol. Rapid Commun.* **2007**, *28*, 2272-2276.

(29) Godwin, A.; Hartenstein, M.; Muller, A. H. E.; Brocchini, S. Narrow molecular weight distribution precursors for polymer-drug conjugates. *Angew. Chem. Int. Ed.* **2001**, *40*, 594-597.

(30) Hu, Z. C.; Liu, Y.; Hong, C. Y.; Pan, C. Y. Synthesis of well-defined glycoconjugate polyacrylamides via preactivated polymers prepared by ATRP. *J. Appl. Polym. Sci.* **2005**, *98*, 189-194.

(31) Huang, C. Q.; Hong, C. Y.; Pan, C. Y. Formation of flower-like aggregates from self-assembling of micelles with PEO shells and cross-linked polyacrylamide cores. *Chin. J. Polym. Sci.* **2008**, *26*, 341-352.

(32) Davis, K. A.; Matyjaszewski, K. Atom transfer radical polymerization of *tert*-butyl acrylate and preparation of block copolymers. *Macromolecules* **2000**, *33*, 4039-4047.

(33) Rathfon, J. M.; Tew, G. N. Synthesis of thermoresponsive poly(*N*-isopropylmethacrylamide) and poly(acrylic acid) block copolymers via post-functionalization of poly(*N*-methacryloxysuccinimide). *Polymer* **2008**, *49*, 1761-1769.

(34) Matyjaszewski, K.; Coca, S.; Jasieczek, C. B. Polymerization of acrylates by atom transfer radical polymerization. Homopolymerization of glycidyl acrylate. *Macromol. Chem. Phys.* **1997**, *198*, 4011-4017.

(35) Bao, Z.; Bruening, M. L.; Baker, G. L. Rapid growth of polymer brushes from immobilized initiators. *J. Am. Chem. Soc.* **2006**, *128*, 9056-9060.

(36) Monge, S.; Haddleton, D. M. Synthesis of precursors of poly(acrylamides) by copper mediated living radical polymerization in DMSO. *Eur. Polym. J.* **2004**, *40*, 37-45.

(37) Barbey, R.; Lavanant, L.; Paripovic, D.; Schuwer, N.; Sugnaux, C.; Tugulu, S.; Klok, H. A. Polymer brushes via surface-initiated controlled radical polymerization: Synthesis, characterization, properties, and applications. *Chem. Rev.* **2009**, *109*, 5437-5527.

(38) Krishnan, R.; Srinivasan, K. S. V. Controlled/"living" radical polymerization of glycidyl methacrylate at ambient temperature. *Macromolecules* **2003**, *36*, 1769-1771.

(39) Cañamero, P. F.; de la Fuente, J. L.; Madruga, E. L.; Fernández-García, M. Atom transfer radical polymerization of glycidyl methacrylate: A functional monomer. *Macromol. Chem. Phys.* **2004**, *205*, 2221-2228.

(40) Rostovtsev, V. V.; Green, L. G.; Fokin, V. V.; Sharpless, K. B. A stepwise Huisgen cycloaddition process: Copper(I)-catalyzed regioselective "ligation" of azides and terminal alkynes. *Angew. Chem. Int. Ed.* **2002**, *41*, 2596-2599.

(41) Wu, P.; Feldman, A. K.; Nugent, A. K.; Hawker, C. J.; Scheel, A.; Voit, B.; Pyun, J.; Frechet, J. M. J.; Sharpless, K. B.; Fokin, V. V. Efficiency and fidelity in a click-chemistry route to triazole dendrimers by the copper(I)-catalyzed ligation of azides and alkynes. *Angew. Chem. Int. Ed.* **2004**, *43*, 3928-3932.

(42) Tornoe, C. W.; Christensen, C.; Meldal, M. Peptidotriazoles on solid phase: [1,2,3]-triazoles by regiospecific copper(I)-catalyzed 1,3-dipolar cycloadditions of terminal alkynes to azides. *J. Org. Chem.* **2002**, *67*, 3057-3064.

(43) Huisgen, R. Kinetics and mechanism of 1,3-dipolar cycloadditions. *Angew. Chem. Int. Ed.* **1963**, *2*, 633-645.

(44) Bergbreiter, D. E.; Chance, B. S. Click-based covalent layer-by-layer assembly on polyethylene using water-soluble polymeric reagents. *Macromolecules* **2007**, *40*, 5337-5343.

(45) Huang, C.-J.; Chang, F.-C. Using click chemistry to fabricate ultrathin thermoresponsive microcapsules through direct covalent layer-by-layer assembly. *Macromolecules* **2009**, *42*, 5155-5166.

(46) Geng, J.; Mantovani, G.; Tao, L.; Nicolas, J.; Chen, G.; Wallis, R.; Mitchell, D. A.; Johnson, B. R. G.; Evans, S. D.; Haddleton, D. M. Site-directed conjugation of "clicked" glycopolymers to form glycoprotein mimics: Binding to mammalian lectin and induction of immunological function. *J. Am. Chem. Soc.* **2007**, *129*, 15156-15163.

(47) Opsteen, J. A.; van Hest, J. C. M. Modular synthesis of block copolymers via cycloaddition of terminal azide and alkyne functionalized polymers. *Chem. Commun.* **2005**, 57-59.

(48) Sumerlin, B. S.; Tsarevsky, N. V.; Louche, G.; Lee, R. Y.; Matyjaszewski, K. Highly efficient click functionalization of poly(3-azidopropyl methacrylate) prepared by ATRP. *Macromolecules* **2005**, *38*, 7540-7545.

(49) Ladmiral, V.; Mantovani, G.; Clarkson, G. J.; Cauet, S.; Irwin, J. L.; Haddleton, D. M. Synthesis of neoglycopolymers by a combination of click chemistry and living radical polymerization. *J. Am. Chem. Soc.* **2006**, *128*, 4823-4830.

(50) Sweeney, E. C.; Tonevitsky, A. G.; Temiakov, D. E.; Agapov, I. I.; Saward, S.; Palmer, R. A. Preliminary crystallographic characterization of Ricin agglutinin. *Proteins* **1997**, *28*, 586-589.

(51) Nicolson, G. L.; Blaustein, J. Interaction of *Ricinus communis* agglutinin with normal and tumor-cell surfaces. *Biochim. Biophys. Acta, Biomembr.* **1972**, *266*, 543-547.

(52) Fujii, K.; Brownstein, S.; Eastham, A. M. Reactions of trifluoroacetic acid with poly(vinyl alcohol) and its model compounds. Effect of neighboring hydroxyl groups on reaction. *J. Polym. Sci., Part A-1: Polym. Chem.* **1968**, *6*, 2377-2386.

(53) Holbert, G. W.; Ganem, B. Trifluoroacetylation of alcohols - newly detected reaction of CF_3CO_3H. *J. Chem. Soc. Chem. Comm.* **1978**, 248-248.

(54) Erberich, M.; Keul, H.; Moller, M. Polyglycidols with two orthogonal protective groups: Preparation, selective deprotection, and functionalization. *Macromolecules* **2007**, *40*, 3070-3079.

(55) Chen, J. P.; Yang, H. J.; Hoffman, A. S. Polymer protein conjugates. 1. Effect of protein conjugation on the cloud point of poly(*N*-isopropylacrylamide). *Biomaterials* **1990**, *11*, 625-630.

(56) Roberts, L. M.; Lamb, F. I.; Pappin, D. J. C.; Lord, J. M. The primary sequence of *Ricinus communis* agglutinin - comparison with Ricin. *J. Biol. Chem.* **1985**, *260*, 5682-5686.

(57) Wu, C.; Zhou, S. Q. Thermodynamically stable globule state of a single poly(*N*-isopropylacrylamide) chain in water. *Macromolecules* **1995**, *28*, 5388-5390.

(58) Kubota, K.; Fujishige, S.; Ando, I. Single-chain transition of poly(*N*-isopropylacrylamide) in water. *J. Phys. Chem.* **1990**, *94*, 5154-5158.

(59) Xia, Y.; Yin, X.; Burke, N. A. D.; Stover, H. D. H. Thermal response of narrow-disperse poly(*N*-isopropylacrylamide) prepared by atom transfer radical polymerization. *Macromolecules* **2005**, *38*, 5937-5943.

(60) Feil, H.; Bae, Y. H.; Feijen, J.; Kim, S. W. Effect of comonomer hydrophilicity and ionization on the lower critical solution temperature of *N*-isopropylacrylamide copolymers. *Macromolecules* **1993**, *26*, 2496-2500.

(61) Chung, J. E.; Yokoyama, M.; Aoyagi, T.; Sakurai, Y.; Okano, T. Effect of molecular architecture of hydrophobically modified poly(*N*-isopropylacrylamide) on the formation of thermoresponsive core-shell micellar drug carriers. *J. Controlled Release* **1998**, *53*, 119-130.

(62) Ganachaud, F.; Monteiro, M. J.; Gilbert, R. G.; Dourges, M.-A.; Thang, S. H.; Rizzardo, E. Molecular weight characterization of poly(*N*-isopropylacrylamide) prepared by living free-radical polymerization. *Macromolecules* **2000**, *33*, 6738-6745.

(63) Schilli, C.; Lanzendorfer, M. G.; Muller, A. H. E. Benzyl and cumyl dithiocarbamates as chain transfer agents in the raft polymerization of *N*-isopropylacrylamide. *In situ* FT-NIR and MALDI-TOF MS investigation. *Macromolecules* **2002**, *35*, 6819-6827.

(64) Ozyurek, Z.; Komber, H.; Gramm, S.; Schmaljohann, D.; Muller, A. H. E.; Voit, B. Thermoresponsive glycopolymers via controlled radical polymerization. *Macromol. Chem. Phys.* **2007**, *208*, 1035-1049.

(65) Pasparakis, G.; Cockayne, A.; Alexander, C. Control of bacterial aggregation by thermoresponsive glycopolymers. *J. Am. Chem. Soc.* **2007**, *129*, 11014-11015.

(66) Jones, M. S. Effect of pH on the lower critical solution temperatures of random copolymers of *N*-isopropylacrylamide and acrylic acid. *Eur. Polym. J.* **1999**, *35*, 795-801.

(67) Yin, X.; Hoffman, A. S.; Stayton, P. S. Poly(*N*-isopropylacrylamide-co-propylacrylic acid) copolymers that respond sharply to temperature and pH. *Biomacromolecules* **2006**, *7*, 1381-1385.

(68) *New trends in natural and synthetic polymer science*; Vasile, C.; Zaikov, G. E., Eds.; Nova Science Publishers, Inc.: New york, 2006.

(69) Sánchez-Chaves, M.; Arranz, F. Preparation of dextran-bioactive compound adducts by the direct esterification of dextran with bioactive carboxylic acids. *Polymer* **1997**, *38*, 2501-2505.

(70) Heredia, K. L.; Bontempo, D.; Ly, T.; Byers, J. T.; Halstenberg, S.; Maynard, H. D. *In situ* preparation of protein−"smart" polymer conjugates with retention of bioactivity. *J. Am. Chem. Soc.* **2005**, *127*, 16955-16960.

(71) Chen, G.; Hoffman, A. S. Preparation and properties of thermoreversible, phase-separating enzyme-oligo(*N*-isopropylacrylamide) conjugates. *Bioconjugate Chem.* **1993**, *4*, 509-514.

(72) Takei, Y. G.; Aoki, T.; Sanui, K.; Ogata, N.; Okano, T.; Sakurai, Y. Temperature-responsive bioconjugates. 1. Synthesis of temperature-responsive oligomers with reactive end groups and their coupling to biomolecules. *Bioconjugate Chem.* **1993**, *4*, 42-46.

CHAPTER 5

CONCLUSIONS AND OUTLOOK

5.1 Summary

The main goal of the research is the modification of microfluidic surfaces with glycoprotein receptors, namely boronic acid and lectin, for glycoprotein analysis. The interaction analyses between a select group of solution-phase glycoproteins and a unique boronic acid capture surface was demonstrated by surface plasmon resonance spectroscopy (SPR). The boronic acid derivative, 4-[(2-aminoethyl)carbamoyl]phenylboronic acid, AECPBA, was synthesized and then immobilized on carboxymethyl dextran surfaces using simple coupling methods. From SPR spectroscopy responses, it was found that model glycoproteins interact strongly with the AECPBA surface and subsequently can be readily released from the AECPBA surface using borate buffer. A striking difference between the glycoproteins fetuin and asialofetuin (desialylated fetuin), in terms of glycoprotein binding to the AECPBA surface, indicated that the interaction of glycoproteins with the immobilized AECPBA is dictated by the terminal saccharide of the heteroglycan chain. Surprisingly, secondary interactions of glycosylated and non-glycosylated proteins with the carboxymethyl dextran hydrogel matrix were observed. Importantly, it was demonstrated that use of tris(hydroxymethyl)aminomethane buffer allows for decreased secondary interactions of non-glycosylated proteins on the AECPBA/dextran surface, as noted with the model protein ExtrAvidin.

After having demonstrated the capability of AECPBA immobilized on a surface to bind glycoproteins and subsequently be regenerated, AECPBA was used to modify poly(methyl methacrylate), PMMA, surfaces. This is relevant to the future fabrication of microanalytical devices that afford a global capture of glycoproteins prior to further fractionation by glycoprotein

subtype. AECPBA was covalently attached to carboxylic acid-terminated PMMA surfaces by carbodiimide coupling. Analysis of the surface by X-ray photoelectron spectroscopy revealed increasing amounts of surface-immobilized AECPBA with increasing carboxylic acid surface coverage on the PMMA. Greater-than-monolayer coverage of AECPBA was obtained for surfaces that had the highest carboxylic acid coverage examined. A continuous decrease in the contact angle of the surface at pH > 6, upon inspection by contact angle titration method, is consistent with a surface containing boronic acid (ionizable) groups. The binding—using glycine- and tris-buffered saline—and elution—using borate-buffered saline—of glycoproteins were accomplished with the aid of Tween 20, as a dynamic coating agent, which suppressed the hydrophobic interactions between the proteins and exposed underivatized regions of PMMA. Non-glycosylated proteins did not exhibit non-specific adsorption under the binding buffer system employed.

A synthetic strategy for efficient incorporation of multiple functionalities, namely *Ricinus communis* agglutinin lectin (RCA_{120}) and its complementary sugar lactose, into a polymer backbone that exhibits temperature-responsive behavior in aqueous media was presented. This synthetic strategy is relevant for developing microfluidic glycoprotein separation methods that do not require the use of externally added eluting agent. In particular, the use of *Ricinus communis* agglutinin as the glycoprotein receptor would allow the capture and enrichment of unique glycoproteins. A terpolymer, initially consisting of *N*-isopropylacrylamide and the functionalizable monomers *N*-acryloxysuccinimide and *tert*-butyl acrylate, was synthesized by atom transfer radical polymerization (ATRP) using the CuBr/Me_4cyclam catalytic system. The resulting thermoresponsive terpolymers exhibited a decrease in phase transition temperature with increased amount of *N*-acryloxysuccinimide and *tert*-butyl acrylate in the terpolymer. However,

polymerization of the three monomers was inefficient, and a dramatic decrease in monomer conversion was noted when the *N*-acryloxysuccinimide and *tert*-butyl acrylate monomer feed was increased. A significant improvement in monomer conversion was observed when glycidyl methacrylate was polymerized with *N*-isopropylacrylamide and *tert*-butyl acrylate, revealing a 93% conversion, as opposed to a 12% conversion with *N*-acryloxysuccinimide as the comonomer under identical ATRP conditions. The oxirane ring of the glycidyl methacrylate units of the terpolymer was further elaborated by propargylamine under mild conditions so as to contain individually-addressable "clickable" units in the terpolymer chain. To demonstrate its feasibility for post-polymerization modification, the propargyl groups and the *tert*-butyl groups were selectively and sequentially modified so as to yield a terpolymer possessing two different types of biologically-relevant moieties. An azide-functionalized sugar, 1-azido-1-deoxy-*β*-D-lactopyranoside ("azido-lactose"), was attached through the propargyl groups via click chemistry, with $CuBr(PPh_3)_3$ as the catalyst. The carboxylic acid functionalities of the terpolymer were revealed by *tert*-butyl group hydrolysis. Aqueous carbodiimide coupling was then subsequently used for attachment of a lectin protein, *Ricinus communis* agglutinin, that has a high binding specificity for lactose. The thermoresponsive property of the terpolymer through the course of the synthetic route was preserved, as demonstrated by turbidimetry experiments.

5.2 Conclusions

The results presented here demonstrate the capacity of AECPBA-derivatized carboxymethyl dextran and poly(methyl methacrylate) surfaces to capture glycoproteins from solution, and the ability of said capture surfaces to have their surface contents efficiently eluted at a later time; these outcomes bode well for use of these and similar surfaces in microfluidic devices for global capture, release and identification of glycoproteins.

The terpolymer poly(*N*-isopropylacrylamide–lactose–RCA_{120}) was successfully prepared by a combination of atom transfer radical polymerization (ATRP), click chemistry, and biologically-relevant post-polymerization modification reactions. This terpolymer exhibited thermoresponsive behavior where binding and elution of glycoprotein analytes can be facilitated by temperature manipulation and one that does not require introduction of eluting agents through the mobile phase, an important feature that allows direct integration of microfluidic devices to mass spectrometry. Because the synthetic route proposed here possesses surface-amenable synthetic protocols, this can be easily adapted in the fabrication of microfluidic devices to capture and isolate a unique glycoprotein from a large set of previously captured glycoproteins.

5.3 Outlook

Glycoprotein analysis seems to be lagging behind other classes of biomolecules in terms of opportunities for their high-throughput analysis and detection, as is evident from the limited publications in this area.[1] It is therefore highly desirable to fabricate a μTAS that can enable the identification of glycosylation sites, composition of glycans, and even quantification; the information from such analyses would benefit the biomedical field in the discovery of biomarkers and in aiding diagnosis and therapy. Owing to the heterogeneity of the glycoprotein pool that is embedded in very complex biological fluids, a μTAS necessarily requires some kind of preconcentration modality to reduce sample complexity and facilitate in the identification of a glycoprotein that manifests aberrant glycosylation.

In the future, the receptor-modified poly(methyl methacrylate) surfaces are envisioned to be integrated into a μTAS for glycoprotein screening. In particular, a serial affinity approach is anticipated for glycoprotein screening. As a proof-of-concept, two microfluidic devices/chips will be fabricated with the channels modified with the boronic acid derivative AECPBA and the

poly(NIPAAM–lac–RCA_{120}), respectively. In order to function for serial glycoprotein processing, the two devices/chips can be arranged side-by-side with the chips integrated via removable interconnecting tubes, similar to the concept from thinXXS Microtechnology (*www.thinXXS.com*). Alternatively, they can be integrated via vertical stacking with flow-through holes to allow the transfer/flow of fluid from the top device (boronic acid) to the bottom device [poly(NIPAAM–lac–RCA_{120})].[2-4] This will require a much sophisticated system that will involve valve assemblies, rotors, and stators similar to the work of Yin and co-workers[2] and Bynum and co-workers.[3] The poly(NIPAAM–lac–RCA_{120}) device will be integrated to a heating device (e.g. film heaters containing resistive heater lines)[5] to provide a means to manipulate the temperature in the channel. The flow of fluid will be facilitated by hydrodynamic pumping. For the serial processing approach via the side-to-side chip arrangement, the workflow will be as follows: (1) the sample containing non-glycosylated and glycosylated proteins will be introduced into the boronic acid device to capture and preconcentrate the glycoproteins; the unbound non-glycosylated proteins will be collected as waste. (2) The boronic acid device will be connected to the poly(NIPAAM–lac–RCA_{120}) device using interconnecting tubes. (3) The bound fraction will be eluted from the boronic acid channel and then pass through the poly(NIPAAM–lac–RCA_{120}) channel whereby galactose-containing glycoproteins are captured; the rest of the glycoprotein pool remains intact and will be collected for further fractionation (if desired). This device will be maintained at a temperature below the LCST of the poly(NIPAAM–lac–RCA_{120}). (4) The temperature in the channel will be increased to that above the LCST, while maintaining buffer flow, to elute the bound glycoproteins.

5.4 References

(1) Bindila, L.; Peter-Katalinić, J. Chip-mass spectrometry for glycomic studies. *Mass Spectrom. Rev.* **2009**, *28*, 223-253.

(2) Yin, H.; Killeen, K.; Brennen, R.; Sobek, D.; Werlich, M.; van de Goor, T. Microfluidic chip for peptide analysis with an integrated HPLC column, sample enrichment column, and nanoelectrospray tip. *Anal. Chem.* **2005**, *77*, 527-533.

(3) Bynum, M.; Baginski, T.; Killeen, K.; Keck, R. Integrated microfluidic LC-MS. *Pharm. Technol.* **2010**, *34*, s32-s39.

(4) Gurung, S. Passive alignment of microfluidic chips using the principle of elastic averaging. M.S., Louisiana State University, 2007.

(5) Huber, D. L.; Manginell, R. P.; Samara, M. A.; Kim, B. I.; Bunker, B. C. Programmed adsorption and release of proteins in a microfluidic device. *Science* **2003**, *301*, 352-354.

APPENDIX. AMERICAN CHEMICAL SOCIETY'S POLICY ON THESES AND DISSERTATIONS

If your university requires a signed copy of this letter see contact information below.

Thank you for your request for permission to include **your** paper(s) or portions of text from **your** paper(s) in your thesis. Permission is now automatically granted; please pay special attention to the implications paragraph below. The Copyright Subcommittee of the Joint Board/Council Committees on Publications approved the following:

> Copyright permission for published and submitted material from theses and dissertations
> ACS extends blanket permission to students to include in their theses and dissertations their own articles, or portions thereof, that have been published in ACS journals or submitted to ACS journals for publication, provided that the ACS copyright credit line is noted on the appropriate page(s).
>
> Publishing implications of electronic publication of theses and dissertation material
> Students and their mentors should be aware that posting of theses and dissertation material on the Web prior to submission of material from that thesis or dissertation to an ACS journal may affect publication in that journal. Whether Web posting is considered prior publication may be evaluated on a case-by-case basis by the journal's editor. If an ACS journal editor considers Web posting to be "prior publication", the paper will not be accepted for publication in that journal. If you intend to submit your unpublished paper to ACS for publication, check with the appropriate editor prior to posting your manuscript electronically.

If your paper has **not** yet been published by ACS, we have no objection to your including the text or portions of the text in your thesis/dissertation in **print and microfilm formats**; please note, however, that electronic distribution or Web posting of the unpublished paper as part of your thesis in electronic formats might jeopardize publication of your paper by ACS. Please print the following credit line on the first page of your article: "Reproduced (or 'Reproduced in part') with permission from [JOURNAL NAME], in press (or 'submitted for publication'). Unpublished work copyright [CURRENT YEAR] American Chemical Society." Include appropriate information.

If your paper has already been published by ACS and you want to include the text or portions of the text in your thesis/dissertation in **print or microfilm formats**, please print the ACS copyright credit line on the first page of your article: "Reproduced (or 'Reproduced in part') with permission from [FULL REFERENCE CITATION.] Copyright [YEAR] American Chemical Society." Include appropriate information.

Submission to a Dissertation Distributor: If you plan to submit your thesis to UMI or to another dissertation distributor, you should not include the unpublished ACS paper in your thesis if the thesis will be disseminated electronically, until ACS has published your paper. After publication of the paper by ACS, you may release the entire thesis (**not the individual ACS article by itself**) for electronic dissemination through the distributor; ACS's copyright credit line should be printed on the first page of the ACS paper.

Use on an Intranet: The inclusion of your ACS unpublished or published manuscript is permitted in your thesis in print and microfilm formats. If ACS has published your paper you may include the manuscript in your thesis on an intranet that is not publicly available. Your ACS article cannot be posted electronically on a publicly available medium (i.e. one that is not password protected), such as but not limited to, electronic archives, Internet, library server, etc. The only material from your paper that can be posted on a public electronic medium is the article abstract, figures, and tables, and you may link to the article's DOI or post the article's author-directed URL link provided by ACS. This paragraph does not pertain to the dissertation distributor paragraph above.

Questions? Call +1 202/872-4368/4367. Send e-mail to copyright@acs.org or fax to +1 202-776-8112. 10/10/03, 01/15/04, 06/07/06

VITA

Jennifer Macalindong De Guzman was born on July 17, 1979, in Lipa City, Batangas, Philippines. She spent her elementary and high school years in three locations, namely Manila, Lipa City, and Rizal, in the Philippines. She obtained her bachelor's degree in chemistry in April 2000 in the University of the Philippines at Los Baños Laguna and graduated *cum laude*. In the same year, she took the Chemistry Licensure examination administered by the Professional Regulation Commission in the Philippines. She obtained the 6^{th} highest examination score (Top 6) out of ~ 600 examinees. She went on and pursued a teaching career in the Institute of Chemistry at the University of the Philippines at Los Baños Laguna for 3 years (2001–2004). In 2004, she obtained an admission for the doctorate program in the Department of Chemistry at Louisiana State University, and started her graduate studies. While pursuing graduate studies, she got married, and both she and her husband are currently living in Baton Rouge, Louisiana.